TU/e EINDHOVEN UNIVERSITY OF TECHNOLOGY

Fibre-optic sensing for application in oil and gas wells

Citation for published version (APA):
Lumens, P. G. E. (2014). *Fibre-optic sensing for application in oil and gas wells*. [Phd Thesis 1 (Research TU/e / Graduation TU/e), Applied Physics and Science Education]. Technische Universiteit Eindhoven. https://doi.org/10.6100/IR769555

DOI:
10.6100/IR769555

Document status and date:
Published: 01/01/2014

Document Version:
Publisher's PDF, also known as Version of Record (includes final page, issue and volume numbers)

Please check the document version of this publication:

• A submitted manuscript is the version of the article upon submission and before peer-review. There can be important differences between the submitted version and the official published version of record. People interested in the research are advised to contact the author for the final version of the publication, or visit the DOI to the publisher's website.
• The final author version and the galley proof are versions of the publication after peer review.
• The final published version features the final layout of the paper including the volume, issue and page numbers.

Link to publication

General rights
Copyright and moral rights for the publications made accessible in the public portal are retained by the authors and/or other copyright owners and it is a condition of accessing publications that users recognise and abide by the legal requirements associated with these rights.

• Users may download and print one copy of any publication from the public portal for the purpose of private study or research.
• You may not further distribute the material or use it for any profit-making activity or commercial gain
• You may freely distribute the URL identifying the publication in the public portal.

If the publication is distributed under the terms of Article 25fa of the Dutch Copyright Act, indicated by the "Taverne" license above, please follow below link for the End User Agreement:

www.tue.nl/taverne

Take down policy
If you believe that this document breaches copyright please contact us at:

openaccess@tue.nl

providing details and we will investigate your claim.

Download date: 14. Sep. 2026

Fibre-optic sensing for application in oil and gas wells

PROEFONTWERP

ter verkrijging van de graad van doctor aan de
Technische Universiteit Eindhoven, op gezag van de
rector magnificus prof.dr.ir. C.J. van Duijn, voor een
commissie aangewezen door het College voor
Promoties, in het openbaar te verdedigen
op woensdag 16 april 2014 om 16.00 uur

door

Paul Gerard Edmond Lumens

geboren te Geleen

De documentatie van het proefontwerp is goedgekeurd door de promotoren en de samenstelling van de promotiecommissie is als volgt:

voorzitter:	prof.dr.ir. G.M.W. Kroesen
1e promotor:	prof.dr. H.C.W. Beijerinck
2e promotor:	prof.dr. L.P.H. de Goey
copromotor:	dr. A. Franzen *(Shell)*
leden:	prof.dr.ir. K. Kopinga
	prof.dr.ir. J.D. Jansen *(Technische Universiteit Delft)*
	dr.ir. J.M.V.A. Koelman *(Shell)*
	Prof.Dr. W. Ertmer *(Leibniz Universität Hannover)*

Unrestricted **SR.14.10061**

Fibre-optic sensing for application in oil and gas wells
by
P.G.E. Lumens (PTI/RS)

PhD-on-Design thesis, publicly defended on Wednesday April 16, 2014 to obtain the doctoral degree from Eindhoven University of Technology.

A catalogue record is available from the Eindhoven University of Technology Library.

ISBN: 978-90-386-3567-5

This document is unrestricted.
Copyright Shell Global Solutions International, B.V. 2014.

Shell Global Solutions International B.V., Rijswijk

Further electronic copies can be obtained from the Global Information Centre.

Summary

Fibre-optic sensing for application in oil and gas wells.

Fibre-optic sensing has the potential to revolutionise *well and reservoir surveillance* in the *oil and gas* industry. Benefits come from the passive nature of fibre-optic sensors, the potential for cost-effective installations, combined with the possibility of densely-distributed measurements along the entire length of the fibre. Information obtained with fibre-optic sensors installed in oil and gas *wells* contributes to efficiency, safety and ultimate recovery.

A variety of fibre-optic sensors enables measurement of physical effects such as *temperature*, *pressure*, *chemical composition*, *strain* and *acoustics*. A suitable data-infrastructure and processing capabilities to translate those measurements into valuable information are crucial elements of any sensing system. The basis is formed by suitable fibre-optic *sensors* in the well and an *interrogation unit* at surface. This thesis focuses on the development of sensing hardware based on two fibre-optic techniques: *fibre Bragg gratings* and *Rayleigh scattering*.

Fibre Bragg gratings (*FBGs*) are *point sensors* that can be distributed along the length of a fibre-optic cable. One of the key enablers for cost-effective FBG-based sensing systems is a *low-cost* and *robust* interrogation unit. The successful development of such interrogation unit for use in a high-temperature desert environment is presented (Chapter 3). This development aims at stimulating commercial low-cost realisations. These can be evaluated in-house in combination with a dedicated test setup (Chapter 4).

Distributed Acoustic Sensing (*DAS*) is a fully *distributed* sensing technique using *Rayleigh scattering* from naturally-occurring scatter sites along the length of a standard optical fibre. The backscattered energy can be interpreted to realise quasi-microphones all along the fibre. DAS has received much attention recently because of its potential application in down-hole surveillance such as in fracturing monitoring, flow monitoring, as well as in geophysical monitoring. With a focus on *geophysical applications*, this thesis describes the development of suitable *interrogation units* (Chapter 5) and the successful verification of new prototypes in *field trials* (Chapter 6). To further widen the geophysical application scope, the sensitivity of the fibre-optic *sensing cable* for seismic waves impinging *perpendicular* to its *axial* direction required to be enhanced (Chapter 7). This thesis introduces the development of such cable concepts, and presents results of successful laboratory and field trial tests (Chapter 8).

Distributed sensing techniques offer the potential of reducing cost while increasing the spatial resolution. However, the continuous measurement along the cable length introduces uncertainties in the conversion from optical length in the fibre to a location in the down-hole environment. While several methods for *depth calibration* have been proposed, this thesis illustrates the development of a novel method: the *Magnetic Depth Locator* (Chapter 9). Installation of multiple magnet assemblies in the well provides for permanent depth referencing points, which makes it very suitable for safeguarding the depth-accuracy required by *time-lapse* well and reservoir monitoring (Chapter 10).

Multiple fibre-optic sensing technologies can be combined in a down-hole environment. The resulting abundance of measurements continuous in time and distance along the fibre, presents a unique opportunity for robust well and reservoir surveillance in the oil and gas industry.

Samenvatting

Glasvezelmeettechnieken voor toepassing in olie- en gasputten.

Het gebruik van op *glasvezel* gebaseerde *meettechnieken* in de *olie- en gas*industrie biedt revolutionaire mogelijkheden voor de *bewaking en bemonstering van putten en reservoirs*. Voordelen zijn ondermeer het passieve karakter van *glasvezelsensoren*, de mogelijkheid tot kostenreductie, in combinatie met een groot aantal meetposities over de lengte van de glasvezel. De informatie die met glasvezelsensoren wordt verkregen in olie- en gas*putten* draagt bij aan de efficiëntie en veiligheid van de productie en aan maximalisatie van de totale winning.

Een verscheidenheid aan glasvezelsensoren maakt het meten van fysische grootheden zoals *temperatuur*, *druk*, *rek*, *akoestiek*, en *chemische samenstelling* mogelijk. Een geschikte infrastructuur en voldoende verwerkingscapaciteit om deze metingen te vertalen naar bruikbare informatie zijn cruciaal voor een dergelijk meetsysteem. De basis hiervoor wordt gevormd door de juiste glasvezelsensoren in de put en een *uitleesapparaat* aan het oppervlak. Dit proefschrift richt zich voornamelijk op de ontwikkeling van meetsystemen gebaseerd op twee glasvezeltechnieken: *fibre Bragg gratings* en *Rayleigh verstrooiing*.

Fibre Bragg gratings (*FBG's*) zijn *puntsensoren* die op iedere gewenste positie aangebracht kunnen worden in een glasvezelkabel. Een belangrijke eis aan een financieel aantrekkelijk meetsysteem gebaseerd op FBG's is een *goedkoop* en *betrouwbaar* uitleesapparaat. De succesvolle ontwikkeling van een dergelijk uitleesapparaat voor gebruik in een warme woestijnomgeving wordt in Hoofdstuk 3 besproken. Deze ontwikkeling is bedoeld om de invoering op commerciële basis te stimuleren tegen een concurrende prijs. Dergelijke commercieel ontwikkelde uitleesapparaten kunnen intern geëvalueerd worden met behulp van een speciaal ontwikkelde testopstelling (Hoofdstuk 4).

Distributed Acoustic Sensing (*DAS*) is een techniek die metingen op iedere willekeurige positie *over de gehele lengte* van de glasvezel mogelijk maakt door analyse van het fenomeen van Rayleigh verstrooiing: deze verstrooiing wordt veroorzaakt door interactie tussen het ingestraalde licht en verstrooiingscentra die in het materiaal van een standaard glasvezel aanwezig zijn en wordt beïnvloed door akoestische trillingen van de glasvezel. De teruggekaatste energie kan geïnterpreteerd worden alsof het microfoontjes zijn, verdeeld over de gehele kabel. DAS heeft recentelijk veel aandacht gekregen vanwege de toepassingsmogelijkheden voor de bewaking van putten, zowel voor het monitoren van fracturing operaties of van gas- en vloeistofproductie, als ook voor geofysische metingen. Met de nadruk op *geofysische toepassingen*, beschrijft dit proefschrift de ontwikkeling van geschikte *uitleesapparatuur* (Hoofdstuk 5) en de succesvolle verificatie van resulterende prototypes in *veldproeven* (Hoofdstuk 6). Het geofysische toepassingsgebied kan verder verbreed worden door de gevoeligheid van de *meetkabel* te vergroten voor seismische golven die *loodrecht* op de *axiale* richting van de kabel binnenkomen (Hoofdstuk 7). Dit proefschrift introduceert de ontwikkeling van prototypes van dit soort kabelstructuren en toont de resultaten van succesvolle laboratorium- en veldproeven (Hoofdstuk 8).

Gedistribueerde meettechnieken zoals DAS bieden de mogelijkheid tot kostenverlaging in combinatie met een verbeterd ruimtelijk oplossend vermogen. Echter, de meting over de gehele lengte van de kabel introduceert een onzekerheid in de vertaling van optische lengte in de glasvezel naar de corresponderende locatie in de ondergrondse omgeving. Naast verscheidene

andere voorgestelde methodes voor *diepte-ijking*, wordt in dit proefschrift de ontwikkeling van een veelbelovend alternatief geïllustreerd: de *Magnetic Depth Locator* (Hoofdstuk 9). Het inbrengen van permanente magneten in een houder op een goedbepaalde positie in de put levert stabiele referentiepunten op om de diepte vast te stellen. Dit maakt deze techniek erg geschikt voor het bewaken van de dieptenauwkeurigheid die is vereist voor *time-lapse* herhaalde monitoring van putten en reservoirs (Hoofdstuk 10).

Op glasvezel gebaseerde meettechnieken kunnen met elkaar worden gecombineerd in een ondergrondse omgeving. De overvloed aan metingen die dit oplevert, continue verdeeld over de tijd en de positie in de glasvezel, is een unieke mogelijkheid voor de bemonstering en bewaking van putten en reservoirs in de olie- en gasindustrie.

Acknowledgements

The work described in this thesis results from a joint effort in a collaborative work environment. I would like to acknowledge the efforts of many, without whom the results presented – and this thesis itself – would not possibly have been realized.

In my view, the success of a project benefits from a team in which members support each other on a technical level as well as balance each other behaviourally. The In-Well Technology (IWT) team is such a team and I am grateful to be part of it. I would like to thank *all* team members, both in Rijswijk and in Houston, for the great atmosphere and the excellent work. In particular, I would like to mention some of the people I have worked with most closely. First of all, my fellow DGS team members Gijs Hemink, Jon La Follett and Brendan Wyker. Excellent technical assistance has been provided by Lex Groen and Arthur van Rooyen. Bill Birch deserves special mention because of his pivotal role in getting me familiar with field operations and well design.

Due to the collaborative and global organizational structure of Shell, interaction with many other individuals and entities is natural. Being exposed to and teaming up across so many different cultures is socially very enriching. I appreciate the collaboration with the Areal Monitoring team, and in particular the extensive geophysical advice and discussion with Samantha Grandi and Kees Hornman. I also would like to extend a word of thanks to the experimental services teams and the wide range of other functions contributing to our projects. Last but not least, the fruitful collaboration with a range of operating units throughout the world should be highlighted, in particular in Brunei, Oman, The Netherlands, the United States and Canada.

Innovation is not limited within one company but flourishes most through cooperation within – and between – industries, and with academia. Therefore, I would also like to thank development partners, suppliers and academic relations for their valuable contributions.

Writing a PhD thesis is a significant challenge in its own right, even after the results are available to be incorporated. I am very grateful for all support and facilitation that I have received from both Shell and Eindhoven University of Technology.

Combining thesis obligations with being employed in an industrial research centre is a less common route towards a PhD. Substantial organisational efforts are required to create the right boundary conditions. None of this would have started without the vision and support of Hans den Boer and Vianney Koelman, both instrumental in initiating this effort. While the project progressed, Juun van der Horst and Hans Potters have been extremely supportive and facilitating.

Throughout my career in Shell, Andre Franzen has provided me with a wealth of guidance. In various roles – supervisor, colleague and co-advisor – he has sharpened my fibre-optic and reporting skills and hence has been crucial in realizing this thesis.

Herman Beijerinck should definitely be called the nurturer of this PhD work. As former director of the technological design programme SAI-DTI, he is the cornerstone of such industry-academia cooperation. He has also raised the role of first advisor to a next level through his excellent and indispensable advice, on technical, personal development and reporting aspects.

I also want to highlight my gratitude for all support received from my parents, my love and my close friends, without which this effort would have been immeasurably more difficult.

Finally, a word to the reader: I appreciate your interest in my work. This thesis describes work done up to August 2013. While I do realize that the value of a thesis is short-lived in view of continuous industry developments, I hope that it will help industry to advance one step further and that it provides a useful introduction to people new to the topic.

Paul Lumens
Rijswijk, September 2013

Table of contents

Summary V
Samenvatting VII
Acknowledgements IX
1. Introduction 1
1.1. Energy challenge 1
1.2. Wells, Reservoir and Facilities Management 2
1.3. Focus on in-well diagnostics by fibre-optic techniques 4
1.4. Fibre-optic sensing technologies 5
1.5. Deployment 8
1.6. PhD on design 9
1.7. Content of thesis 9
2. Field deployment and design strategy 11
2.1. Down-hole environment 11
2.2. Operating range 13
2.3. Safety 15
2.4. Reliability 15
2.5. Design process 16
2.6. Deployment 17
3. Interrogation unit for multi-point sensors 19
3.1. Quasi Distributed Pressure Sensing 19
3.2. Requirements interrogation unit 21
3.3. Selection of interrogation scheme 22
3.4. Tuneable filter based interrogator prototype 23
3.5. Validation by experimental testing 27
3.6. Conclusions 28
4. Towards deployment of Quasi Distributed Pressure Sensing 29
4.1. Development cycle 29
4.2. Interrogation units in initial field trials 30
4.3. Test setup 31
4.4. Typical test results 32
4.5. Conclusions 35
5. Delocalized sensing: Distributed Acoustic Sensing 37
5.1. Sensing system 37
5.2. Rayleigh scattering 38
5.3. Fibre-link probing schemes 39
5.4. Acoustic probing schemes 41
5.5. Lab evaluation 43
5.6. Trade-off: stability vs spatial resolution 44
5.7. Continuous development 46

6. DAS for Geophysics: deployment 49
6.1. Field trial resourcing 49
6.2. Vertical Seismic Profiling 50
6.3. DAS signal quality 52
6.4. Angle-dependent sensitivity 55
6.5. Cemented vs tubing-conveyed cable deployment 57
6.6. Micro-seismic monitoring 59
6.7. Conclusions 61
7. DAS for Geophysics: transfer function 63
7.1. Traditional down-hole fibre-optic cable 63
7.2. Fibre-optic sensitivity to strain 64
7.3. Modelling of axial and radial strain coupling 65
7.4. Axial strain coupling in practice 69
7.5. 2D directivity 70
7.6. Lessons learned 71
8. DAS for Geophysics: directionally-sensitive cable design 73
8.1. Applications 73
8.2. Helically-shaped fibre 76
8.3. Inertial members 77
8.4. Proof of principle 80
8.5. Field trial 81
8.6. Outlook 81
9. Depth calibration for DAS: design 83
9.1. Well-logging accuracy 83
9.2. Depth accuracy 83
9.3. Application 86
9.4. Magnetic Depth Locator 88
9.5. Reliability 89
9.6. Sub-channel accuracy 93
9.7. Conclusions 93
10. Depth calibration for DAS: deployment 95
10.1. Towards a deployable system 95
10.2. Assembly development 96
10.3. Integrated approach 97
10.4. Test-well trial 99
10.5. Way forward 100
11. Concluding remarks 101
11.1. Strategic approach to develop in-well fibre-optic sensing tools 101
11.2. Commercial success 102
References 105
List of patents 111

List of publications 113
Curriculum Vitae 115
Bibliographic information 117

1. Introduction

This thesis describes the development of fibre-optic sensing technologies for application in oil and gas wells, to optimize production and safety. The design process ranges from early application research, definition of product requirements, via product development, to field trial deployment, which is an essential part in Shell's technology maturation strategy. The work described can only be realized as part of an integrated team effort, with a long-term goal of commercial-scale application in Shell's assets.

1.1. Energy challenge

The work presented in this thesis relates to the development of novel fibre-optic sensing technologies as part of a corporate product development programme in Shell. One of the largest *international oil companies* (*IOC*), Shell dedicates substantial resources to the development and implementation of the actual fibre-optic hardware- and software tools. The reasons for such focus can be linked to the growth in global population and energy demand over the next century.

Rapid population growth in combination with increasing prosperity in developing countries is expected to lead to a surge in energy consumption over the next decades. Despite implementation of energy saving measures, forecasts indicate an increase in energy demand in 2035 ranging from 55% up to 95% compared to 2000 [1] [2]. Renewable energy sources are expected to provide a substantial part of the required energy. However, a range of sources will be needed to supply the energy required over the coming decades. To do this in a sustainable way, a part of the world's energy mix can come from renewables, with *fossil fuels* and nuclear power providing the remainder. Moreover, oil – and potentially gas [3] – are the basis for many products in today's industrialised world, e.g., plastics products or industrial chemicals, and it is unlikely that sufficient alternatives become available over the next decades [4].

As a result, the challenge for oil and gas companies is to supply sufficient amounts of oil and gas – together referred to as *hydrocarbons* – well into the future in a sustainable way. This needs continuous improvements throughout the production cycle. Displayed in Figure 1.1, the integrated value chain ranges from *upstream* to *downstream*. Activities to *explore* and *produce* hydrocarbons are collectively referred to as upstream activities, and are the focus of this work. Production locations include onshore oil and gas wells, offshore platform-based or subsea production-systems, as well as production of, e.g., sugarcane as an ingredient for bio-fuels. *Downstream* activities include all efforts to process and *refine* the hydrocarbons, eventually resulting in products that can be sold. Products include fuels, e.g., diesel or kerosene, but also chemicals, e.g., plastics, as feedstock for other industries. Shell, together with most other IOCs, is active in the entire value chain ranging from exploring new hydrocarbon sources all the way to marketing and selling of refined products.

The fibre-optic sensing technologies discussed in this thesis are tailored to upstream applications, although they also offer significant potential for application to downstream. In upstream, the challenge is to increase hydrocarbon production as the era of "*easy oil*" is over: easily-drillable sources of light-oil are becoming increasingly scarce. Instead, hydrocarbon resources that are more difficult to recover from challenging environments have to be pursued. Such production environments include deep water – currently up to approximately 3,000 meters of water depth [5] – and arctic environments with seasonal operations windows due to heavy ice formation, both illustrated in Figure 1.1. Apart from finding new resources, significant benefit can come from increasing the *ultimate recovery* from existing fields. The amount of oil in a *subsurface reservoir* is called *oil in place*. Only a fraction of this oil, the *recovery factor*, can be recovered and is considered to be a

Figure 1.1: **Integrated value chain of a state-of-the-art IOC and pictorial diagram of modern hydrocarbon recovery. 'Easy oil' is gone, advanced processes to extract more difficult resources have to be used and are the focus of the work presented in this thesis. The onshore field (1) uses fracturing techniques in long horizontal wells to extract gas or oil from shales. Steam is injected in onshore field (2) to lower the oil viscosity and consequently increase the recovery factor. New resources are increasingly found in challenging areas, such as deep sea environments (3) or in arctic conditions (4). All these more complex production conditions require monitoring to ensure efficient operation.**

reserve. The portion that is not recoverable is not included unless and until additional – and often newly developed – methods are implemented to produce it. Historically, only about 35% to 45% of the hydrocarbons in place in a field have on average been produced [6]. With conventional production technologies it is often not economically feasible to produce more. However, incremental improvements will already lead to significant benefits: for example, an improvement of the recovery factor by only 2% can be equated to approximately one year of today's global oil demand [7]. Hence it is obvious that to maximize production and meet growing energy demand in a sustainable way, the efficient management and optimisation of production operations and systems is crucial. The next sections will illustrate that monitoring, especially by means of fibre-optic sensing, can provide crucial information in this optimisation process.

1.2. Wells, Reservoir and Facilities Management

Optimisation of production operations provides a significant contribution to increase ultimate recovery. This includes processes from modelling the reservoir, via optimised well design, to novel technologies which help in maximizing production from these wells. The first step is to assure that operation of current production facilities is as efficient as possible. Streamlining of,

e.g., processes, maintenance schedules, and subsurface models guarantees that all hydrocarbons that can be recovered with the selected production concept are actually produced. Although this might result in a production increase of only a few percent, the absolute volumes represent a significant value and are a substantial contribution to global energy demand.

The Shell group consists of a varied range of *operating units* (*OUs*), the majority being independent *joint-ventures*. Operating through-out such a range of *assets* means dealing with a variety of processes, communication styles and technologies. In practice, improvements are not only implemented top-down – from headquarters to the OUs – but are to a large extent also initiated in the OUs. The resulting variety in requirements poses a challenge for designing novel solutions, as will be further discussed in Chapter 2. Nevertheless, this cross-fertilisation approach is actually highly beneficial, since it draws from the extensive and varied experience available amongst operations staff, and enhances engagement in a continuous improvement loop throughout the organisation.

Further step-changes in ultimate recovery can be realised by applying so-called *enhanced oil recovery* (*EOR*) techniques. This involves techniques to increase the mobility of the oil in order to ease oil flow into production wells. One method involves the injection of *surfactants* (detergents) with the aim to reduce the surface tension between water and oil in the reservoir, thereby mobilizing oil which would otherwise remain in the reservoir as residual oil. *Steam injection*, as displayed in Figure 1.1 (#2), is another technique that heats very viscous – *heavy* – oil in order to reduce viscosity and hence help extraction [6]. Unwanted is the situation in which the injected steam or surfactants 'short-cut' to a producer well through a small highly-permeable zone, instead of increasing the mobility of the oil itself. It is crucial to monitor how the injected fluids propagate *down-hole* through the reservoir, and act accordingly – for example by redistributing injection fluids to different sections of the reservoir.

Wells, Reservoir and Facility Management (*WRFM*) is the overarching term for such feedback control. As illustrated in Figure 1.2, WRFM aims at deriving optimisations for a particular process from the analysis of objective facts and measurement data. Such process can relate to basic scheduling

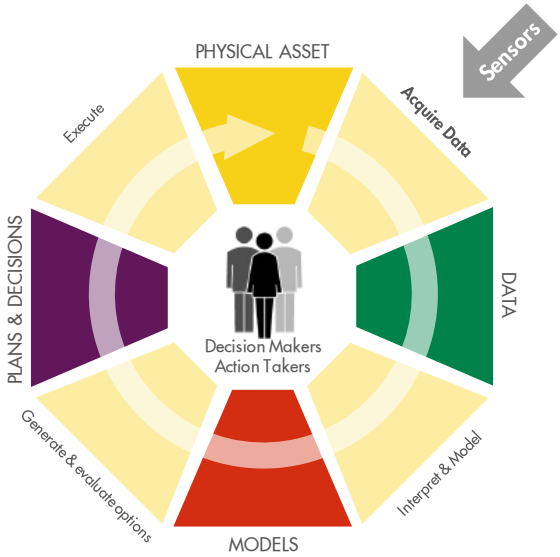

Figure 1.2: **Increasing production and optimizing hydrocarbon recovery requires a measure-model-decide-intervene improvement loop. Availability of down-hole sensor measurements is often a bottleneck in realizing this improvement loop.**

of maintenance for, e.g., a flow valve, but also to – significantly more complex – optimisation of steam injection patterns. Different processes require different cycle times: well-optimisation can happen on a daily basis, and therefore often requires automated measurement and analysis capabilities. Field-optimisation can have annual cycles and requires more complex measurements which need expert analysis. Summarizing, regardless whether such process requires basic failure monitoring for well-optimisation or reservoir-wide steam monitoring for field-optimisation, the common denominator is the necessity of having suitable sensors. Obtaining sensors suitable for down-hole measurements is not trivial as will be further discussed in the next section.

1.3. Focus on in-well diagnostics by fibre-optic techniques

Sensors for use in oil and gas wells, reaching multiple kilometres into the subsurface, are used to measure a wide range of parameters. Examples include: pressure and temperature distributions along the well, the presence of certain chemicals, acoustic signals resulting from seismic activities or due to activities in the well-bore, and mechanical stress on structural components.

A range of different sensors can be used, either temporarily hung-off in the well or permanently installed as part of the well construction. In the past, electrical point sensors were the only means to measure. Recently developed fibre-optic sensors provide a very promising alternative. They provide distributed measurements, are passive, potentially low-cost, have a long service life and a small form-factor.

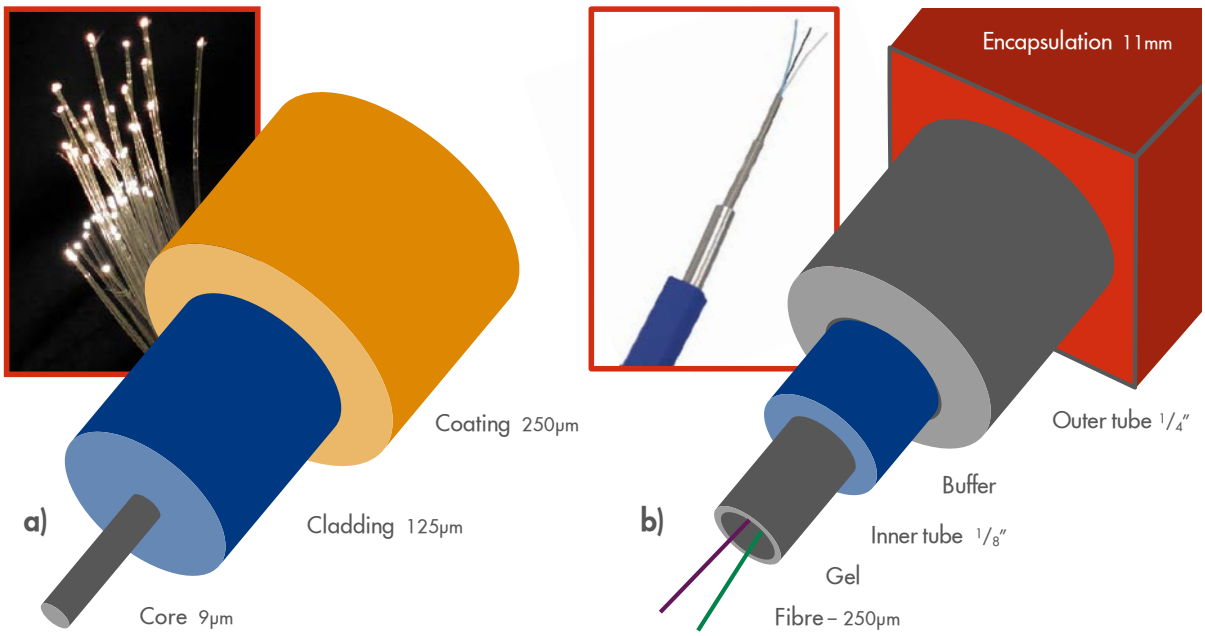

Figure 1.3: **Build-up of a typical optical fibre and traditional down-hole fibre-optic cable. (a) A single-mode fibre consists of several layers: light typically is transmitted through the core, in which it is contained due to the refractive index contrast with the cladding. One or more coatings are typically added to provide increased strength to the optical fibre. (b) For down-hole applications, one or more fibres are typically packaged in a metal control line. Inside this metal outer tube, the fibre is usually contained in a smaller, ⅛" size, metal tube and a plastic buffer material in between them.**

As displayed in Figure 1.3a, an optical fibre typically consists of three layers [11]. The light propagates in the *core*, guided by the contrast in *refractive index* between the core and the surrounding *cladding*. Both core and cladding are made of glass, with the required difference in refractive index typically provided by the addition of *dopants* to the core. Depending on the size of the core and the refractive index profile between core and cladding, light either propagates in one single *propagation mode* in a *single-mode* fibre, or in multiple modes in a *multi-mode* fibre. The typical optical wavelength used in a single-mode core of 9 μm is around 1550 nm, whereas multi-mode fibres have typical core diameters of 50 or 62.5 μm and wavelengths between 850 and 1300 nm are typically used. Around the cladding, with a typical diameter of 125 μm, one or more coatings provide additional strength to the optical fibre.

For down-hole installations, such bare optical fibres are traditionally packed in *control-lines*, metal tubes of typically ¼" diameter (Figure 1.3b). Inside the control-line, the fibre is – often immersed in a *gel* – packaged in a second, typically ⅛" size, *inner tube* and often surrounded by a plastic *buffer* material. A plastic *outer encapsulation* is often added around the control-line to improve grip for clamping the cable in the well. All these layers together prevent any stress on the optical fibre which could lead to damage, or even worse, a fibre break.

Although so far mainly used in low- to medium-temperature environments and provided the cable has not been damaged during installation, optical fibre in such control-lines has a service-life track-record of ten years or longer, typically based on extensive testing in the telecommunications industry [8]. This is one of the advantages resulting from the passive nature of an optical fibre, compared to a larger reliability risk involved with active electronic components down-hole. Fibre-optic sensors do consequently not cause *Electro-Magnetic Interference* (*EMI*) nor are they sensitive to EMI, e.g., due to other down-hole equipment such as electrical pumps.

The component cost of the simple cable construction as presented in Figure 1.3b provides significant potential for a *lower-cost* sensor compared to electrical sensors, especially in combination with volume-produced optical fibres from the telecommunications industry. The most significant part of the cost of a fibre-optic sensing system is in the interrogation unit at surface. However, this unit can often be used for a number of wells, and servicing or replacement is straightforward since it is easily accessible and can simply be (un-)plugged. Some sensing concepts require a sort of mechanical – passive – transducer to convert the measurement quantity into a measurable impact on the fibre. Most fibre-optic sensing technologies, however, provide distributed measurements all along the length of the standard cable as displayed in Figure 1.3b. While the basics of commonly-used sensing techniques will be introduced in the next Section, the explanation above indicates that fibre-optic sensors provide a potentially low-cost and ruggedized means of measuring signals relevant to monitoring of wells and reservoirs all along the extent of the well.

1.4. Fibre-optic sensing technologies

Many sensing techniques have been proposed to transform optical fibres into sensors. The concept of *fibre Bragg gratings* (*FBG*) is applied in many applications [9]. A FBG is a local periodic variation of the refractive index in the core of an optical fibre. FBGs are nowadays *inscribed* in a *photosensitive* fibre by using an intense ultraviolet source, and are typically between 1 and 10 mm long. The periodic refractive index variation, as illustrated in Figure 1.4a, leads to a similar effect as seen in atomic crystal layers: *Bragg* reflection at a wavelength related to the periodicity of the structure. The reflected wavelength will change if the periodicity or the refractive index changes, as depicted in Figure 1.4b. This feature enables the use of FBGs as sensors. For example as

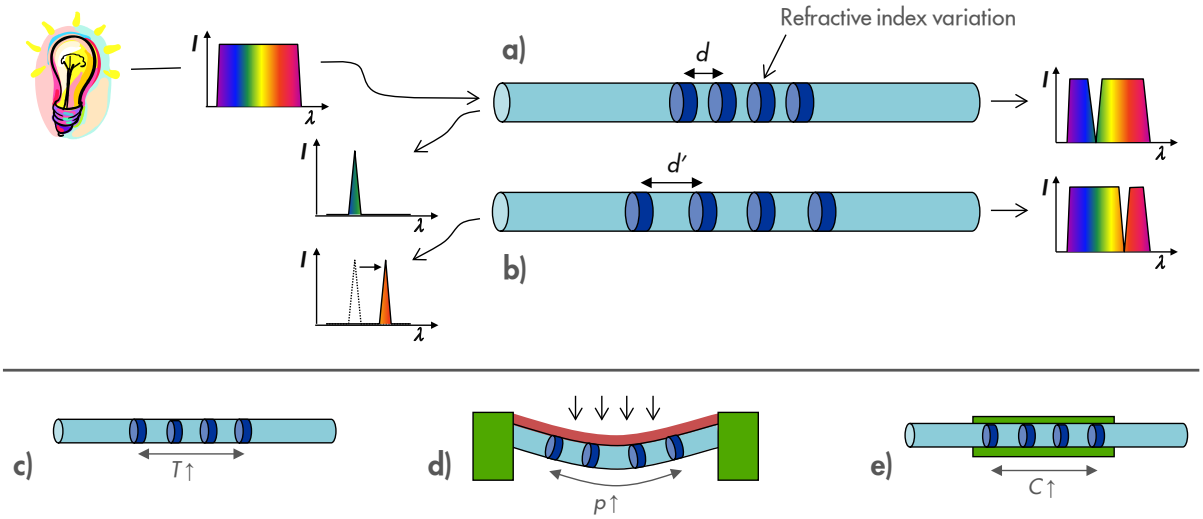

Figure 1.4: **The working principle and some applications of Fibre Bragg Gratings. (a) A fibre Bragg grating is a spatially limited periodic variation of the refractive index in the core. Only incident light intensity *I* at a particular wavelength *λ* will be reflected. This wavelength is proportional to the period *d* of the refractive index variation. (b) A change in length of the fibre will change the periodicity to a value *d'*, which will lead to a corresponding change in reflected wavelength. (c) Such length change of the fibre can be related to temperature *T*, but also to applied strain on the fibre. (d) Pressure can be measured by connecting the FBG to a membrane. (e) A chemical sensor can be created by coating the FBG with a polymer which exerts strain as a result of a chemical reaction with a specific chemical.**

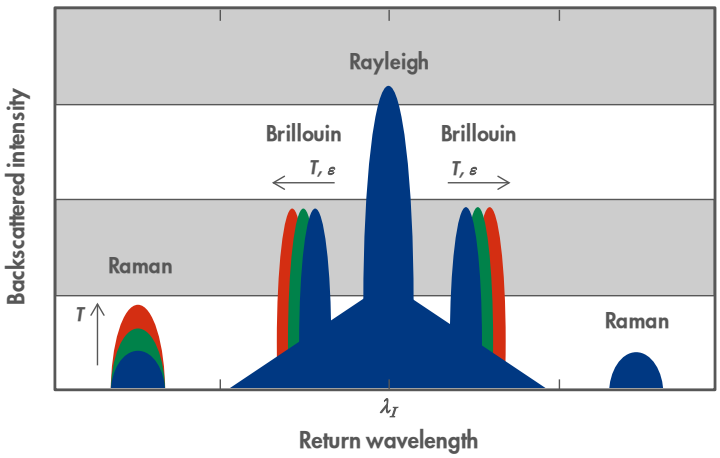

Figure 1.5: **Distributed sensing technologies and the scattering mechanisms used. DAS uses phase shifts derived from Rayleigh scattering, which has the same wavelength λ_I as the incident light. Brillouin scattering, often used in strain detection systems, is characterized by side-lobes around the wavelength of the incident light. The wavelength of the scattered light changes as a function of temperature *T* and strain *ε*. DTS uses Raman scattering to determine temperature changes along the fibre. Temperature is derived from the ratio between the two Raman scattering wavelength ranges, with one being temperature dependent and the other not. This thesis focuses on the use of Rayleigh scattering for Distributed Acoustic Sensing.**

temperature sensor (Figure 1.4c), since a temperature increase will lead to expansion of the glass and hence to a change in periodicity. Similar, strain on the FBG changes the periodicity as well, therefore a FBG is a *strain sensor*. This can be exploited as, e.g., a *pressure sensor* by attaching a FBG to a membrane (Figure 1.4d). A *chemical sensor* can be realised by coating the FBG with a specific polymer which swells when in contact with a specific chemical substance (Figure 1.4e).

FBGs were first demonstrated in 1978, initially for use as a wavelength filter [10]. Even earlier, fibre-optic sensors already existed based on a *Fabry-Perot* interferometer: light passes through a partly reflecting layer and is reflected by a totally reflecting mirror some distance behind it [11]. An interferometric cavity is formed with a series of resonance wavelengths similarly defined by cavity length and refractive index. Fabry-Perot sensors are true single point-sensors. Combination of multiple sensors – *multiplexing* – on one fibre is hindered by the second reflector as it is required to form a cavity to reflect light of all wavelengths. In contrast, a FBG only reflects part of the energy in a limited wavelength band around its peak wavelength and lets the remainder pass through. This can be used to incorporate multiple FBG sensors onto a single optical fibre by, e.g., *wavelength division multiplexing* (*WDM*), using FBGs with different peak wavelengths for each of the sensors [11]. An alternative is *time division multiplexing* (TDM), which distinguishes the sensors by time-of-flight of a short interrogation pulse. Such schemes lead to a *quasi-distributed* array of point sensors[1] positioned along the extent of the well.

A truly distributed sensing system can be realised by using naturally occurring reflections all along a typical optical fibre. These reflections result from the interaction of light in a fibre with *inhomogeneities*, which are much smaller than the wavelength of the light. Such inhomogeneities are most often impurities unavoidably present in the glass and dopants that are being included as part of typical fibre manufacturing processes. This phenomenon enables truly distributed interrogation all along the fibre, without any modifications in the fibre: just by sending a light-pulse into the fibre, energy scattered from each position along the fibre can be detected and its location determined by travel time. The measurement quantity depends on the type of *backscattering* being analysed. Three different backscatter mechanisms are indicated in Figure 1.5, differing in the interaction between a photon in the light pulse and scatter centres in the fibre.

Raman scattering, or the *Raman effect*, results in backscattered light at two spectrally shifted wavelengths compared to the incident light [12]. The intensity of the so-called *anti-Stokes* band is temperature-dependent, while the so-called *Stokes* band is practically independent of temperature. While Stokes-light provides a correction for intensity variations along the fibre, the local temperature of the optical fibre can be derived from the ratio of the anti-Stokes and Stokes light intensities. This technique is commonly called *Distributed Temperature Sensing* (*DTS*). Shell contributed to the introduction of DTS as the first distributed sensing technology in the oil and gas industry, some twenty years ago. Nowadays, typical DTS systems can locate the temperature to a spatial resolution of 0.5 m, a resolution of 0.5°C, over distances greater than 30 km.

Brillouin scattering also results in two side-lobes, however, with wavelengths depending on, e.g., strain or temperature [13]. Brillouin-based fibre-optic sensing is mainly used for static strain and temperature measurements. Brillouin scattering has applications in the oil and gas industry, for example for structural monitoring of pipelines and offshore installations.

---

[1] Apart from the term '*quasi-distributed*', multiple other terms can equivalently be used, including '*multi-point sensors*' and '*multiplexed point-sensors*'. For the application of such sensors to pressure measurements, as will be described in Chapters 3 and 4, we have chosen to use the name '*Quasi-Distributed Pressure Sensing*' (*QDPS*).

The third scattering mechanism described in Figure 1.5 is *Rayleigh scattering*: elastic scattering of photons, resulting in backscattered energy at the same wavelength as the incident light. Rayleigh scattering is the basis for *Distributed Acoustic Sensing* (*DAS*): a technique that essentially allows the realisation of microphones all along the fibre. Such distributed acoustic sensor provides a wide range of monitoring opportunities, as will be discussed in detail in Chapter 5 and further.

The work in this thesis focuses on two fibre-optic sensing concepts: FBGs and DAS. The design of interrogation units for FBGs will be studied for applications such as pressure sensors. After that, the majority of this thesis will consider the development of DAS technology and its use in geophysical applications.

1.5. Deployment

The novel fibre-optic sensors as described in this thesis, and for that matter most technology development for upstream operations, are not products that Shell aims to sell. In contrast, consumer electronics firms require development of new technology because it directly impacts the attractiveness of their products. Oil and gas *operators* are responsible for the overall process to maintain hydrocarbon production, not only in a sustainable but also safe way. Most technical *oilfield services* are outsourced to specialized *service companies*. For Shell, technology is an enabler to optimise production and to obtain a *license-to-operate*: it differentiates Shell from competitors when, e.g., bidding for a license to explore and produce with a host government. Commercial *deployment* of individual technologies is mostly outsourced to service companies. However, the development of key technologies is crucial for Shell and hence *innovation* is a key driver in its strategy[2].

Design requirements for down-hole equipment can be compared best to *space exploration*: a long service life, combined with high safety requirements and operating accuracy. As will be described in detail in Chapter 2, wells are challenging environments, amongst others because of the presence of aggressive chemical conditions, high pressures, high temperatures and stringent uptime requirements. Equipment often has to operate for more than ten years without any possibility of repair, while the explosive environment requires high safety standards. Moreover, while exposed to these conditions, measurements with high accuracy are still needed to provide information on, often subtle, changes in the reservoir. For example, in Chapter 3 we measure optical wavelength shifts in the order of only 1 *picometer*, kilometres deep in the subsurface: an aspect ratio of $1{:}10^{15}$.

Testing the accuracy and reliability of new designs under such extreme down-hole conditions also poses a challenge: laboratory-scale tests can often not be complete for two reasons. First, because it is difficult to build suitable test-equipment to emulate the extreme conditions, such as a pressure of 200 bar. Second, because it is often the combination of multiple conditions that poses a limit to the operating envelope, e.g., a pressure of 200 bar combined with a temperature of 300°C. Such combined experiments are even harder to design and execute, and specifying the most realistic combination of conditions is often a challenge in itself.

---

[2] Note that traditionally most IOCs see their investment in R&D as a competitive advantage, and hence several aspects of this introduction apply not only to Shell but to IOCs in general. For several reasons this introduction has been mainly focused on Shell. First, Shell has been an early investor in R&D related to the fibre-optic sensing technologies described in this thesis. Second, Shell has traditionally been amongst the largest R&D spenders in the oil and gas sector [14], and as such differentiates Shell to some extent from other IOCs.

The combination of challenging operating conditions and limitations to laboratory tests requires the demonstration of technologies in *field trials*. Initial phases of design, modelling and lab tests, are relatively quickly followed by installation of prototypes in real operating environments. This approach provides the most realistic test scenarios, and also demonstrates the technology already in an early stage to the assets: the users.

1.6. PhD on design

The work presented in this thesis is executed within a competitive industrial research centre. Pursuing set goals and demonstration of designs and procedures in field trials has top priority. Fundamental understanding fulfils an important supporting role, but is not the main objective.

I work in the *In-Well Technology* (*IWT*) team: a global team of approximately 25 people, consisting of fibre-optic specialists, researchers, deployment advisors and lab technicians. Staff is distributed over locations in Rijswijk (The Netherlands) and Houston (USA), with individual projects drawing from the manpower and expertise from both locations.

The typical work environment is collaborative. Efforts throughout a range of functions within the organization are needed: scientific staff in collaboration with experimental support, research teams that are global teams, and technology centres in collaboration with assets around the world.

Consequently, the work presented here is not the effort of an individual, it reflects a team effort. My role in this team related to the topics described in this thesis is best described as 'initiator' of the development of new sensor tools or applications. These new ideas are most often the result of a wide brainstorming process. The first evaluation and development activities were then executed by myself. These activities include a significant degree of experimental efforts, which were conducted in close collaboration between myself and lab technicians. If an idea proved to be interesting, it was often further evaluated in a wider team. The lead in such team was often not with myself, but I could still provide important expert input based on my knowledge and experience gained in the initial evaluations. In cases where my input was significantly more limited, this will be specifically indicated.

The combination of work resulting from a highly collaborative environment, focusing on technological designs for direct application rather than academic publication, fits well with the "*PhD on design*" track commonly used in the three universities of technology in the Netherlands [15]. Eindhoven University of Technology plays an active role in filling in the landscape along this new axis of a two-dimensional space of PhDs.

1.7. Content of thesis

The structure of this thesis reflects the industrial setting, in which research and development activities are executed and aimed at deployment of the resulting technologies in the company's operations. Similarly, the contents of this thesis are structured in a *dual panel* approach: a first chapter describes the design based on modelling studies and laboratory experiments. Feedback obtained from the execution of field trials is provided in a second chapter, together with a flavour of the next steps towards commercial-scale deployment.

This thesis describes the *main thread* throughout the work, focused on the methodologies and results to realise a technological design which fulfils the requirements of its end-users. A

substantial amount of work forms the basis, with only a selection published in this thesis: inherent to the aim of industrial research to obtain a competitive edge, some further details are confidential and are only published in company-internal reports. Whereas the reader should understand the full extent of the projects described, the thesis itself is aimed at providing sufficient information on the goal, approach, novelty and results of the work.

The work presented in this thesis focuses on two fibre-optic sensing concepts: fibre Bragg gratings (FBG) and Rayleigh scattering, as already briefly introduced in Section 1.4. First, an introduction to the challenging requirements in oil-field environments and the design strategy typically used in Shell will be provided in Chapter 2.

The focus of Chapter 3 and 4 will be on the development of a read-out unit – an *interrogation unit* – for temperature, pressure and chemical sensors based on FBGs. These sensors are, cascadeable, point sensors for quasi-static measurements, with stringent requirements for the long-term measurement stability.

The remaining, and largest, part of this thesis is devoted to acoustic measurements based on Rayleigh scattering: Distributed Acoustic Sensing (DAS). Efforts start with development of a suitable interrogation unit in Chapter 5, followed by field testing the resulting DAS system for geophysical applications in Chapter 6. The results have proven very successful, and as a result commercial deployment has already started for specific applications, such as Vertical Seismic Profile (VSP) acquisition.

Further improvements can be realised by enhancing the sensitivity of the fibre-optic cables: an analysis of the sensitivity of current state-of-the-art cables is provided in Chapter 7, which forms a basis for further cable designs. The concept, development and first tests of these revolutionary cable designs are presented in Chapter 8. The combination of the new developments in interrogation units and sensor cables has the potential to compete with the sensitivity of current state-of-the-art sensors, geophones, but at a significantly reduced cost and an enlarged deployment envelope.

Finally, Chapter 9 and 10 deal with one last source of uncertainty in fibre-optic measurements in a well-bore: depth calibration. In order to relate measurements to the corresponding reservoir features, the calibrated position of the sensor cable is required. A novel design suitable for permanent deployment will be presented and tested.

Together, the fibre-optic technologies described in this thesis provide a suite of down-hole sensors which – especially when used in combination – provide a step-change in real-time information obtained from the subsurface. Such additional information is crucial to achieve sustainable and optimised hydrocarbon production in increasingly complex production systems.

2. Field deployment and design strategy

The sensors under development are aimed for deployment in wells within Shell Operating Units. The combination of harsh environmental conditions, high accuracy and hostile deployment conditions is not found in many other industries. The design of new sensing technologies is a tangled interplay between Operating Units having specific applications and requirements on the one hand, and specialised companies developing and manufacturing deployable versions of required sensors on the other hand.

2.1. Down-hole environment

A hydrocarbon well has an aspect ratio up to 1:10^5, more extreme than a human hair: whilst a hair is typically around 100 μm thick [16], few people have hair longer than 1 m; well-bores can extend 10 kilometre or more into the subsurface with a diameter (at the bottom) as small as 0.1 m. The path of a well may be *vertical*, but it can also be accurately *steered* during drilling to *deviate* in deeper layers into, e.g., a *horizontal* trajectory, or a more complicated *fishhook* or *snake*-like trajectory. Such trajectories ensure penetration of one or multiple reservoirs, and create the need for information about down-hole conditions.

Drilling a well, such as the simplified well in Figure 2.1a, employs several stages [17]. First a very thick-walled pipe – a *conductor* – is mechanically pile-driven into the soft unconsolidated surface burden to provide structural strength to the well. A *rotating drill-bit* is then typically used to drill the hole. After a section has been drilled, the drill-bit is removed and a series of tubulars, *casings*, are lowered into the hole. The choice of cased sections depends on mechanical strength requirements to, e.g., contain or exclude down-hole pressures or prevent ingress of aquifer water.

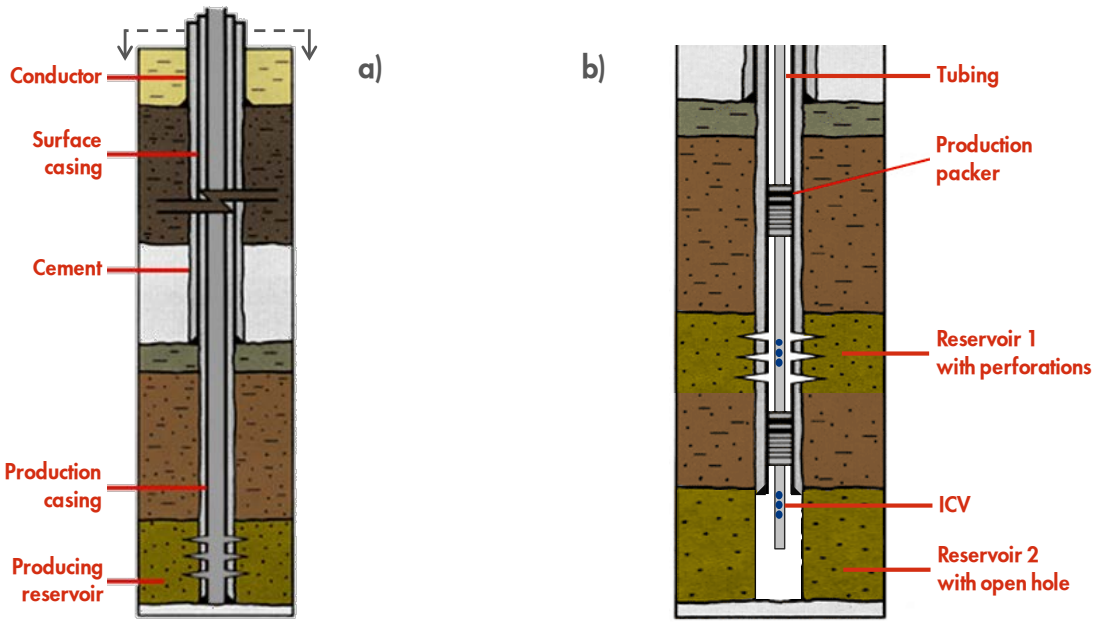

Figure 2.1: **Some typical *well schematics*. (a) The result of drilling a well: a well with one or more cemented casing strings and perforations in the production interval, prior to completion. (b) A completion is added, in this case consisting of a tubing string with production packers to produce from two zones. [18]**

The casings are subsequently cemented in place by filling the void between hole wall and casing with *cement*, as illustrated in Figure 2.1b. This seals the hole from the intersected rock layers. A hole section can be 100 m but also kilometres deep, and is followed by a repeated *drill-case-cement* cycle for the next section. Subsequently smaller hole- and casing-diameters allow drilling of next sections through the inner diameter of the previous casings until *total depth* (*TD*) of the well has been reached.

Depending on the reservoir(s) to be produced and the design of the well, fluid inflow can be from an *open hole* section, or through *perforations* in the casing. Figure 2.1a indicates a well producing from one reservoir. Initially cased and cemented throughout the production interval, shaped ballistic charges are used to perforate the casing to allow inflow of hydrocarbons into the well. Figure 2.1b indicates a well which produces from two reservoirs. In the top reservoir, the well is also cased and subsequently perforated to allow inflow. However, in the bottom reservoir, the well is simply left uncased. Inflow is now possible along the entire depth interval of this open hole section.

To produce from a well the final task is to install *production tubing*. As indicated in Figure 2.1b, this involves lowering a tubing string into the well and placing sealing *packers* to ensure fluids flow through the tubing instead of through the casing. The advantage of such a *completion* includes protection of the casing against potentially highly corrosive fluids, which can eventually lead to compromised integrity of the pipe walls. By forcing fluid flow through the tubing, the fixed casing is protected while the tubing can be periodically replaced. Another advantage of the completion is the ability to control inflow. Considering again the example of producing from two reservoirs in Figure 2.1, it is beneficial to control inflow from the two intervals independently. For example, to optimise production from each: full *draw-down* of the fluids might provide high production initially, but reservoir conditions could cause ultimate recovery to be better if produced at a moderate rate. Such inflow is controlled by installing *In-flow Control Valves* (*ICV*s) instead of simply having perforations in the tubing at intervals where inflow is desired.

This well-configuration with ICVs is an example of a situation in which down-hole *in-well monitoring* is beneficial: by positioning, e.g., pressure, temperature, chemical or acoustic sensors in the well, the in- or outflow can be quantified and the contribution of each ICV can be monitored. Permanent (sensor) instrumentation is typically attached to the outside of the tubing

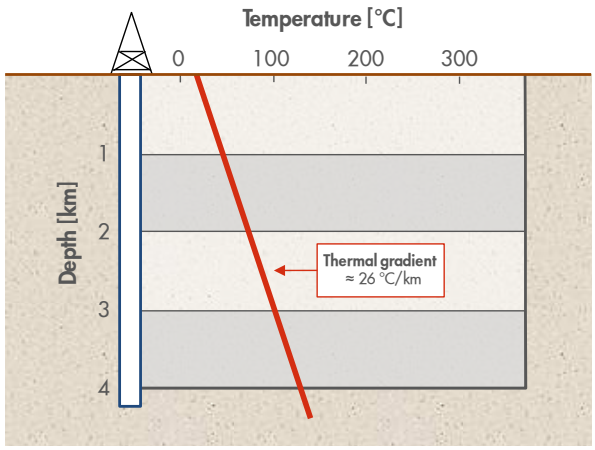

Figure 2.2: **Rate at which temperature increases with depth is called the thermal gradient. This gradient can be measured in oil and gas wells during drilling, or by means of static temperature surveys once wells are completed.**

string, or sometimes on the outside of the casing. However, the – *annulus* – spacing between either tubing and casing, or casing and hole, sometimes less than 2", imposes significant size constraints on down-hole instrumentation.

This introduction to well construction is not intended to provide a full understanding of *well engineering* principles, but should provide the reader with an appreciation of the mechanical environment in which down-hole sensors are installed. Section 2.5 will provide an introduction to the design process to develop fibre-optic sensors suitable for deployment in such well environments. The next Sections will first introduce other important parameters defining the operating range of a typical down-hole sensor.

2.2. Operating range

Apart from the size limitations as discussed in Section 2.2, other important parameters for down-hole operation of sensors are the prevailing *temperature*, *pressure* and *chemical* constituents. These will be further discussed in this Section.

The temperature in the subsurface typically increases with depth as displayed in Figure 2.2. The world-wide average thermal gradient is about 26ºC/km, and ranges from a low of about 18°C/km, to a high of approximately 55°C/km [19]. Local variations are caused by differences in heat flow from the earth's hot core to the surface as a result of variations in thermal conductivities of different rock types. Typically, temperatures up to 85°C can be expected in a well of two kilometre depth.

Pressure also increases with depth. The rock is exposed to the *overburden pressure* as plotted in Figure 2.3, which is a combination of *lithostatic pressure* and *fluid pressure*. Lithostatic pressure is due to the weight of the rock above, and its magnitude mainly depends on the density of the overlying rocks and the local gravity. The lithostatic pressure gradient is on average around 13 kPa/m and increases with depth. Rock typically consists of a matrix of heavily *compacted grains*. The void between the grains, *porosity*, where fluids sit, and the connectedness of this porosity determine the ease with which fluids can flow through the *pore spaces*, the rock's *permeability*. Grain-to-grain contacts in the *rock matrix* support the lithostatic pressure throughout the subsurface. Sensors in a well-bore are therefore mainly subjected to the fluid pressure, or *pore pressure*, which is exerted against the rock grains by the fluids within the pore spaces. When the fluids in rocks are free to move in response to small changes in pressure and are connected to the surface by permeable rocks such as sandstone, the pressure in the pores is caused only by the weight of the column of fluid in the rocks above and is called *hydrostatic pressure*. If easy fluid communication with the surface is inhibited by rocks of low permeability, then abnormal or non-hydrostatic pore pressures can result. However, for the purpose of estimating which pressures a sensor would typically have to cope with, the hydrostatic pressure provides a sufficient first estimate. For a column of fresh water (no *salt* content) with a density of 1.0 g/cm^3, the hydrostatic gradient is 9.81 kPa/m. The gradient increases with increasing *salinity* of the water to about 10.52 kPa/m for typical water in the pore spaces [19].

Over the reservoir depth, pressure gradients vary depending on which fluid is present, from a very low pressure gradient for the gas interval to close-to-water gradients in oil. This variation in pressure gradients can be used to detect interfaces between water, oil and gas by having a

distributed array of pressure sensors in the well-bore. Pressure sensors for this application will be discussed further in Chapter 3.

It is only in the reservoir itself, which most often is less than 100 m thick, that hydrocarbons – oil and gas – are partially filling the pores. Over the total length of a well, the pressure gradient of water provides a good estimate as it is the dominant fluid in the pore spaces, indicating that typically pressures up to approximately 200 bar are expected in a 2 km deep well.

Apart from pressure and temperature, a range of chemical constituents and reactions should be considered in the design of down-hole sensors. *Hydrogen-sulfide* (H_2S) is not only fatal for humans at extremely low concentration (50 – 200 ppm), but also severely corrodes metal down-hole. Appropriate packaging materials should be selected to maximize the sensor's life. Other specific conditions can cause a range of chemical reactions of produced fluids, resulting in, e.g., the formation of *hydrates*, *wax*, *asphaltines* and a variety of chemical *scales*. These can cause clogging of the well-bore, but also of sensor interfaces if appropriate measures to reduce build-up are not implemented in the design [20].

More extreme conditions can be expected as a result of applying specific production techniques. For example, for enhanced oil recovery (Section 1.2), steam or chemicals are often injected to reduce oil viscosity and hence improve flow towards production wells. Steam temperatures down-hole can easily increase above 200ºC (because of elevated pressure), with a typical maximum temperature of 300ºC. Chemical surfactants can be strongly acidic or basic, to such extent that organic tissue may dissolve and only high-grade metals endure long exposure.

Summarizing, down-hole sensors have to withstand aggressive chemicals, in combination with considerable temperatures and pressures: typically 85 ºC and 200 bar in a 2 km deep well, with higher steam temperatures and potentially over-pressured zones. This harsh environment, which – as we will see in the next Sections – introduces significant design challenges to provide for a safe and reliable sensor deployment.

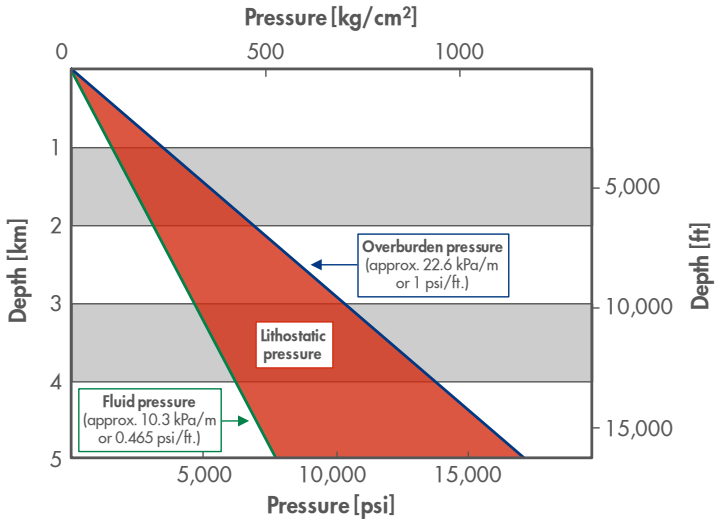

Figure 2.3: **Overburden pressure, which is also called geostatic pressure, is equal to the sum of the hydrostatic pressure plus the lithostatic pressure. This pressure may also be thought of as the weight of the overlying (pore fluid + sediment) per unit area. Overburden pressure increases with depth and averages about 22.6 kPa/m or 1 psi/ft. In many cases, sensors are only subject to the hydrostatic pressure.**

2.3. Safety

Safety is a *critical* issue for the oil and gas industry [21]. Field personnel is exposed to many high-risk activities and challenging environments. Drilling activities require hoisting and lifting of heavy and sizeable materials. And last but not least, both drilling and production operations involve dealing with inflammable and pressurized hydrocarbons, which require a thorough understanding and strict control of operating procedures.

These safety risks have a direct impact on the work of research teams and require significant efforts. In every project phase, from initial design to field trials, safety is an important factor and each risk should be reduced to a level *as low as reasonable practicable* (*ALARP*) [22]. Risks are related to the design of sensors, as well as to operational aspects. Transport during field trials should be carefully planned, selected and audited. Dedicated safety training should be completed before entering high-risk sites. Prototypes and their packaging should be designed such that handling can be done in a safe manner.

The most important safety aspect in the design of fibre-optic down-hole sensors is related to leak paths. They are a potential risk for fibre-optic sensors since they rely on cables to communicate to surface. If improperly designed and installed, cables can become a leak path from pressurized, hydrocarbon-carrying, down-hole zones to surface. Cable constructions and deployment procedures are carefully designed to avoid these risks. The data obtained by such sensors can instead be used to enhance safety by providing information about the subsurface conditions and the integrity of the well. As such, down-hole sensing adds to Shell's strong drive towards zero incidents.

2.4. Reliability

Sensors are installed in an environment of heavy steel pipes and equally massive tools. The contrast could not be bigger with the tiny and fragile optical fibres that form the basis of accurate down-hole fibre-optic sensors. During *running-in-hole*, the sensors are continuously subjected to crushing and friction forces between casing and tubing, or between hole wall and casing. For this reason, the optical fibres in down-hole cables are packaged in multiple concentric metal tubes, as illustrated in Section 1.3. If point sensors are included in the cable, the packaging of these sensors has to be equally sturdy. However, the sheer difference in weight and scale between sensor components and other well construction components makes foolproof design an illusion. Drill crews are typically not well equipped nor trained to handle sensitive equipment, and hence a sufficiently ruggedized design needs to be combined with extensive supervision and training to avoid damage during installation.

If successfully installed, sensors have to operate with – usually – high accuracy under harsh conditions: pressure, temperature and chemicals, as discussed in Section 2.2. Well completions typically last from five years up to the lifetime of the well. If sensors are deployed behind casing, retrieval is impossible and hence sensors have to last the entire lifetime of the well, or need to be designed for a specific task where the lifetime is known. Wells can be in production for more than forty years [23].

This combination of rough deployment conditions, harsh environmental conditions and high accuracy is not found in many other industries. For example, the aircraft industry, where similar sensing technology is deployed, relies on equipment inspection and maintenance after each flight, which is a huge contrast with up to forty years of operations without service. The space industry

provides us with probably the best analogy to upstream operating conditions [24], with harsh conditions both during deployment and during service life, but also virtually no possibility for service during the equipment's lifetime. However, one big difference between both industries is the scale of commercial operations: while, e.g., a limited number of satellites is launched every year, approximately 100,000 wells are drilled by oil companies each year [25]. Summarizing, the oil and gas industry provides an almost unique challenge to the level of *reliability* required of each sensor design, combined with cost constraints driven by the scale of deployments.

2.5. Design process

To create suitable sensors, requirements with respect to reliability, operating range, safety and accuracy have to be considered, incorporated and tested during the *design process*. Starting from an actual challenge in an operating environment (an *application*), a typical design process consists of the following steps: defining a list of requirements, executing research and market studies to find potential solutions, selecting the best options, and further mature and test these options towards a deployable prototype [26]. In Shell, such process involves a range of *stakeholders*, as illustrated in Figure 2.4, which especially has major implications for the definition of requirements and the relation with contractors.

A major – and crucial – challenge is the definition of a *list of requirements*. Shell consists of a heterogeneous group of *Operating Units* (*OU*s), each of them operating fields they need to explore and produce differently as local environmental conditions, as well as political and economical backgrounds vary. Differences in operating environments result in a range of applications for a

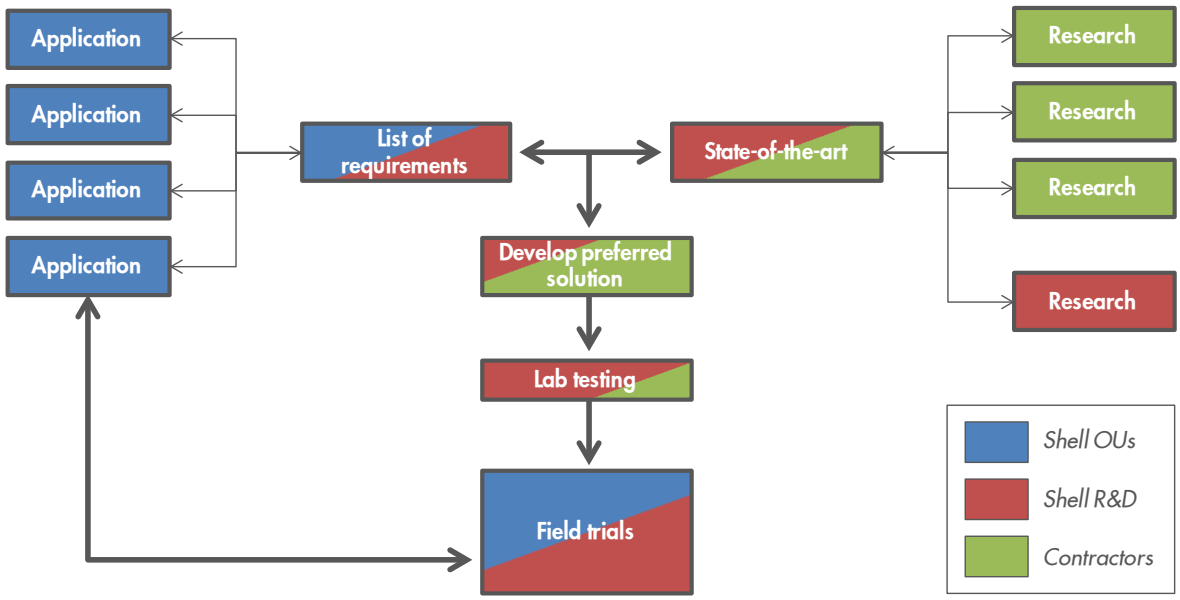

Figure 2.4: **Typical design process in fibre-optics product development in Shell. Each application refers to an actual challenge found within the operating environment of one or more Shell Operating Units, and can range from a relatively low-risk application of such technology (often used as a 'demonstrator') towards more complex applications. Primary involvement from Shell OUs is indicated in blue and contractors in green. My own involvement typically is in 'Shell R&D' activities, indicated in red.**

sensor which measures a certain parameter. Inherently, such range of applications results in a variety of requirements for such sensor. To keep development efforts focused and hence improve the *probability of success*, selecting the right applications up-front is a challenging and important step. This process is centred in Shell R&D. The selection of requirements is ideally converging and benefits from synergies between different applications. However, sometimes it is beneficial to simply focus on one application which represents significant business value. Further development of additional applications can then build on the momentum gained by the realization of a first application. Especially because of the different strategies possible, the step of defining the list of requirements is a crucial part in the design process.

As introduced in Section 1.5, Shell is an *operator*. As such, new technology is needed to be able to operate assets more efficiently, and to obtain and maintain a license-to-operate. While technology is needed to run the business, most technical aspects are sourced in from specialised companies and institutes who engineer and manufacture the technologies used. Maintaining all these technical functions is not Shell's core business. Not many industries showcase the same characteristic combination of depending heavily on technology to optimise production on the one hand, while outsourcing the majority of technical services on the other hand. Probably the best comparison would be airlines, which also rely heavily on technology, e.g., aircraft, but do not manufacture them themselves. A key difference, however, is Shell's substantial involvement with development of new technologies, while airlines are clearly much less actively involved with the development of new airplanes.

In the case of fibre-optic sensors, Shell does not intend to create their own fibre-optics interrogators or even production of fibre-optic components. The aim is to stimulate the fibre-optic sensing industry to come up with an appropriate solution for the applications in question. To do this, some research is done in-house to create an understanding of the important parameters. Meanwhile, potentially suitable base technologies are also being investigated in the active community of the fibre-optic sensing or oilfield service industries. An important step is assessing the *state-of-art*, which helps in determining focus for further development and partnership. Then, detailed development and engineering is done together with – and often largely by – *contractors* that have developed suitable technologies. In parallel, application engineering is largely done in-house, e.g., to build suitable analysis tools to convert the measured data into useful information, or to integrate the sensing system into daily operations using standardised workflows. The manufacturer then often develops the solution further into prototypes that Shell R&D tests, first in the lab, but quickly after that in field trials to ensure suitability for a particular application in relevant OUs.

2.6. Deployment

The final aim of technology development in Shell is the *commercial* use in Shell Operating Units. This stage is called *deployment*. Before a technology is ready for deployment, a range of steps to understand, test and validate the approach are undertaken (Figure 2.4), ranging from modelling, via lab tests to field trials. In a *field trial*, the technology is applied in a real operational environment.

Field trials are elaborate because of the scale of typical oilfield operations. Although OUs are generally stimulating new technology with the aim to improve future operations, their main short-term goal is to minimize down-time in their operations and hence sustain daily production. This introduces many limitations to the implementation of a new technology, which is often only a small aspect in the complex operations involved in, e.g., drilling and completing a well. Because

of these boundary conditions, field trials often take a significant amount of time and effort to plan and execute.

Although lab testing is easier, cheaper and faster to execute, there are limits to its usefulness. After optimizing the design and creating an understanding of its performance from lab tests, it is very hard to simulate all conditions that might occur in a field installation. Scales, forces and complexity of the parameter space are significantly different between them. Despite the effort involved with field trials, they are therefore crucial to test and validate a new technology and should be a vital part of the research cycle for the exploration & production industry.

Summarizing, the position of fibre-optics R&D in Shell is at the heart of the design process, involving both component-level *expertise* as well as *system engineering* aspects. Expertise is nurtured through detailed research of key issues as well as involvement in field trials to validate a technology in practice. System-level management of the design process, from the definition of requirements all the way to final testing, is crucial to ensure that integration between various parties and sub-components results in an integral sensing system. The described development efforts are aimed towards commercial deployment of such sensing technology in the regular operations of the Operating Units.

3. Interrogation unit for multi-point sensors

To enable permanent deployment of Quasi Distributed Pressure Sensing for field-wide monitoring, a low-cost interrogation unit is needed. Harsh operating environments translate into high operating temperatures for the unit. An interrogation scheme has been developed fulfilling all requirements and a prototype has been successfully tested.

3.1. Quasi Distributed Pressure Sensing

A *fibre Bragg grating* (*FBG*), as initially introduced in Section 1.4, is a periodic variation of the refractive index of the core of an optical fibre in its axial direction. Sketched schematically in Figure 3.1, the essential feature of such a grating is reflection of light at a specific wavelength. This wavelength is directly proportional to the spatial period of the variation in refractive index. The spatial period is fundamentally influenced by both axial and radial strain [27]. Axial strain is the dominant effect, stretching the fibre and thereby enlarging the grating's spatial period. In this way, the wavelength becomes a function of the exerted strain.

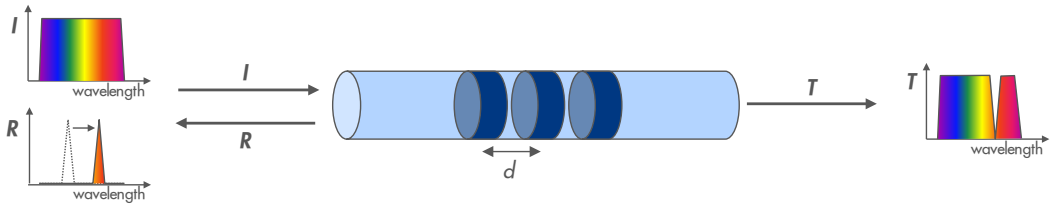

Figure 3.1: **The fibre Bragg grating (FBG) reflects light in a narrow spectral range with a central wavelength defined by a grating period *d*. This schematic view only displays the core of the fibre. Under tensile strain conditions, the central wavelength increases (as displayed), while under compression it shifts towards a shorter one. Here, *I*, *R* and *T* are the incoming, reflected and transmitted intensity, respectively.**

Hence, FBGs can be used as sensors to measure a range of parameters by converting them into strain. Examples include measurement of *temperature*, *pressure* and *chemicals* concentration (Figure 3.2), but also static *strain* in structures or acoustic noise as a result of fluid *flow*. Multiple sensors can be incorporated onto a single optical fibre by, e.g., wavelength division multiplexing (WDM), using FBGs with different peak wavelengths for each of the sensors.

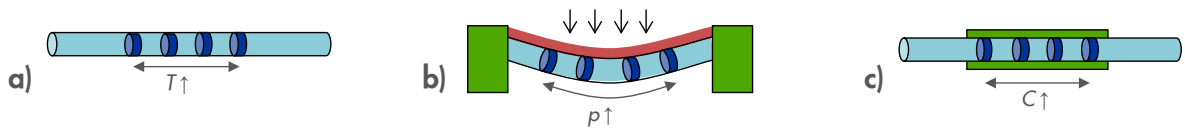

Figure 3.2: **FBG sensors can be used to measure a range of parameters by converting them into strain: (a) An increase in temperature *T* causes expansion of the fibre material and thereby of the grating period. (b) Pressure *p* can be determined by measuring the axial strain induced in a fibre attached to a deformed membrane. (c) FBGs can be coated with specific polymers, which induce a strain when reacting with specific chemicals as a result of an increase in concentration *C* of that particular substance.**

Of particular interest here is the concept of a pressure sensor as depicted in Figure 3.2b. By attaching a FBG to a membrane, the FBG will sense strain as a result of fluid pressure deflecting the membrane. Based on this pressure sensor design, and incorporating multiplexing as described above, Shell, together with industry partners, is developing *Quasi Distributed Pressure Sensing* (*QDPS*): a multi-point and cost-effective sensor array for permanent down-hole pressure measurements.

Monitoring the thickness and depth of the oil layer in a reservoir is an application for which such QDPS system is especially suitable [28]. Gas, oil and water have, in increasing order, different densities, and hence these fluids will vertically separate accordingly under steady-state conditions. An array of pressure sensors can be deployed in a borehole to monitor the hydrostatic pressure profile as a function of depth as depicted in Figure 3.3a. The intersects between gas-oil and oil-water gradients define the extent of the oil layer. The fluid-contacts in the well can in principle be related to the fluid-contacts in the reservoir. If this relation is known, the extent of the oil layer in the reservoir can be determined from measuring the extent of the oil layer in the well. A first version of a QDPS sensor array has been deployed in a field trial and was used to monitor the pressure profile for a duration of more than half a year. A numerical simulation of the thickness-variation of the oil-rim over time as displayed in Figure 3.3b was executed to demonstrate the expected tracking accuracy. Such variations can be the result of changes in, e.g., production rates or water injection rates (to maintain reservoir pressure and hence optimise production). Thin oil-rims increase the risk of producing water rather than oil. Hence, pressure monitoring by means of a QDPS system can provide a basis for feedback control to optimise hydrocarbon production. An example would be by gas- or water-injection to control the oil-rim and drive it towards the producing wells.

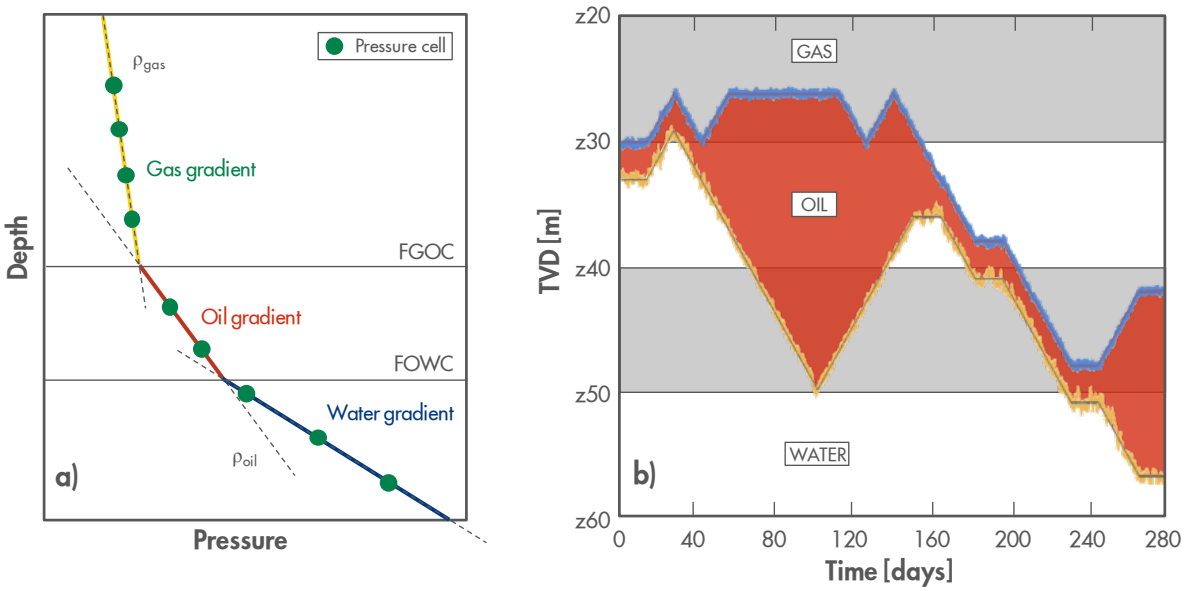

Figure 3.3: **(a) Measurement principle for oil-rim monitoring. The gas-oil contact (FGOC) and the oil-water contact (FOWC) are derived from multiple measurements of the hydrostatic pressure and the fluid densities. (b) Automated interpretation of simulated pressure data (with pressure-noise added), tracking substantial variations in the depth of the oil-water contact over time. Note that the depth is expressed in True Vertical Depth (TVD), which is independent of the deviation of the well trajectory. TVD is offset by an unspecified depth *z*.**

A wide range of other applications for quasi-distributed sensing systems exist. A market study was conducted to identify a common set of system requirements, including pressure, temperature and chemical sensing applications [29]. The *oil-rim monitoring* application as described above is, within the selected range of applications, representative of a challenging application in terms of the high precision required. One of the other main insights from this study is that most of the envisioned low-cost applications only require the measurement of a limited number of sensors and a significantly limited acquisition rate. This insight will prove itself very useful, as we will see in the next sections.

FBG-based sensors currently under development have significant potential to meet the established requirements. However, a sensing system does not only consist of the sensors themselves, but also requires an interrogation unit to read out one or more sensors. As will be discussed further in the next section, there is still a gap in the specifications of current commercially-available interrogation units.

3.2. Requirements interrogation unit

Translating system requirements for the complete sensor system – based on the earlier discussed market study – into requirements for the interrogation unit, leads to the *user-requirements* as stated in Table 3.1 [30].

To enable large-scale implementation of permanent distributed sensing systems, and especially QDPS systems, the interrogation units should be *cost-effective*, both for initial purchase as for maintenance during operation. Examples of important deployment locations are large, scattered oilfields in desert environments. A suitable interrogator unit should be *robust* enough to be placed just next to the well in the open air and should have *low power consumption*. *Ambient temperatures* in such environments can reach values up to 60°C. Other possible deployment locations would be below sea level or even in a down-hole environment.

Table 3.1: User-requirements for a low-cost high-temperature FBG interrogation unit. Repeatability and absolute accuracy are expressed in picometre (pm, 10^{-12} m).

Costs target	**Priority**	
Unit cost	1	< US$8,000 for series production
Environmental target specifications		
Max. ambient temperature	2	60°C
Robustness	3	outdoor, sand, field installation
Power	4	< 100 W
Communication	5	wired to computer or RTU
Max. humidity	5	82%
Application target specifications		
Repeatability	1	≤ 2 pm
Absolute accuracy	1	≤ 4 pm
Number of sensors (wavelength range)	2	≥ 6 (30 nm)
Channels	2	≥ 2
Acquisition time	3	≤ 10 s

Despite the aim of low-cost and high-temperature suitability, the measurement precision is crucial for most identified applications. The peak wavelength values correspond to measurement quantities, like pressure or temperature. A typical FBG sensor response is 20 pm/bar for in-well pressure sensors and 12 pm/°C for temperature sensors.

Repeated measurements of the same FBG peak wavelength under the same conditions will typically show a spread with a normal distribution. The *repeatability* is the standard deviation (1σ) of such a normal distribution [32]. Interesting to note is that the repeatability can be several orders of magnitude better than the interrogator's hardware resolution, since the peak wavelength is the result of a multi-point fit of the, typically, Gaussian shape of a FBG reflection peak [29]. Also note that repeatability and precision are sometimes used in the same context, whereas repeatability is preferred by standards [32] and as such typically used in interrogator datasheets.

The *absolute accuracy* is the sum of the temperature stability and the average deviation from the "real" peak wavelength value. Most important is the temperature stability: the variation in measurements of a constant FBG peak wavelength due to varying the interrogator's temperature over its operating temperature range.

Comparing typical commercial specifications to the user-requirements stated in Table 3.1, indicates that the main challenge is to improve the robustness while significantly reducing the price. The reduced *acquisition rate* and *wavelength range* offer opportunities for a trade-off to realise this challenge. Interesting opportunities are offered by recent developments in the optical telecommunications industry towards lower-cost, more accurate and more compact components.

Since Shell is not aiming at producing suitable interrogation units themselves, the objective is to stimulate the commercial realisation of a suitable interrogation unit. A project was initiated to facilitate commercial realisation by suggesting feasible ideas through its deliverables: knowledge and a prototype of a low-cost high-temperature FBG interrogation scheme.

As such, the **objective** is the *development of a low-cost high-temperature FBG interrogation unit.*

3.3. Selection of interrogation scheme

In order to develop an interrogation unit fulfilling the user-requirements of Table 3.1, a structured design process was followed as represented in Figure 3.4. As outlined in the previous sections, the project started off with a market survey of applications within Shell and present state-of-the-art interrogation technology. Based on the resulting necessary and feasible user-requirements, the next step entails evaluation of several design approaches. Eventually this feeds into selection of a suitable interrogation scheme for further development into a stand-alone prototype.

Figure 3.4: Flow-chart of the subsequent phases in the project and respective milestones and deliverables.

An interrogation unit to read out one or more FBG sensors, is mostly an integrated combination of light source, detector and analysis module. The light source sends light into the fibre. A detector then analyses the reflected light to find the peak reflection(s) and determine its wavelength(s).

A literature study identified three concepts, based on a tuneable laser, tuneable filter, and spectrometer, respectively. Initial design considerations resulted in the selection of two schemes for further experimental evaluation. Only an overview of the evaluation study will be provided here. The selected interrogation scheme will be discussed in more detail in Section 3.4.

The *tuneable laser based interrogation scheme* employs a tuneable laser to step through the wavelength range, while a photo-detector measures the reflected intensity for each wavelength step. This setup is conceptually very interesting because of its modular approach and low costs. On the other hand, the tuneable laser suffers from reliability issues, the tuning step size of 200 pm is rather coarse and the temperature stabilised FBG calibration reference is not rugged over the full temperature range yet. Further improvement of these issues, without significant cost increase, would result in a potentially interesting option for the future.

The *tuneable filter based interrogation scheme* is based on a combination of a broadband light source and a tuneable filter, which sweeps the wavelength to which the photo-detector is exposed. This concept presently already offers an extremely high sweep resolution due to continuous tuneable filter tuning. An extensive multi-point calibration simultaneously for each FBG measurement guarantees the accuracy under all conditions.

Further details of the evaluation study can be found in [29]. Eventually, the *tuneable filter based interrogation scheme* was selected for further development into a stand-alone prototype.

3.4. Tuneable filter based interrogator prototype

Figure 3.5 schematically displays the *tuneable filter based interrogation scheme* in more detail [30]. It uses a Super Luminescent Light Emitting Diode (SLED) broadband light source in combination with a tuneable filter to identify the wavelength response of both a calibration path and an interrogation path. The interrogation path uses a circulator to send light into the FBGs and to direct the reflected light into a photo-detector (#1). The calibration is done in parallel by splitting part of the light into the calibration path, which measures the absorption spectrum of a gas cell with a second photo-detector (#2). An optical switch is used to enable measurements of two optical fibres, i.e. channels, with FBG sensors.

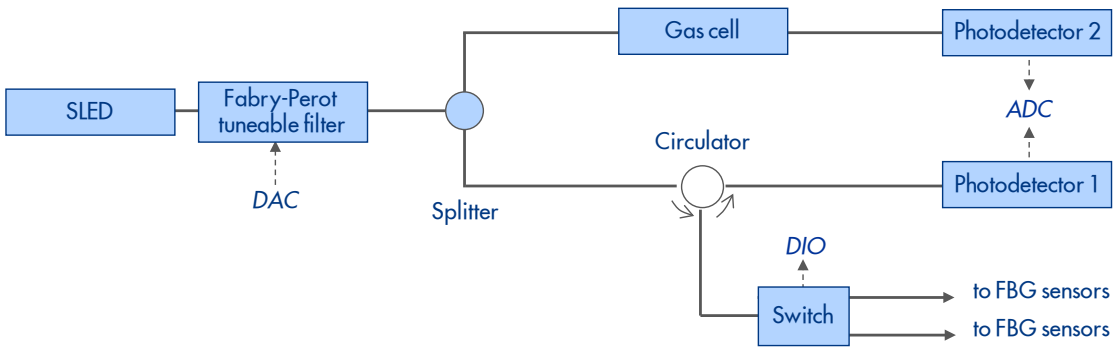

Figure 3.5: Schematic representation of the optical assembly for the tuneable filter based interrogation scheme. The figure also displays analogue and digital control and measurement instances.

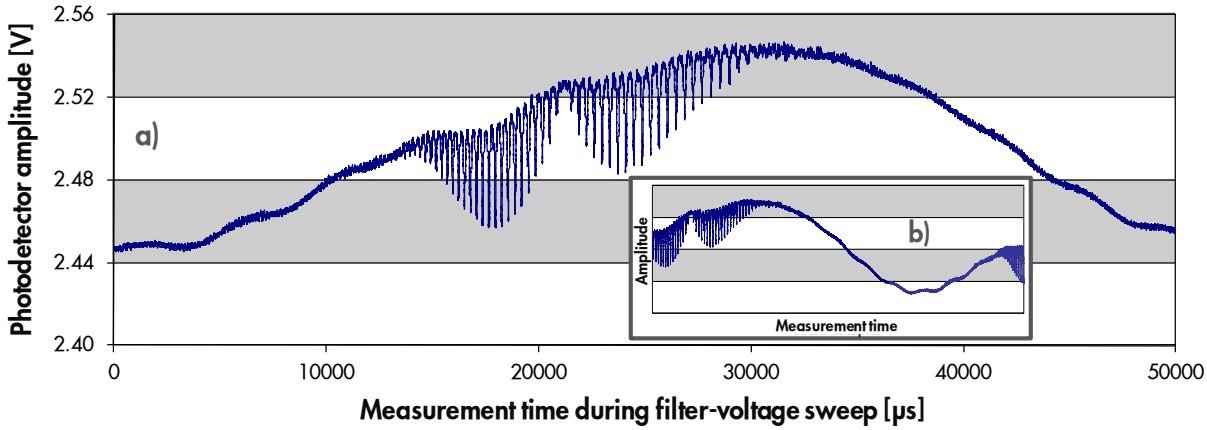

Figure 3.6: **Spectral measurement of molecular absorption lines of hydrogen cyanide ($H^{13}CN$) in a gas cell at a filling pressure of 100 Torr, as measured by recording the transmission through the cell while sweeping the tuneable filter, at (a) room temperature and (b) at a temperature of 70°C.**

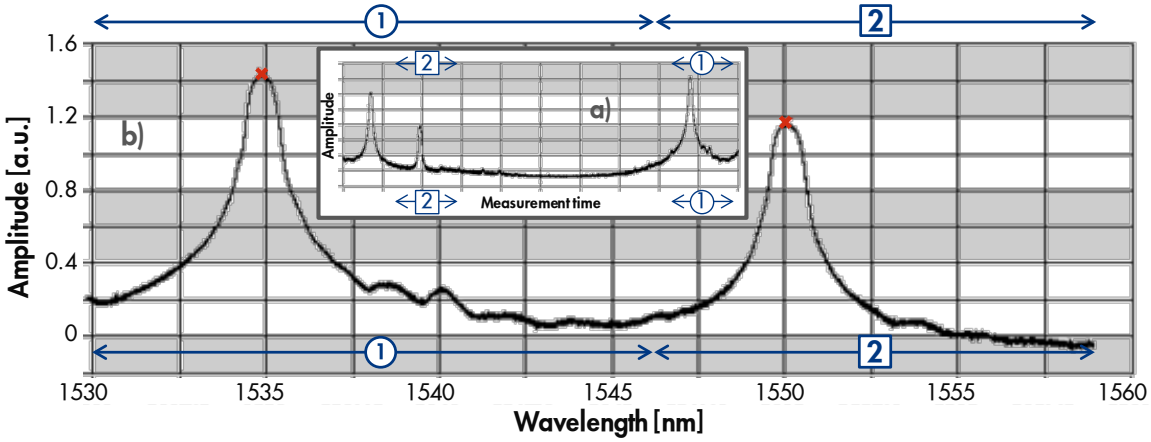

Figure 3.7: **(a) Raw photo-detector recording of the reflected intensity from a fibre with two FBGs while sweeping the tuneable filter at elevated temperature. By using the gas cell calibration, the optimal wavelength range for each part of the spectrum can be selected (indicated by number 1 and 2). (b) These wavelength ranges can be combined into one continuous and calibrated spectral response, and the peak reflection wavelength of each FBG can be determined (red crosses). Note that some part of the sweeped range in (a) is not used to construct (b), because no gas cell calibration peaks are available in the related wavelength range.**

To avoid pollution with e.g. desert sand, a fan-less thermodynamic approach was chosen. An extensive market survey considering products from more than 40 suppliers was conducted to guarantee sufficiently low wavelength-dependencies and temperature-dependencies. To minimize the eventual unit cost of the interrogation unit, only volume-produced optical components from the telecommunications industry were considered. Based on extensive tests up to ambient temperatures of 70°C, components from 10 suppliers were selected for use in the prototype.

Nonetheless, some components unavoidably have large temperature-dependencies. The tuneable filter exhibits the largest temperature-dependency: for an identical control voltage, the filter's transmission wavelength is different for different temperatures. Accurate temperature-stabilisation of such components would be a possibility, however, would require an extensive – and expensive – thermodynamic design and hence increase power consumption.

The novelty of our design is the implementation of a fully-automated online wavelength-calibration instead, compensating each measurement for potential temperature influences over the entire wavelength range [31]. A hydrogen cyanide gas cell is especially suited as calibration reference [33]. Figure 3.6a shows the transmission spectrum of such gas cell, measured by a photo-detector while sweeping the tuneable filter through the wavelength range of interest. Clearly visible are the gas cell's multiple molecular absorption lines, uniformly spread over the wavelength range of interest. Each of these lines is extremely stable and well determined, with an inaccuracy of only 0.5 pm due to a collisional shift of the line position over the full temperature range.

The measurement in Figure 3.6a was done at room temperature. Figure 3.6b shows the results of an identical voltage sweep of the tuneable filter, but at a temperature of 70°C. These results show that the tuneable filter's relation between control voltage and transmission wavelength is indeed highly temperature-dependent. Furthermore, Figure 3.6b also shows that parts of the gas cell spectrum are measured twice. This is a result of the periodic transmission peaks of the Fabry-Perot filter used [34]. Although at first sight this duplication seems to complicate the interpretation of the measurements, it is actually crucial to guarantee that all parts of the spectrum are eventually measured.

In order to exploit these gas cell measurements for calibrating the parallel FBG measurement, a peak-search algorithm is necessary to detect all gas cell absorption lines and also place them in the right order. Although increased noise levels at elevated temperatures impose a challenge, a reliable algorithm could be developed successfully.

A high-capacity processing unit is required to run the extensive peak-search algorithm used for the online multi-point calibration. For this purpose, an integrated data acquisition and processing unit was selected. This – entirely autonomous – unit is the basis for all control, measurement and data processing tasks. Capabilities include voltage drive and measurement at rates of at least 100,000 samples per second, as is necessary to realise the high optical resolution of approximately 1 pm. Extensive testing showed that this processing unit fulfils the requirements up to ambient temperatures of 70°C and potentially beyond.

Figure 3.7 demonstrates application of the calibration results to an FBG sensor measurement with two FBGs in series in one fibre. Figure 3.7b shows the measurement over time during a sweep of the tuneable filter. This measurement is taken at an elevated operating temperature. Analogous to the gas cell measurement in Figure 3.6b, the wavelength spectrum is not centred

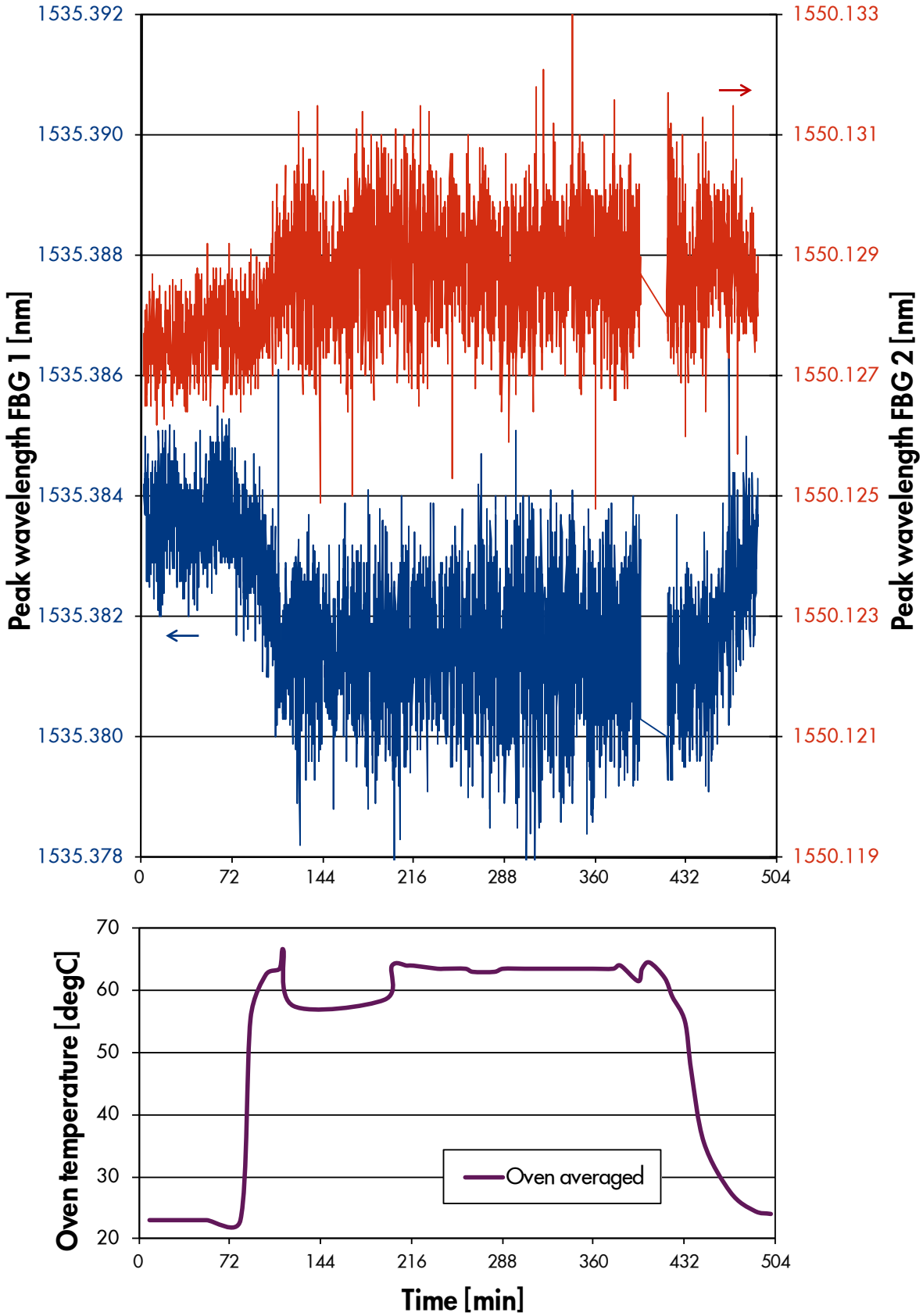

Figure 3.8: **Peak wavelength of two temperature stabilised FBGs, while the interrogator is placed in an oven and the oven temperature is varied between room temperature and more than 60°C. The grid lines in the upper figure are spaced at 2 pm.**

and parts of the spectrum are duplicated. Using the wavelength-calibration obtained from the simultaneous gas cell measurement, wavelengths can be attributed to measurement points and partial spectra can be combined. In this way, as illustrated in Figure 3.7a, one continuous – and calibrated – spectral response can be assembled. This spectrum can be used to determine the peak reflection wavelength of each FBG, now being accurately calibrated.

Summarizing, this combination of a low-cost optical design in combination with a continuous referencing methodology enables a multi-point calibration in order to guarantee the accuracy of every FBG optical spectrum, at all temperatures and at all times. Validation tests are described in the next section.

3.5. Validation by experimental testing

Figure 3.9 shows the setup used to validate the performance of the interrogator prototype. The interrogation unit was placed in an oven to enable testing over a temperature range from room temperature up to 70°C. The interrogation unit was connected to a pair of FBGs and to a PC, which were all placed outside of the oven. To guarantee constant FBG peaks, temperature stabilised FBGs were used.

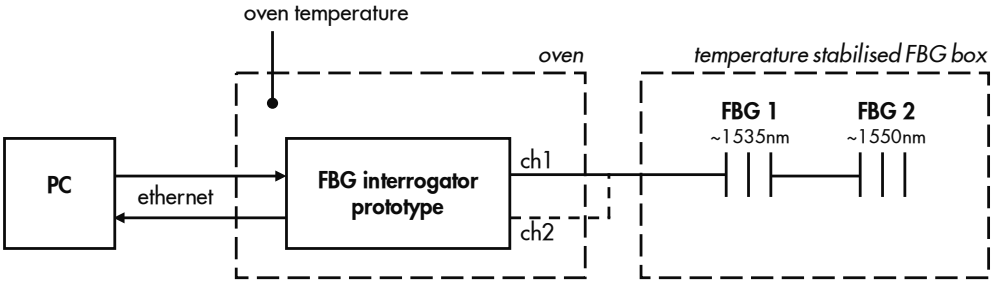

Figure 3.9: Schematic overview of the setup used for testing the FBG interrogator prototype.

The SLED broadband light source is the bottleneck component for high-temperature operation. Due to self-heating and a case temperature rating of 70°C maximum, its over-temperature protection is activated **above 63°C ambient temperature**.

The average acquisition rate is **8 seconds** for all sensors in one channel, which is mainly caused by the time required for the peak-search algorithm. The acquisition rate is well in line with the maximum requirement of 10 seconds.

The most important test result is displayed in Figure 3.8, showing the peak wavelengths of two temperature stabilised FBGs while the temperature of the oven with the interrogation unit was varied between room temperature and more than 60°C.

The repeatability is the standard deviation in repeated measurements of the same constant FBG peak at room temperature. From the data in Figure 3.8 it can be concluded that the **repeatability** is better than **0.6 pm**. This is a factor two better than most commercial high-end interrogators.

The maximum difference between the average measured wavelength and the calibrated peak wavelength value of the respective temperature stabilised FBG is 1.0 pm. This is the absolute accuracy of the interrogator at room temperature. For increasing temperatures, some residual temperature dependence in one or more optical components is seen. This could be investigated further, although the temperature dependency is already sufficiently reduced to a maximum of 2

pm. Including the repeatability, this results in a temperature stability of 2.5 pm. Adding the absolute accuracy at room temperature to the temperature stability, results in an **absolute accuracy** over the full temperature range better than **3.5 pm**. This fulfils the absolute accuracy requirement of 4 pm.

3.6. Conclusions

Summarizing, this Chapter reported on the development of a low-cost high-temperature interrogation unit for fibre Bragg gratings. A market survey of state-of-the-art FBG interrogation technologies with a focus on oil- and gas-well applications resulted in a list of user-requirements (see Table 3.2). The evaluation of various interrogation schemes led to the selection of the *tuneable filter based interrogation scheme* for further development into a stand-alone prototype.

The *tuneable filter based interrogation scheme* presently already offers an extreme high sweep resolution due to the continuous tuneable filter tuning. Accepting the temperature-dependencies of low-cost components, an extensive multi-point calibration simultaneously to each FBG measurement guarantees the required accuracy under all conditions.

Laboratory tests, at room temperature and at various elevated temperatures, showed that the prototype fulfils all user-requirements. The repeatability of 0.6 pm is a factor two better than most commercial high-end units. The temperature stability is better than 2.5 pm over a temperature range from 20°C up to 63°C. The absolute accuracy of 3.5 pm is also well below the requirement, as summarised in Table 3.2.

Hence it can be stated that all requirements – financially and technically – were fulfilled. This result confirms the feasibility of low-cost Quasi Distributed Pressure Sensing systems and their potential for commercial-scale realization. In Chapter 4 we discuss the implementation path towards field-wide deployment, including the design of a test programme for evaluation of commercially-introduced interrogation units.

Table 3.2: Final test results for the tuneable filter based stand-alone prototype, compared to user-requirements. Specifications marked with "n.i." were not (conclusively) investigated. The unit cost for the tuneable filter based interrogation scheme is based on estimated volume-pricing for the required components.

Costs target	**User-requirements**	**Tuneable filter based prototype**
Unit cost	< US$8,000	US$7,000
Environmental target specifications		
Max. ambient temperature	60°C	63°C
Robustness	field installation, sand	fanless, metal enclosure
Power	< 100 W	< 40 W
Communication	wired to PC or RTU	Ethernet
Max. humidity	82 %	n.i.
Application target specifications		
Repeatability	≤ 2 pm	0.6 pm
Absolute accuracy	≤ 4 pm	< 3.5 pm
Number of sensors	≥ 6 (30 nm)	6 (31 nm)
Channels	≥ 2	2
Acquisition time	≤ 10 s	8 s

4. Towards deployment of Quasi Distributed Pressure Sensing

In order to enable initial field trials of Quasi Distributed Pressure Sensing (QDPS) systems, standard lab-grade interrogation units had to be used in combination with a thermal switch to prevent operation above the maximum operating temperature. While sensor development continues, a test programme has been set-up to evaluate the high-temperature performance of newly developed interrogation units.

4.1. Development cycle

The realisation of a low-cost *Quasi Distributed Pressure Sensing* (QDPS) system requires development of a fibre-optic pressure sensor that can compete on specification, cascadability, price and reliability against most other (and much more expensive) down-hole sensors on the market. The development path, together with an industry partner, eventually led to a field trial of the first version of such sensors in 2008. An array of nine sensors was installed and pressure readings were acquired for almost a year. The results proved, at a significantly reduced cost, its suitability for down-hole pressure measurements. Further improvements to optimise long-term stability and reliability resulted in a 'Mark II' sensor design, which was installed at the end of 2012 for a second field trial [35].

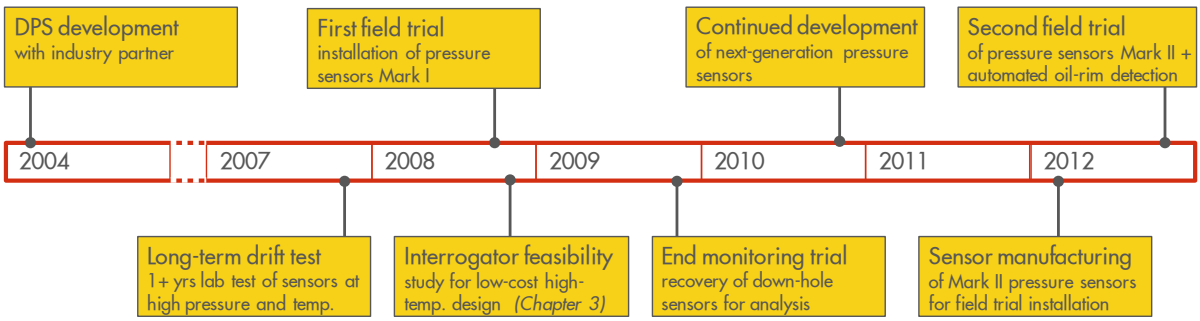

Figure 4.1: Milestone events in QDPS development timeline.

The extent of the development cycle as described above, and summarized in Figure 4.1, is a good illustration of a typical design process in Shell as earlier introduced in Section 2.5. Field trials are essential to evaluate performance of new or modified designs, especially in view of the diverse parameter-space and extreme length-scales typical of down-hole environments, as introduced in Chapter 2. One step further, integration of a new technology into the daily operations of each operating unit should also be part of the system design. The aim is to provide actionable information to the engineer. In this particular case, acquired pressure data has to be transported to the office, stored and finally interpreted. All these steps have to be integrated in the operating unit's data management system, and most importantly, should provide an automated way of interpretation of the data [36]. For *oil-rim monitoring* (Section 3.1) this means that, rather than, e.g., looking at pressure data intermittently downloaded onto a USB drive, the interpreted position of oil-water and gas-oil contacts should be made available in the company-wide online database.

Field-wide deployment can only start after the prolonged field trial campaign and sensor development phase have been concluded. Since more robust and lower-cost interrogation units

are especially an enabler for such larger-scale deployment, development of interrogation units has so far been limited to a study to confirm the feasibility of suitable interrogation units (the topic of Chapter 3). Now that the project has progressed further towards deployment, the need for such interrogation units becomes increasingly relevant. The aim is to encourage vendors to provide suitable units through a combination of: generating suitable interrogation concepts within Shell (Chapter 3), sharing such concepts with the industry, as well as evaluating commercially-available candidate interrogation units.

4.2. Interrogation units in initial field trials

The first two field trials of QDPS systems for oil-rim monitoring have been executed in an oil-field in a desert environment. Figure 4.2 shows the instrument cabinet installed next to the well. Due to the surface extent of such oil-fields, a power grid and wired data network is typically not available. Hence, this installation includes solar cells and a wireless communications link.

Note the large size of the instrument cabinet. Due to the unavailability of interrogators that can withstand high operating temperatures, lab-grade interrogation units have been deployed. The enclosure has been designed such that some shade is provided and hence reduce the temperature to which the interrogation unit is exposed. Nevertheless, a temperature control had to be incorporated to switch the unit off at higher temperatures to avoid damage due to high temperatures.

This is undesirable since data is lost when temperatures are high, which could include a significant part of the day, especially in summer in desert environments. Moreover, as we know from Chapter 3, inaccuracies can already occur at temperatures lower than the damage-threshold. Furthermore, the setup includes a separate processing unit. The combination of all such

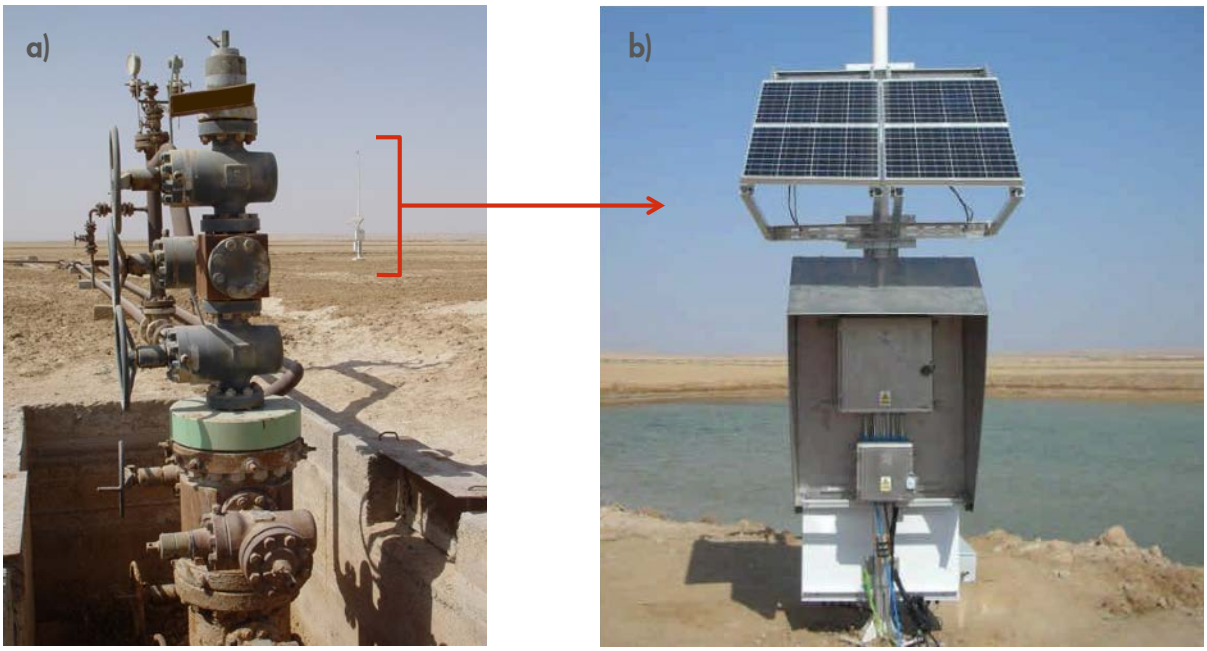

Figure 4.2: Exterior view of the QDPS instrument cabinet, illustrating (a) its position next to a well in a desert environment with minimal infrastructure, and (b) instrument cabinet dimensions to house laboratory-grade components providing an automated acquisition system.

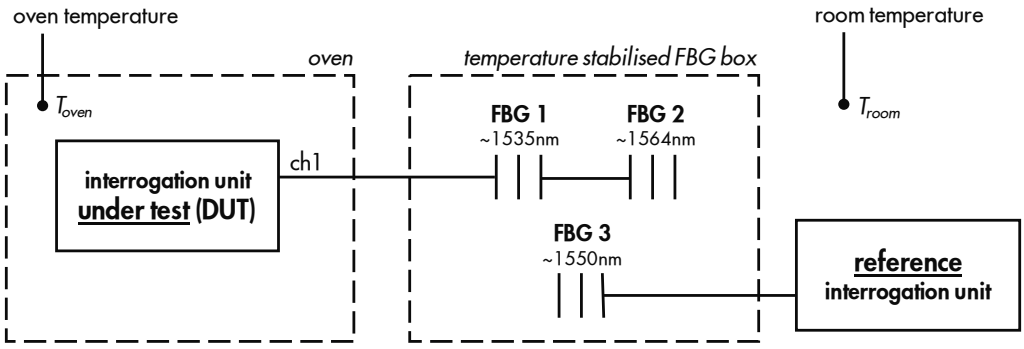

Figure 4.3: Schematic overview of setup used for testing a FBG interrogation unit.

additional components is too costly for field-wide deployment. Therefore, crucial for the success of QDPS field-wide deployment is the availability of more robust and lower-cost interrogators.

4.3. Test setup

In order to allow in-house evaluation of potentially suitable interrogation units, a laboratory setup has been designed and realised. Since the operating temperature range is a crucial parameter for the envisioned applications, the setup focuses on testing the measurement repeatability and absolute accuracy at various operating temperatures and temperature gradients. However, other parameters, such as robustness, power consumption and reliability, are also important criteria in the evaluation process.

The measurement setup generally consists of an oven and a reference measurement, as depicted in Figure 4.3. An oven with a temperature stability of approximately 0.1 K has been used to house the interrogation unit to be tested. The temperature in the oven and in the laboratory has been continuously monitored by calibrated thermometers. To protect the interrogation unit from overheating, a safety switch is installed to disable the oven in case the oven temperature unexpectedly exceeds the interrogation unit's temperature rating [37].

The interrogation unit is connected to two temperature-stabilised FBGs in series. Located outside of the oven, the stability of the temperature-stabilised FBG wavelengths at room temperature is better than 1 pm. Such wavelength stability is sufficient to prove the absolute accuracy requirement of 4 pm (Section 3.2). However, the FBG stability might not be sufficient to evaluate the actual specification: Some laboratory-grade interrogation units have absolute accuracy specifications in the order of 1 to 2 pm (although only at low temperatures).

A third reference FBG connected to an additional interrogation unit at room temperature has been added as an extra reference for possible temperature-dependent variations in the FBGs. All three FBGs are part of the same temperature-stabilised assembly, and as such can be considered to be subject to identical temperature variations. The reference interrogation unit is used to characterise the reference FBG: an industry-standard, accurate Micron-Optics sm125-500 laboratory-grade interrogation unit [38]. The variation in the mean of the reference FBG can be used to correct the other two FBGs, which can possibly improve the accuracy that can be determined.

An interrogation unit is typically subjected to a temperature pattern as plotted in Figure 4.4a. Ideally, interrogation units are tested from room temperature up to 65°C. The interrogation unit-

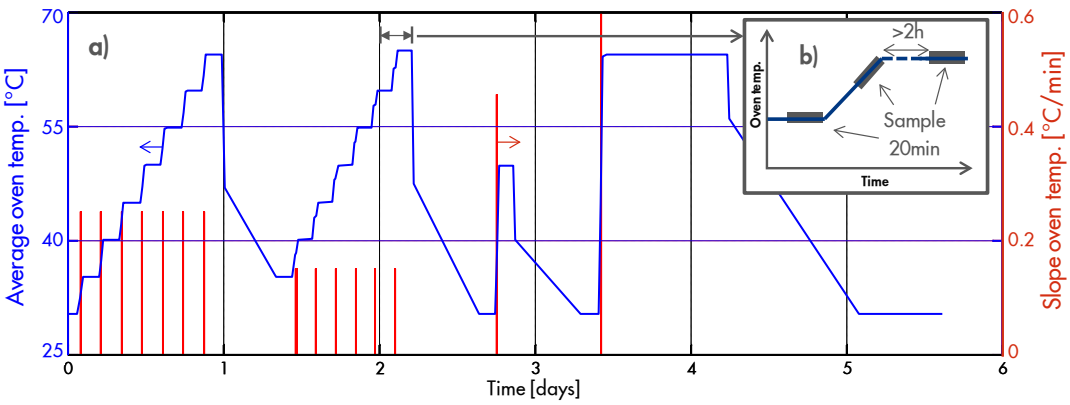

Figure 4.4: **Typical oven temperature sequence for testing an interrogation unit up to a temperature of 65°C. (a) The interrogation unit is tested at various stable intermediate temperatures as well as during temperature ramps. (b) The analysis procedure considers data-sets both during the second half of a temperature ramp (considered worst-case) and after two or more hours of temperature stabilisation (considered best-case).**

under-test (or *device-under-test*: *DUT*) is subjected to low and high temperatures for both short and longer periods of time, in order to get a first impression of longer-term stability. Although proper evaluation of long-term stability requires tests of one or more years, the current six day test programme is designed to facilitate vendors in providing a unit for initial evaluation. Temperature gradients range from 0.15°C/min to 1°C/min. Logging surface temperatures in a typical desert environment indicated that temperature gradients of 0.15°C/min are regularly occurring and 0.25°C/min is a typical higher bound. Higher temperature gradients are added to explore boundaries of the unit's operating envelope.

As illustrated in Figure 4.4b, a wait time of two hours or more has been incorporated before each next temperature change, to allow full stabilisation of the DUT. After stabilisation, data is acquired for 20 minutes at the DUT's optimal sample rate. Such dataset is considered to be representative of best-case performance. Another dataset taken in the second half of each temperature gradient is considered a worst-case, since the DUT is internally also exposed to the temperature gradient and is potentially not stabilised yet. Together, these results provide a good estimate of the practically achievable performance.

To accommodate the interests of commercial interrogation unit manufacturers, the test results obtained so far are *not* presented in this thesis and will only be used for internal evaluation and selection purposes. Each manufacturer is provided with the test results of its own unit, and is at liberty – in case of a positive test – to disclose that its unit is approved to comply with Shell's requirements as set out in Section 3.2.

4.4. Typical test results

In this section, we discuss the performance of the test setup. For this purpose, we present test results of an interrogation unit that was available in our laboratory. The temperature rating of this interrogation unit is limited to 50°C, and is as such not a suitable candidate for low-cost field

deployment. Nevertheless, the results, as displayed in Figure 4.5, are representative of the envisioned test and analysis scheme.

Data has been continuously acquired with a 0.5 Hz measurement rate. Only the average values and the standard deviation in 20-minute datasets – as depicted in Figure 4.4b – have been used for evaluation purposes. Consequently, each dataset contains typically 600 datapoints. The standard deviation given is the standard deviation in each series; the average value has a statistical error that is a factor of $1/\sqrt{600}$ smaller and is negligible in all cases. The data-points are represented by blue dots (average value) and red bars (standard deviation in series) in Figure 4.5.

Reference measurement

Before evaluating the device-under-test, it is crucial to verify the ultimate stability of the temperature-stabilised FBGs and the reference interrogation unit first. Figure 4.5e shows a total room temperature variation of 2°C, which is close to the upper bound of temperature variations in the laboratory. Normal FBGs have a typical temperature sensitivity of 12 pm/°C, which would result in unacceptable wavelength variations up to 24 pm as a result of the variation in room temperature. The FBGs have been actively temperature-stabilised to mitigate this potential error source. Figure 4.5d shows that the remaining wavelength fluctuation is less than 0.5 pm, which is equivalent to a temperature stabilisation as accurate as 0.05°C. This stability is sufficient to evaluate the requirements as set out in Section 3.2.

Since all three FBGs are part of the same temperature-stabilised assembly, the reference FBG can be considered representative of the stability of the other two FBGs. If even better reference stability is required, the temperature-dependent behaviour of the reference FBG can be used to correct the two other FBG measurements for this systematic long term effect in the temperature stabilisation loop. Due to the very small statistical error in the average values, this is a valid procedure.

The repeatability within a measurements series, represented by the maximum value of the standard deviation of all series, is 0.9 pm. This value is consistent with the specifications of the reference interrogation unit. Summarizing, we conclude that both the repeatability and long-term stability of the reference measurement performs as expected and can indeed be used to guarantee the evaluation accuracy to the desired level.

Device-under-test

Using the temperature-dependent behaviour of the reference FBG, any room temperature variations can be excluded from the evaluation of the DUT. We investigate stability over temperature and time as a practical measure for monitoring applications, where mainly variations over time are of importance. We do not worry about absolute calibration. The resulting temperature stability of the interrogation unit under test, represented by the maximum variation in the average values after correction, is 0.8 pm (Figure 4.5a/b). A correction has been applied for the influence of room temperature variations on the FBGs, although in this case the correction is negligible due to the well-performing temperature-stabilisation. The measured temperature stability represents the (minor) correlation between the oven temperature to which the DUT is subjected and the measured wavelengths, as careful inspection of Figure 4.5a and Figure 4.5b indicates. The repeatability, represented by the maximum standard deviation, is 1.4 pm. These results are in line with the specifications of the interrogation unit. However, this

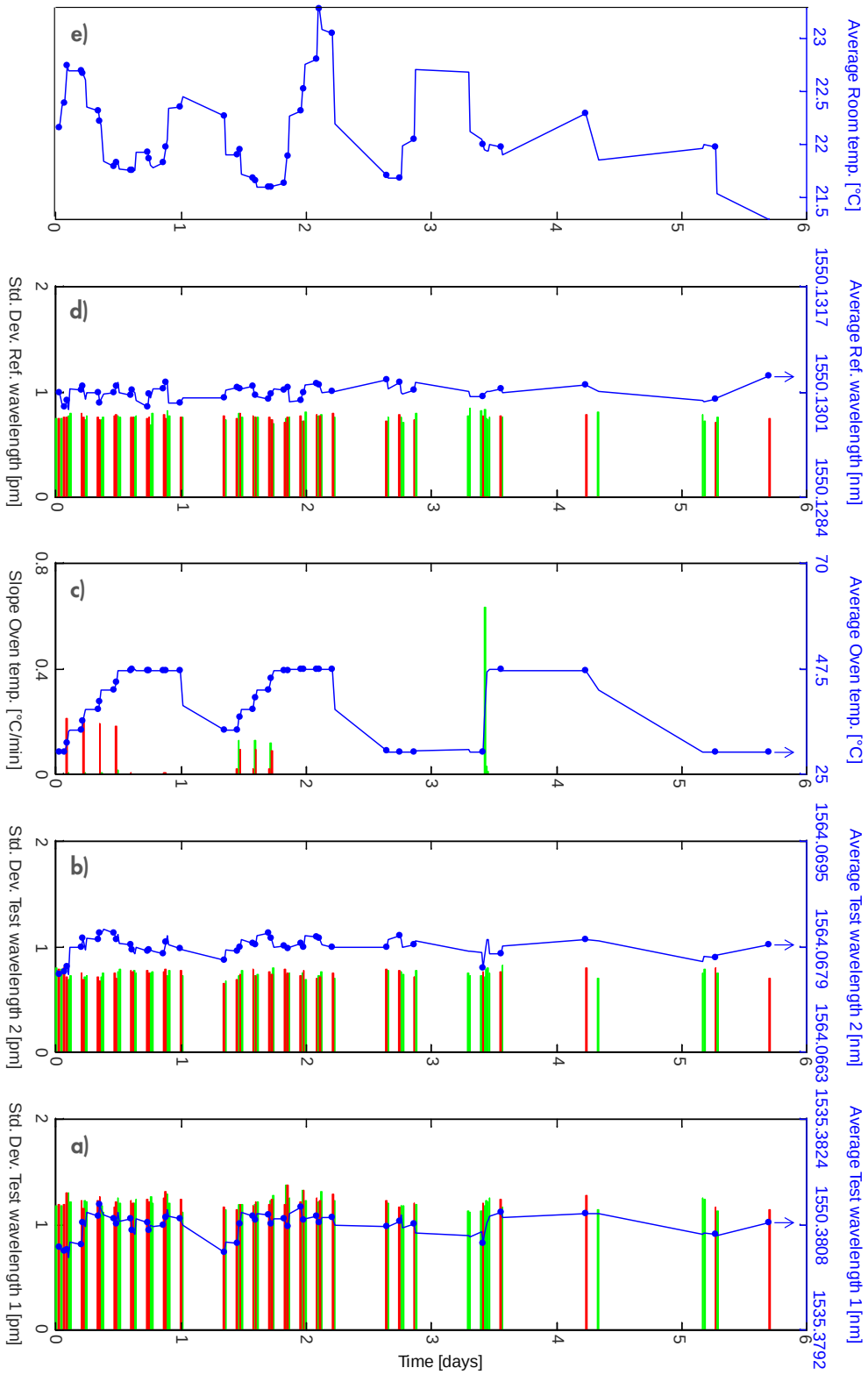

Figure 4.5: **Overview of measurement data for testing of an interrogation unit available in the lab. Measurement steps indicated by blue dots and red bars are used to calculate final results, selected as described in Figure 4.4b. The remaining (intermediate) measurements, not used for the final results, are indicated by green bars. Each data-point represents a 20-minute dataset, in this particular case sampled at 0.5 Hz. Longer-term drift tests have been executed towards the end of the test sequence (between day 4 and 6), resulting in a lower density of data-points.**

interrogation unit is only rated up to 50°C and as such is not a good candidate for the envisioned field applications.

Nevertheless, the results indicate that the setup can be used to accurately characterize the temperature stability and repeatability of interrogation units better than approximately 1 pm. As such, the described testing programme provides a fast and representative tool to evaluate the temperature-performance of interrogation units. Determination of the absolute accuracy is impossible, because it depends on the absolute wavelength calibration of the reference measurement.

4.5. Conclusions

Shell does not intend to produce interrogation units themselves. Instead, the goal is to encourage vendors to provide suitable interrogation units. The first step in support of this goal was an early-stage study of the technical feasibility for the envisioned applications. A next step involves the set-up of a test programme aiming at evaluation of candidate interrogation units. Such evaluation provides a first selection criterion, followed by a more detailed qualification of the integrated system of down-hole FBG sensor and interrogation unit.

Low-cost high-temperature interrogation units are an enabler for field-wide deployment of QDPS systems, but also, e.g., temperature or chemical sensing systems. Only few – potentially suitable – interrogation units have recently either become commercially available or have been announced. The main technical challenges for such interrogation units are: sustain performance at high operating temperatures, combined with a ruggedized packaging to withstand field deployment, and provisions for incorporation in a remote operations network.

5. Delocalized sensing: Distributed Acoustic Sensing

Distributed Acoustic Sensing (DAS) is a fibre-optic sensing technique allowing the measurement of acoustic strains at all positions distributed along the length of an optical fibre. The initial focus of the development was on the interrogation unit, which has been developed together with a third party. The in-company efforts focused on experimental evaluation and understanding of the behaviour of interrogation units, in order to contribute to continuous redefinition of the development focus and applicability base.

5.1. Sensing system

In Chapters 3 and 4, fibre Bragg grating-based (FBG) point sensors are considered. Whereas multiplexing is possible, a dedicated FBG has to be purposely installed at each measurement location. A considerable increase in spatial resolution while simplifying the installation can be provided by true distributed sensing along the entire length of an optical fibre. *Distributed Acoustic Sensing* (*DAS*) is a fibre-optic sensing technique which uses light backscattered from (naturally present) inhomogeneities in a standard telecommunications optical fibre. Analysis of the backscattered signal transforms the fibre into a continuous array of microphones sensitive to dynamic strain imposed on the fibre. By merely installing a cost-effective and small form-factor fibre-optic cable, DAS can provide information on acoustic signals impinging all along the length of the optical fibre. Initial applications in the '80s and '90s mainly involved protection of assets, for example telecommunication cables, railways, or military bases [39]. By burying a fibre-optic cable along the asset's perimeter, acoustic signatures of, e.g., approaching individuals and vehicles can be detected in a simple way without being noticed by the intruder.

Shell was the first energy company to investigate DAS for real-time monitoring of *hydraulic fracturing* operations [40]. Inflow into the well of fluids from tight formations can be increased by means of fractures created by down-hole injection of high-pressure fluids. To optimize the fracturing process, and hence maximize well productivity, monitoring and control of the amount and location of injected fluid is crucial. The first trials were very successful, and were followed by joint product development with one of the DAS manufacturers, *OptaSense* Ltd.. The aim was to develop a range of applications, targeting both geophysical monitoring of the area around a well, as well as monitoring of events in a well, e.g., fluid flow. Flow applications include the hydraulic fracturing application, but also zonal production allocation and performance monitoring of injection wells. The geophysical applications include seismic characterisation *of* the subsurface (for example through *Vertical Seismic Profiling*, Chapter 6) as well as monitoring seismic activity originating *from* the subsurface using artificial sources (*micro-seismic*, Chapter 6). Traditionally geophones are used for these applications, whereas DAS has the potential to provide a distributed and low-cost alternative. The geophysical applications are especially demanding in terms of signal fidelity and repeatability, and have therefore been chosen as a platform for further development of the *interrogation unit*.

The interrogation unit is not the only important component of a distributed sensing system. Such sensing system consists of distinct components as depicted in Figure 5.1: an optical fibre in a sensing cable connected to an interrogation unit, as well as infrastructure and algorithms to analyse the data generated. Infrastructure and algorithms are essential for efficient operational use. The fibre-optic cable is the actual sensor converting a physical stimulus into an optical response, and we will see in Chapter 7 and 8 that significant gain for geophysical applications can

come from the development of improved cable designs. A suitable interrogation unit is the basis for any application, and therefore initial focus was on the development of the interrogation unit and optimisation of the interaction of light pulses with the optical fibre. OptaSense was responsible for development of the interrogation unit. Shell's efforts concentrated on the evaluation of enhanced prototypes, to understand the behaviour of interrogation units and aid in continuous redefinition of the development focus and applicability base. This Chapter will provide an introduction to the DAS concept and the road towards important improvements in the interrogation scheme.

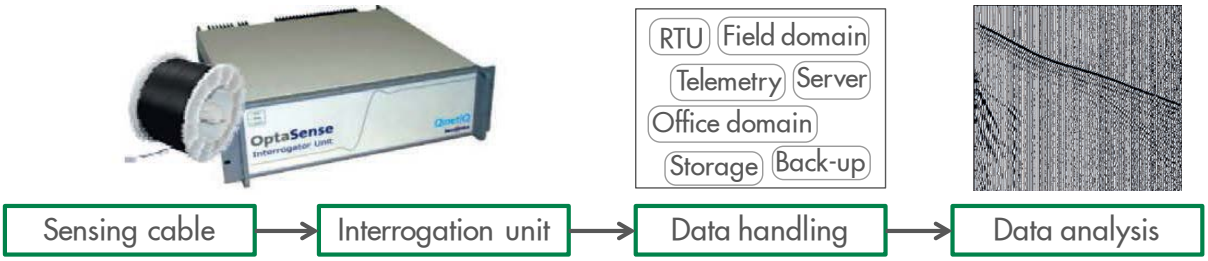

Figure 5.1: **Distributed sensing system, consisting of individual components that only together can deliver useful information. An *interrogation unit* uses a fibre-optic *sensing cable* to make measurements along the length of the cable. The resulting raw data has to be transported from the field in order to be stored and processed, indicated by *data handling*. Next, *data analysis* procedures and algorithms are required to convert raw data into information that can help to optimise field operations and development. The right-hand figure shows a typical result of Vertical Seismic Profile acquisition with DAS, depicting an intensity plot of acoustic amplitude in time (vertical axis) versus distance in the fibre (hor. axis).**

5.2. Rayleigh scattering

The capability of DAS to measure acoustic disturbances in the optical fibre is based on the principle of *Rayleigh scattering*. Similar to optical speckle resulting from diffraction on a rough surface [42], Rayleigh scattering results from the interaction of light in a fibre with *inhomogeneities* much smaller than the wavelength of the light (Figure 5.2a). Such inhomogeneities are mostly impurities in the glass and dopants that are being included as part of typical fibre manufacturing processes [41]. Each of these *scattering sites* can be seen as an independent source with a random amplitude and phase, but at the wavelength of the incident light. Some energy scatters in such a direction that it is trapped in the fibre and transmitted back to the source (Figure 5.2b).

Often, short light pulses are used to probe the fibre. Such a light pulse travels along the fibre while a small fraction of its energy is continuously scattered back to the interrogation unit. Even though the back-reflected Rayleigh scattering equates only to approximately -65 dB/km of the incident light, the backscattered light can be successfully analysed to provide information on the amplitude and phase of the assembly of scattering sites along the length of the fibre.

If the distribution of scatterers in the area covered by the pulse reflection changes, the amplitude and phase of the backscattered light change as well. These changes are a function of imposed strain and temperature. If slow variations in temperature and background strain are ignored, the retrieved signal becomes dominantly a function of acoustic strain on the fibre: the lowest acoustic frequency of interest is typically in the order of 1 Hz, although some applications might require even lower frequencies. On the other end of the spectrum, frequencies of interest can be as high as 500 to 5,000 Hz.

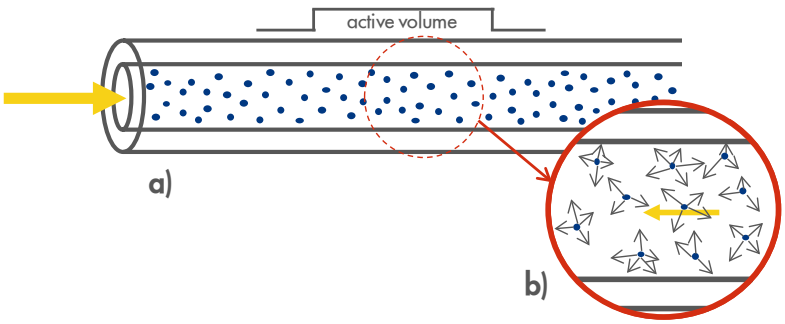

Figure 5.2: **Rayleigh scattering of a light pulse in an optical fibre. (a) Local inhomogeneities are present throughout the fibre. (b) Interaction within the active volume of the pulse causes Rayleigh scattering of the incident light. Local strain or temperature changes cause a change in the overall amplitude and phase of the backscattered light.**

A fibre is sensitive to both axial and radial strain [43]. *Axial strain* directly impacts the optical path length to a particular scattering site. *Radial strain* causes a change in refractive index through the so-called *opto-elastic effect*, resulting in a change in the group velocity of a light pulse and hence an apparent change in optical path length. A bare fibre is approximately four times more sensitive to axial strain than to uniform strain in the radial direction. The sensitivity to radial strain is reduced even further after packaging in typical cable designs. This topic of strain coupling through fibre-optic cables will be further considered in Chapter 7. For now it is important to realize that acoustic strains impact the phase of individual scatterers. The backscattered light results from an almost infinitely large assembly of scatterers, and hence is also influenced by acoustic strain.

5.3. Fibre-link probing schemes

In this Section probing schemes using Rayleigh scattering will be introduced. First the case of using an incoherent light source is discussed (*OTDR*). This is useful because it gives an excellent reference frame for introducing the use of a coherent light source (*C-OTDR*). DAS is based on the latter, coherent, type of light source. The minimum requirement for the use of a coherent probing scheme is that the emitted light is coherent over the duration of the light pulse. As will be explained in Section 5.4, more stringent coherence requirements are posed by the practical implementation of such probing schemes.

OTDR

The first application of Rayleigh scattering for sensing purposes involved the determination of optical loss along a fibre-optic cable, now known as the commonly used *Optical Time Domain Reflectometry* (*OTDR*) diagnostic tool [44]. A small fraction of a light pulse's energy is continuously scattered back into the interrogation unit, as depicted in Figure 5.3a. The backscattered light is analysed as a function of arrival time *t*, to provide spatial resolution at distance *d* in the optical fibre:

$$d(t) = \frac{ct}{2n}, \tag{1}$$

Note that *t* is the time corresponding to the two-way distance *2d* travelled in the optical fibre. The time *t* depends on the local speed of light $c' = c/n$, with *n* the refractive index of the fibre-optic glass.

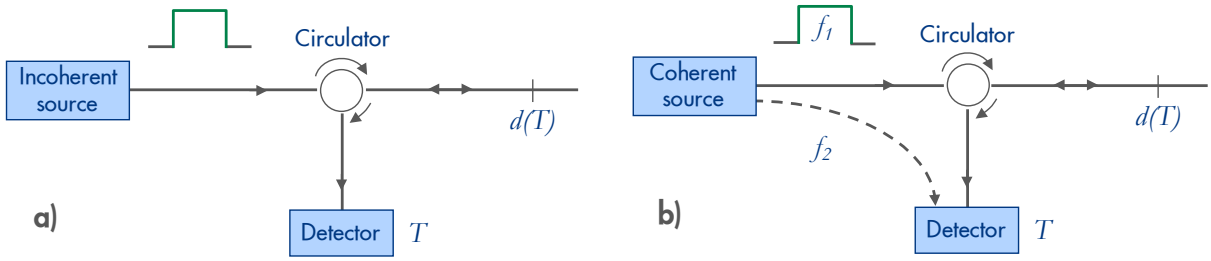

Figure 5.3: **OTDR detection schemes. (a) Incoherent OTDR interrogation scheme, detecting the backscattered intensity in time T from positions d in the fibre, resulting from emitting a light pulse into the fibre. (b) Single-pulse coherent OTDR setup, with a light pulse of frequency f_1 being sent into the fibre, and backscattered light being analysed for resulting amplitude, or, alternatively, for phase by interference with a reference signal of frequency f_2.**

A typical OTDR trace of a fibre assembly consisting of two fibres in series is shown in Figure 5.4a. Uniform loss over the length of each fibre causes an exponential decay in the received signal. The initial large signal is often a result of reflections within the OTDR system or at the front connector and can be disregarded. The splice between the two connecting fibres can be seen at a distance of 1 km in the form of a jump in signal level. Finally, beyond the end of the fibre no signal is backscattered anymore; a narrow peak in the signal is due to a reflection at the end of the fibre.

Despite the random amplitude and phase of individual scatterers (Section 5.2), smooth and repeatable traces can be obtained. The reason for this is the use of an *incoherent* light source: the wavelength of the emitted light has a non-zero spectral width. Hence, these fluctuations in the output of the source also lead to a change in phase of the emitted light over time. This instability leads to a crucial phenomenon in OTDR: *diversity*. The incoherent illumination of the scattering sites leads to diversity in the combinations of *scatter ensembles* and hence a large amount of different overall scatter energy amplitudes and phases are observed. After averaging multiple measurements, all these diverse combinations together lead to a trace representative of the loss along the fibre as displayed in Figure 5.4a.

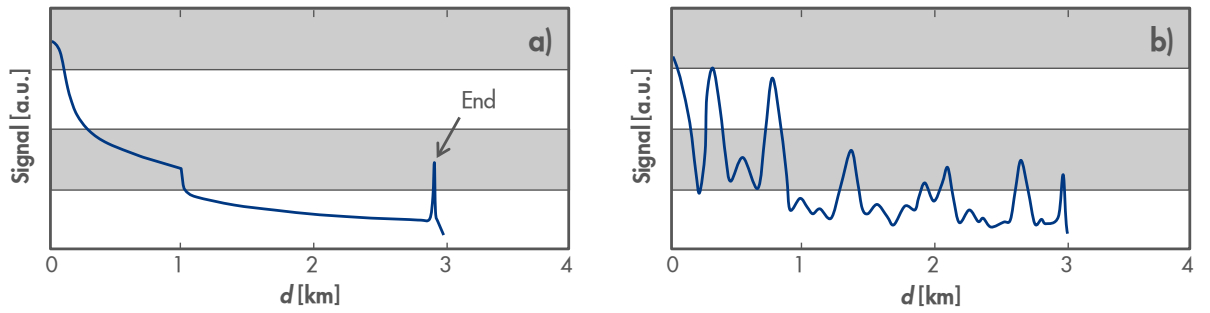

Figure 5.4: **Typical OTDR traces as a function of distance d in the fibre, for (a) conventional incoherent OTDR, and (b) coherent OTDR. Vertical axes in arbitrary units. [44]**

Coherent OTDR

By using a *coherent* light source instead, diversity can essentially be switched off. The result of such individual measurement is illustrated in Figure 5.4b. The observed signal is indicative of the random amplitude and phase of the backscattered signal, as a result of vector summation of the random amplitude and phase of individual scatterers within the pulse reflection. The advantage of using a coherent signal is the possibility of correlating the backscattered signal with a *reference* signal (Figure 5.3b). For example, from the same source, directly routed to the detector (more details in Section 5.4). The resulting *cross-product* term is not only related to the amplitude of the backscattered signal, but has a linear dependence on the phase difference between the backscattered signal and the reference signal. Because of the large amplitude of the reference signal, the correlation product essentially provides amplification to the original backscatter signal. In this way, the signal-to-noise ratio can be increased by 21 dB or more and is now mainly limited by the noise in the backscatter signal rather than by detector noise [45]. Introduction of diversity is necessary to retrieve the backscatter envelope, for example by using a source with alternating frequencies [46], resulting in an improved version of a typical optical loss trace as displayed in Figure 5.4a.

The discussion of OTDR techniques for fibre-link characterisation could be extended further, including improved interrogation schemes as well as other concepts such as those based on taking into account the polarisation of Rayleigh backscattered signal (POTDR [44]) or using other, for example Brillouin scattering mechanisms instead (BOTDR). However, the main goal here is not to find the optimal tool for diagnostics of the optical loss in a fibre-link, but rather to exploit Rayleigh backscattering for sensing dynamic strain, or in other words: acoustic signals. The coherent OTDR concept as discussed so far provides an interesting platform for this objective.

5.4. Acoustic probing schemes

Single-pulse C-OTDR

To measure strain variations with frequencies ranging from several Hertz up to 1,000 Hz or higher, the absolute amplitude and phase of the backscattered signal is not of importance. It is the change over time, between individual measurements, that represents the acoustic signal.

In the simplest realisation, it is sufficient to monitor the *amplitude* of the backscattered signal over time at a particular position in the fibre. As a result of strain, the phase of each individual scattering site changes. Unfortunately, the vector summation of a large amount of scatterers within the pulse reflection does not result in a linear dependence of the overall backscatter amplitude. Some applications, such as the detection of an intruder in perimeter protection, can be sufficiently served with this non-linear amplitude response. However, it is not sufficient if the exact temporal shape of an acoustic waveform is important as in, e.g., seismic applications.

An alternative is correlation with the before-mentioned reference signal of frequency f_2 (Figure 5.3b), to obtain the *phase* change of the backscatter signal directly. The pulse sent into the fibre and the reference signal, also called *local oscillator* signal, are usually derived from the same source. If the reference signal is of the same frequency as the backscatter signal ($f_1 = f_2$), then the cross-product is at baseband, so-called *homodyne* detection. If the reference signal is at a different frequency ($f_1 \neq f_2$), altered from the source signal by an appropriate external modulator, the cross-

product occurs at the difference frequency (*heterodyne* detection [47]). Many variations on this theme have been proposed and realised, for example heterodyne single-pulse detection [48], leading to systems useful for specific applications such as intruder detection.

Dual-pulse C-OTDR

One of the largest challenges for single-pulse systems is the fact that the light source should be coherent over a significant amount of time: the light pulse has to travel along the full length of fibre, which can for example be a 5 km long well with a two-way travel time corresponding to approximately 0.05 ms, to interfere with an – only then generated – reference signal. Achieving such *coherence time* is challenging for current state-of-the-art laser systems, and even more so for cost-effective laser systems [49].

An alternative concept is provided by launching two subsequent pulses into the optical fibre and analysing the interferometric result of the backscattered pulses, as schematically displayed in Figure 5.5. This concept relaxes the coherence requirement to the short time between the two pulses of a pulse pair, typically in the order of 100 ns [51], and consequently provides a potential reduction in noise floor.

The dual-pulse C-OTDR concept is developed into a commercial service by OptaSense, with technical input and evaluation by Shell. As part of a larger Shell-wide team, the author was involved in providing technical feedback based on a combination of modelling and experimental evaluation.

Inherent to the confidential nature of collaboration on a commercial basis, the related information in the following sections will be solely based on publicly available information.

The pulses in a pulse pair have different frequencies (typically differing in the order of 1 to 5 MHz [52]), allowing heterodyne detection. This imposes the requirement for the pulse pair to interfere at the detector. The interference requirement implies that the scatter region for the first

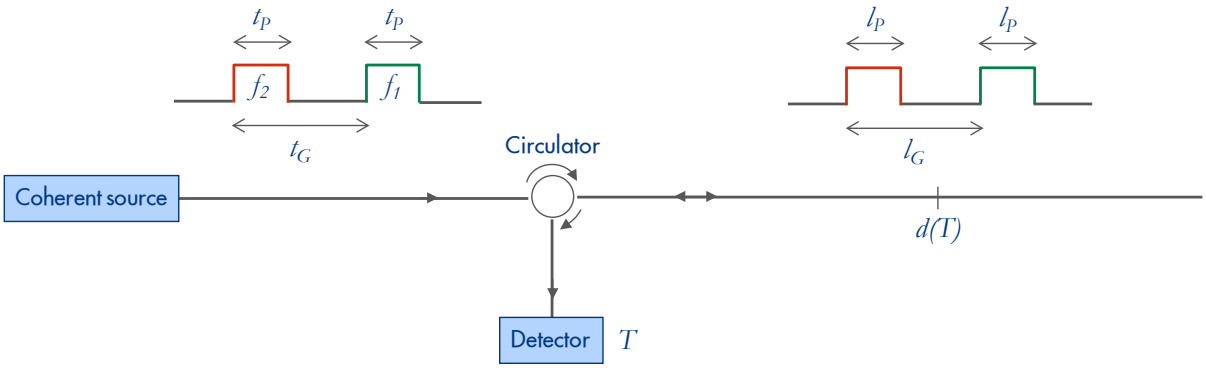

Figure 5.5: **Dual pulse interrogation scheme [50] [51]. A coherent source emits two pulses at optical frequency f_1 and f_2, respectively, with a pulse duration t_P and separated by a time t_G. These pulses travel through the fibre and back-scatter due to Rayleigh scattering. Each sample time T corresponds to a position d along the optical fibre. The detector is selectively sensitive to reflected energy at the beat frequency due to interference between the pulses. In order to interfere, the pulses have to reflect from scattering sites distributed over a pulse length l_P and separated by a gauge length l_G.**

pulse has to be further into the fibre than the scatter region for the second pulse, in order for both backscatter signals to travel back together and interfere. The gauge length l_G between the two pulse reflections is determined by the delay time t_G between the two pulses of a pair (Eq. (1)). The cross-product in the heterodyne detection arrangement contains a phase term with a linear relation to fibre strain. As such a strain sensor was created, defined by the gauge length between the two pulses. The number of such strain sensors along the optical fibre depends on the sample rate of the detector: if the detector samples at a sample interval ΔT, the distance between adjacent measurement channels is governed by Eq. (1) and is defined as the channel length $l_{CH} = c\Delta T/2n$.

5.5. Lab evaluation

The signal response in a field trial can be the result of a wide range of parameters, not all related to the interrogation unit. A laboratory setup can provide a first means to study the response of the interrogation unit itself in a reduced parameter space that is easier to control.

For this purpose, the *table-top* setup of Figure 5.6 has been developed. A fibre has been glued along the (vertical) length of a Perspex cylinder. The cylinder has been pre-loaded within a stiff metal frame, together with a *piezo-electric actuator* (*PZT*). Because the Perspex cylinder is the weakest element in the stack, actuation of the PZT will result in an axial compression of the cylinder. Deformation of the cylinder results in (predominantly) axial strain in the optical fibre. Isolated fibre segments have been attached to the cylinder to study the influence of spatially localised strain sources. Multiple fibre segments within one channel length have been attached to the cylinder to study the response to more distributed strain signals. The PZT is capable of generating signals up to approximately 500 Hz and the induced strain can be monitored by FBGs as well as electrical strain gauges for reference [53].

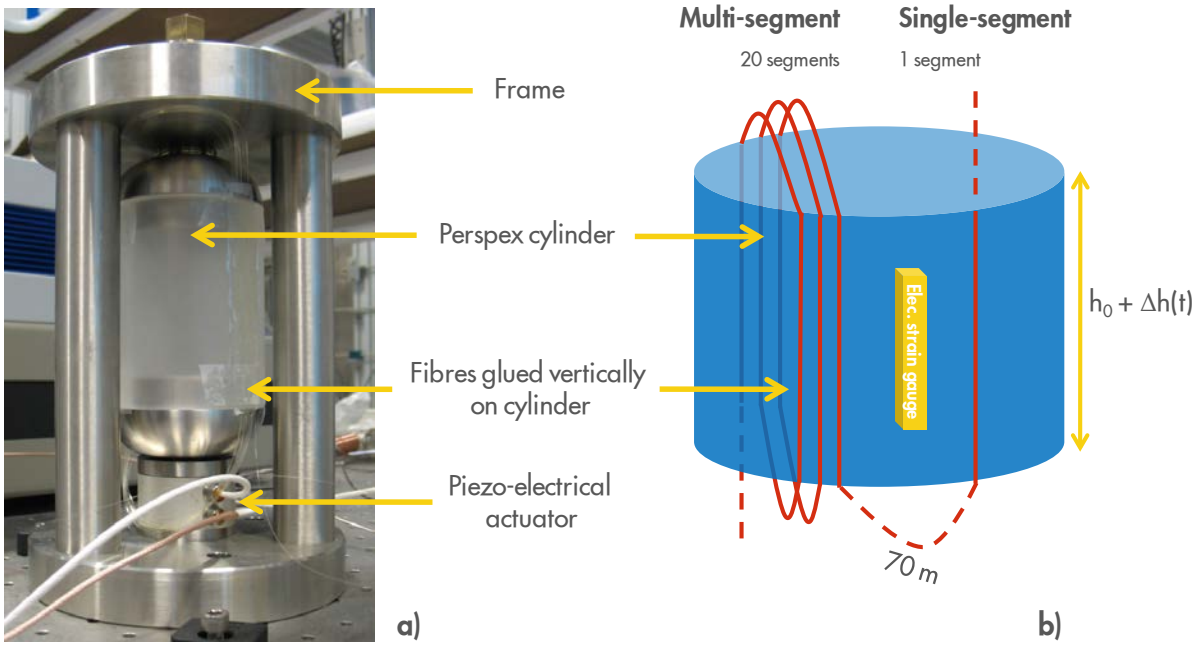

Figure 5.6: **Table-top axial strain test-setup. (a) Picture showing frame, piezo-electric actuator, Perspex cylinder and fibres. The cylinder has a height h_0 of approximately 100 mm. (b) Schematic representation of single- and multi-segments glued to the Perspex cylinder. A strain gauge and FBGs were attached to the cylinder for reference. The piezo-drive induces an amplitude $\Delta h(t)$.**

Testing of an initial prototype interrogation unit resulted in several important observations. These helped in improving the understanding of the functionality and working principles of the interrogation schemes. These tests also provided useful information on the limitations in the performance. Amongst others, signal distortion, non-linear response at higher strain amplitudes, sub-optimal spatial resolution, and signal drift over time were observed. Some of these effects could be attributed to the preliminary design and construction of these first prototypes. However, part of the observations are related to a fundamental characteristic of Rayleigh scattering: *fading*. Fading is a result of the spread in backscattered signal resulting from the combination of the random distributed amplitude and phase of individual Rayleigh scatterers. This will be treated in detail in the next section.

5.6. Trade-off: stability vs spatial resolution

Fading leads to two features in our measurements: (1) strong variations in signal amplitude, even for adjacent locations; (2) signal drift over time for one particular fibre location.

First, the response along the fibre length exhibits strong variations in signal amplitude. One pulse reflection location can provide a large backscattered signal, whereas signal emanating from an only slightly different position might be virtually absent. This is a direct result of the interference of many waves of the same frequency, having different phases and amplitudes, which give a resultant wave whose amplitude, and therefore intensity, varies randomly [42]. If each individual scatterer is modelled by a vector, then it can be seen that if a number of vectors with random angles are added together, the length of the resulting vector can be anything from zero to the sum of the individual vector lengths – a random walk[54] [55].

Second, for each position along the fibre, as inferred from the two-way travel time, the signal might drift over time. At one time the signal might be substantial, whereas later in time the signal might have almost entirely vanished. Strain and temperature influence the optical path length, by physical elongation or by changing the speed of light, and as such essentially 'shift' scattering sites along the fibre. The scattering sites observed in a pulse reflection at a constant two-way travel time therefore have changed. Such new combination of random amplitudes and phases may lead to a randomly different overall backscattered signal amplitude.

Whereas most C-OTDR interrogation schemes (Section 5.3) are only concerned with the overall phase change of backscattered pulses over time, problems arise when a sufficiently strong optical signal is at some point not observed anymore due to fading as described above. Such channel is not accurate anymore and has a far-from-perfect proportionality to fibre strain. Even worse, there might be time periods in which no acoustic signal at all can be retrieved for a certain position in the fibre.

The random distribution underlying fading can be reduced by creating 'diversity' in the acquired signals. As discussed in Section 5.3, diversity in fibre-link diagnostic applications can be created by averaging over, e.g., multiple wavelengths in time. Since we are interested in rapidly-varying acoustic signals, it is not an option to simply average multiple diverse samples *in time*. However, it is possible to acquire signal for multiple pulse pairs at different wavelengths *simultaneously* [52]. Alternatively, diversity can be created *spatially* [57]. Slightly shifted pulse reflections can be used as depicted in Figure 5.7. Data acquisition at an integer *N*-multiple of the repetition rate is the extra

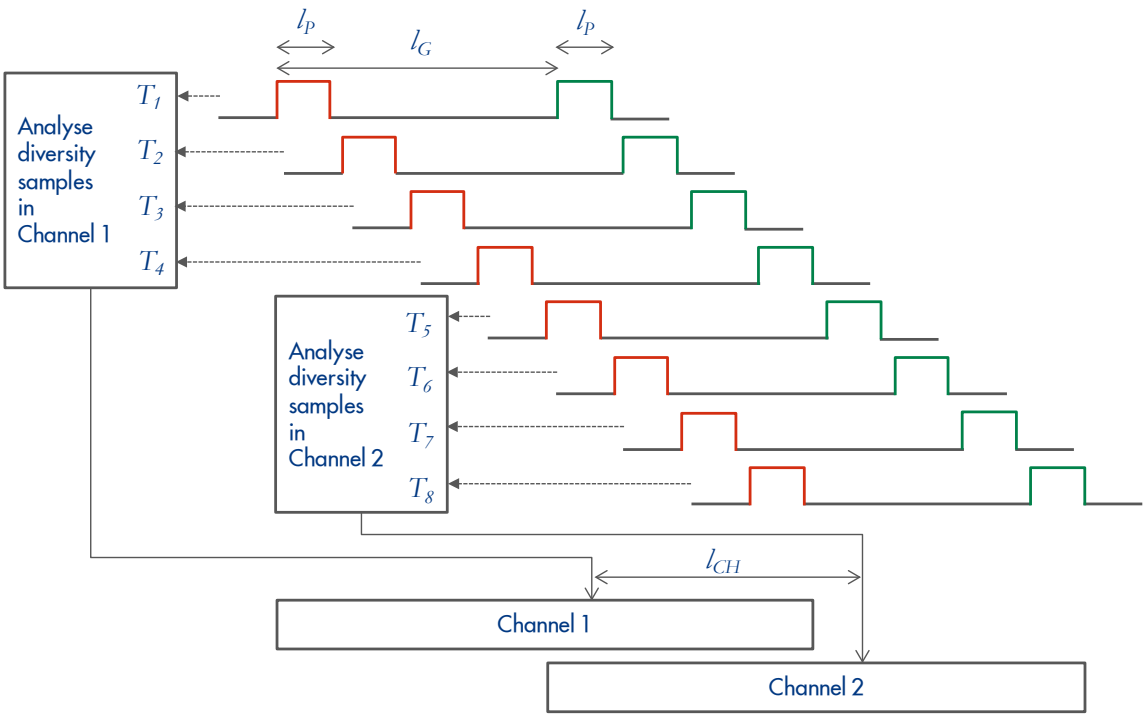

Figure 5.7: **After an optical pulse pair is injected into the optical fibre, the scattered light is sampled at times T_i, corresponding to different locations in the fibre (Eq. (1)). In this example, four subsequent samples are analysed and combined into a single output channel. Each channel represents a fibre length, equal to the channel length l_{CH}, determined by the sample rate and the number of diversity samples. [57]**

requirement to the initial dual-pulse interrogation scheme. A number of N subsequent 'diversity samples' can then be analysed and compared to select diversity samples that exhibit a non-faded response[56]. This spatial diversity scheme provides a significantly reduced probability of suffering from fading: if the probability of observing a non-significant signal amplitude for a single sample is for example 10%, then by using the information from, e.g., four samples reduces this probability to (at best) only 0.01% [52].

A downside of introducing spatial diversity is the enlarged spatial extent covered by each output channel. Instead of each sample providing a channel, multiple spatially-shifted samples are combined into one output channel. At the same sample rate, the channel length is proportional to the number of diversity samples used per output channel. Furthermore, the sensitivity in the traditional dual-pulse scheme extended over one gauge length only. Since now an output channel is representative of multiple spatially shifted diversity channels, the sensitivity is extended over a larger fibre length. For most geophysical applications this is not a significant problem since wavelengths are long. For example, a 100 Hz signal (which is close to the upper bound of typical seismic source signals) at a typical wave velocity in sand formations of 2500 m/s, results in a wavelength of 25 m. Such wavelength is still larger than the typical extent of the sensitivity of a channel, and therefore spatial diversity can be applied. Nevertheless, apart from the extent of a channel, it remains important to know the exact location of the output signal that is built up from the selection of diversity samples.

Summarizing, the concept of introducing spatial diversity is a method beneficial in reducing the impact of fading in coherent Rayleigh-scattering reflectometry, at the expense of a degraded spatial resolution. This represents the usual trade-off that is part of real-life design.

5.7. Continuous development

Prototype interrogation units have been developed and built based on the concept of spatial diversity, now commercially branded as 'OptaSense ODH-3' units. Again, tests were conducted in a laboratory environment to provide a first evaluation of its performance. The setup used is identical to the setup described in Section 5.5, allowing an easy comparison with the results of initial prototypes. Typical test results are provided in Figure 5.8, showing the response to an amplitude scan of a 90 Hz continuous wave [58]. The results of an initial DAS prototype, to some extent behaving as an intensity-detection based C-OTDR system (Section 5.3), are given in Figure 5.8a. Clearly visible is the expected non-linear amplitude response, especially at higher frequencies. Figure 5.8b displays the results for an ODH-3 prototype. As a result of phase-detection in combination with diversity sampling, the strain response is now quasi- linear up to high strain values.

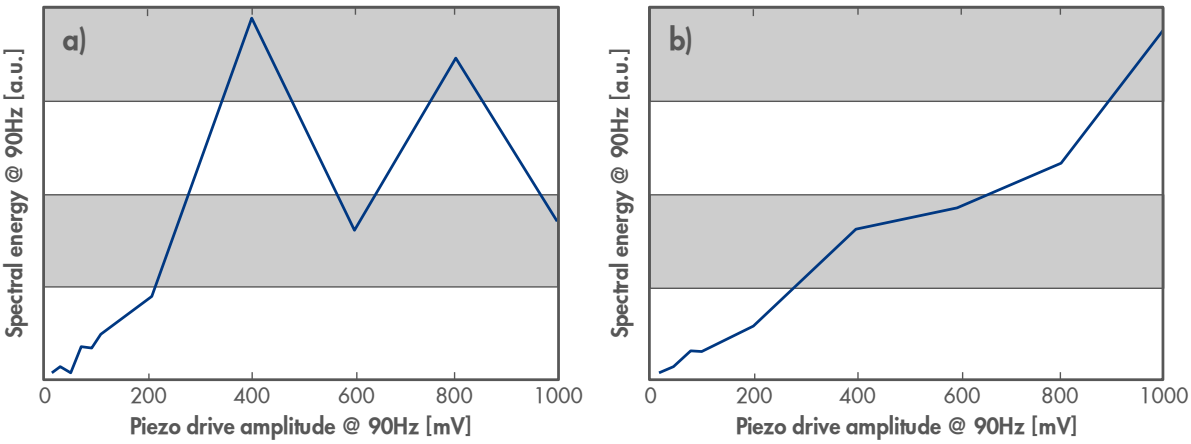

Figure 5.8: Response as a function of the amplitude of the applied strain (in volts) at 90 Hz; (a) initial prototype with random fluctuations at higher amplitudes; (b) ODH-3 with spatial diversity sampling, showing a nearly linear response up to highest strain input.

As such, the ODH-3 interrogation unit with spatial diversity sampling provides a promising technique for, especially, geophysical sensing. Chapter 6 will give an overview of the extensive field trials executed after the first laboratory experiments. The field trials have provided a wealth of information on acoustic sensitivity of the integrated sensing system in a down-hole environment. As expected, we have also gained more insight in the limiting factors.

The interrogation scheme with spatial diversity sampling is especially beneficial for a range of seismic measurements. However, as will be described in Chapter 6, further development is needed in some areas, especially to improve performance as compared to geophones. Also, for other applications other interrogation schemes might be more suitable, depending on requirements such as spatial resolution, signal stability and frequency response.

Without going into any detail, it is worth mentioning the application of flow-assurance measurements in wells. Typical seismic applications are concerned with far-field illumination of the optical fibre with long-wavelength acoustic waves. Instead, flow measurements in a wellbore are concerned with noise-logging of near-field signals of much wider frequency content. Due to the limited extent of features in a wellbore, spatial variation of acoustic waveforms can be large and hence spatial diversity sampling is less effective. Trade-offs can be made in other areas, for example signal stability (fading) is less important when concentrating on the average frequency content of flow noise.

The universal interrogation unit should combine good signal stability and linearity with a good (sub-meter) spatial resolution, and should allow measurement of frequencies ranging from quasi-static up to approximately 10,000 Hz. However, such an interrogation unit is potentially significantly more expensive than appropriate for most permanent monitoring applications. Therefore, the development of special purpose interrogation units is a more likely scenario, each with specific trade-offs for different applications.

While Distributed Acoustic Sensing is already being deployed on a commercial basis for selected geophysical and flow applications, further development work is ongoing and has the potential to enable an additional number of novel applications.

6. DAS for Geophysics: deployment

DAS interrogation units have been tested in a range of field trials. Although preparation and execution of field trials is elaborate, they are necessary to prove the applicability of a new technology in operational situations. Field trials of Vertical Seismic Profiling (VSP) and micro-seismic monitoring are presented. VSP results show the usefulness of the current development for commercial application. Micro-seismic results were less favourable, but clearly indicate the potential for future improvements in the noise floor of DAS interrogation units and – especially – directional sensitivity of fibre-optic cables.

6.1. Field trial resourcing

Interrogation units for *Distributed Acoustic Sensing* (*DAS*) have been developed together with an industrial partner. The concepts and initial laboratory tests (Chapter 5) indicate promising performance for down-hole applications. In a laboratory environment it is typically not possible to fully encompass the parameter space influencing performance. Therefore, testing of newly-developed interrogation units in *field trials* is crucial to prove their use for the actual applications.

The execution of field trials is elaborate, however. Research teams, operating units and contractors have to work together in realising a field trial. Major constraints, e.g., on timing and scope, are often imposed in order to minimize negative effects on asset productivity during the field trial operations. The companies developing fibre-optic interrogation units are typically not familiar with oilfield operations and therefore need considerable support. Research teams are often the only party having the overview of all parts of the project, from new technology to operational constraints, and as such project management is often centred in the research teams. While this role is crucial, it also requires considerable effort to integrate the vast range of different views within such multi-faceted team. Another critical constraint is safety. Risk exposure in oilfield operations is relatively large, and efforts to minimize risk are significant, especially in consideration of the new and unproven technologies trialled. The new technology must not compromise the safety of the operations in any way.

Consequently, field trials, which at first glance might appear like simple and straightforward tests, are often significant efforts with preparation times on the order of months to years. Therefore, careful evaluation and laboratory testing prior to initiation of a field trial is important to gain efficiency. After evaluation in such first steps, the enhanced DAS interrogator prototypes were considered ready for further evaluation in field trials.

The field trial results presented in this Chapter focus on two *geophysical* applications: *Vertical Seismic Profiling* and *micro-seismic* monitoring. The reason to choose geophysical applications for the first field evaluation of the new interrogator prototypes was two-fold. First, these geophysical applications are seen as some of the key applications of DAS. Second, all applications require a suitable level of interrogation hardware, sensing cable and data-analysis. Novel data-analysis methods are an initial bottleneck for many applications, whereas geophysical applications clearly required improved signal fidelity of the interrogation hardware. As such, geophysical applications provided an ideal test-bench for evaluating the novel interrogator prototypes.

6.2. Vertical Seismic Profiling

Vertical Seismic Profiling (VSP) is a borehole seismic measurement primarily used for correlation with surface seismic data or for obtaining images around the wellbore with a higher resolution than surface seismic can deliver. In a general context, VSPs vary in the number and location of sources and geophones. Typical configurations – and the ones used in our measurements – include *checkshot*, *zero-offset*, *offset* and *walk-away* surveys. In such configurations, measurements are made in a wellbore, typically using *geophones* inside the wellbore, and a *source* at the surface near the well (Figure 6.1).

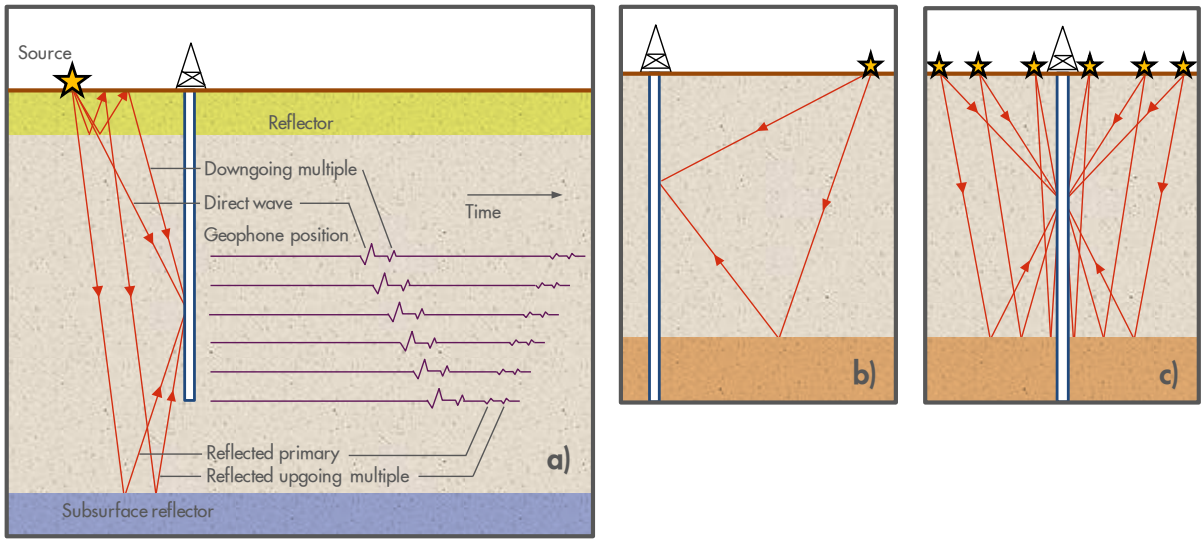

Figure 6.1: **Vertical seismic profiling (VSP) acquisition geometries include: (a) checkshot and zero-offset VSP, targeting direct waves and reflections, respectively; (b) offset VSP; (c) walk-away VSP geometries extend lateral subsurface coverage. Processing involves filtering of several artefacts, for example down-going and reflected multiples [59].**

Following the review paper of Christie et al. [59], the simplest and earliest variety – a common practice since 1940 – is the *checkshot* or *velocity survey*. In a checkshot, a stationary seismic source is used, while a single down-hole receiver is moved along the well-depth, usually locating it at the most relevant reflectors. Checkshots measure the travel time of waves propagating directly from source to receiver with no reflections along the way (Figure 6.1a). The arrival times of these direct waves correspond to the *first arrivals* – or first breaks – in the seismic traces. Since the receiver-depth positions are known, checkshots provide a profile of seismic velocity near the well. Such measurement is required to relate surface-seismic travel-time to depth: in surface seismic, instruments record the time an acoustic wave takes to travel from a surface source to a reflector located at a certain depth and back to the surface to the position of a receiver. In order to determine the depth-position of such a reflector, some estimation of the rock's velocity is needed which can be obtained by acquiring a checkshot.

The checkshot source and receiver combination is similar in a *zero-offset VSP*, as indicated in Figure 6.1a. The aim is now to observe subsurface reflectors, both along the well-bore and below. This requires a higher density of receiver positions than in a check-shot survey and longer trace recordings extending beyond the first arrivals to include later-time reflections. In order to extend the lateral coverage of the subsurface by recording reflections further from the well, the single surface-source can be positioned at a larger distance, termed *offset*, from the well (Figure

6.1b). The data recorded in this way can be processed to obtain a partial image of a subsurface reflector.

The checkshot and the two VSP techniques described so far use a single source position. The *walk-away* VSP collects data from multiple surface source locations along a line that extends from the well (Figure 6.1c). Each line typically has a large number of source positions. Combining reflections acquired from all source positions provides an umbrella-shaped coverage of the formation around and below the well. This results in an image of a cross-sectional slice defined by the direction of the walk-away line. A three-dimensional image can be obtained by acquisition of multiple walk-away lines: a *3D VSP*. This data is then processed to create an image that usually has higher resolution than that from surface seismic surveys. The enhanced detail is ideal for monitoring subtle changes in the subsurface as a result of, e.g., improved oil recovery processes.

The applications and configurations of VSP extend beyond the basic concepts discussed above, including walk-above VSPs, salt-proximity surveys, shear-wave VSPs, reverse VSPs, and drill-noise VSPs. However, the field trial results presented in this Chapter only concern basic checkshot, zero-offset and offset VSP acquisition. Individual shot records acquired in this way are sufficient to evaluate the quality of the DAS interrogation units and systems.

The surface sources used to transmit a seismic signal into the subsurface differ between onshore and offshore operations. The source in offshore environments is often an *air-gun*. On land, *vibrators*, *accelerated weight drops* (*AWD*) and *dynamite* are commonly used. The frequency content of such source signals is typically limited to a range from about 1 Hz to approximately 100 Hz. Air-gun, AWD and dynamite sources emit their energy as a pulse, with peak energies in the above-mentioned frequency range. Vibrators, as displayed in Figure 6.2, are typically used to sweep through a similar frequency range in a time interval on the order of 10 seconds. The received signal is correlated with the sweep signal to obtain the equivalent of a pulsed signal after processing, at the benefit of increased overall source energy and optimised frequency content.

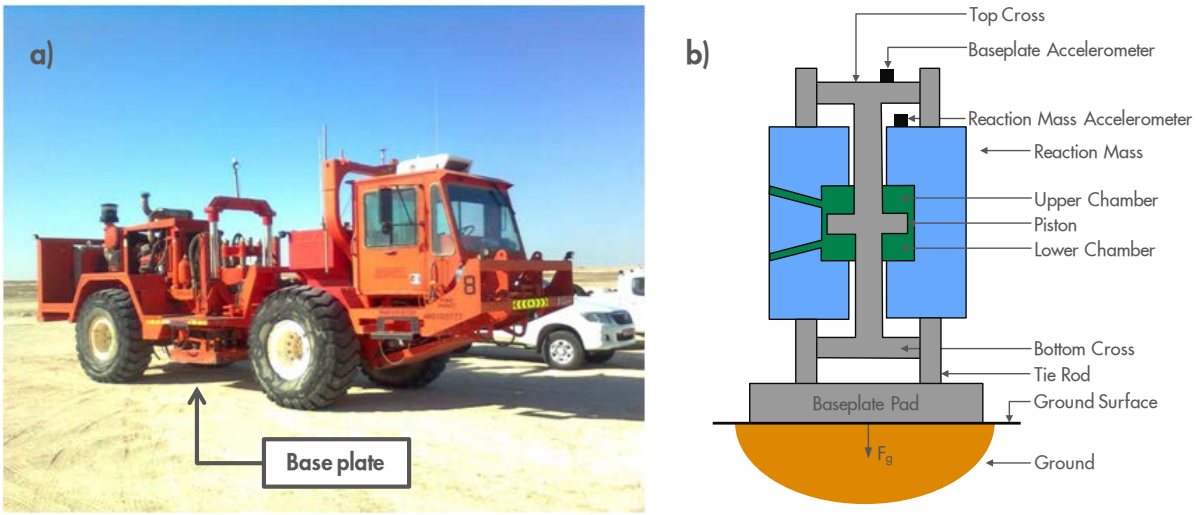

Figure 6.2: **A vibroseis (or 'vibe', 'vibrator') is a commonly used surface source in seismic acquisition on land. (a) Vibrator displayed during a field trial in Oman. Visible is the hydraulically vibrated base plate, which is used to couple vibrations into the subsurface. (b) Schematic model of an AHV-IV vibrator [61]. The necessary force to actuate the base plate is provided by a hydraulic system and a reaction mass. Acceleration sensors monitor the actual displacement.**

The amplitude effectively generated in the subsurface depends strongly on the coupling between source and ground, as well as on the characteristics of the shallowest rock layers. To give a first idea of the forces used, note that a medium-sized vibroseis as shown in Figure 6.2 produces peak forces in excess of 200,000 N [60].

Typically, a down-hole receiver array consists of geophones. A geophone is a mass-spring-system based point-sensor with its signal being proportional to particle velocity at the location of the geophone (more about geophones in Chapter 8) [62]. Production in a well typically has to be stopped to allow geophones to be inserted, also their cross-section causes a significant obstruction to hydrocarbon flow in a well-bore while deployed. As a result of their dimensions as well as the cost of geophones, strings of multiple geophones are only temporarily inserted into the well-bore. These strings contain geophones at a typical spacing in the order of 10 to 20 m. VSP surveys typically start at five to seven geophones, with the maximum number of geophones limited to approximately 100 geophones, largely by economical factors. If a well requires more geophones because of depth and required spatial resolution, a limited array is often shifted to various positions instead, at the expense of an increase in acquisition time.

The virtue of DAS is two-fold. First, it replaces discrete geophones by a continuous fibre, with measurement channels distributed all along the fibre. This results in a significant increase in the number of channels at a reduced cost. Second, compared to mostly temporary geophone deployments, fibre-optic cable has a much smaller footprint and can therefore be permanently installed without significant reduction in the well's flow cross-section. In that way, the permanently installed fibre-optic cable allows repeated measurements without the costs involved with repeated deployment of temporary geophone arrays. This is ideal for time-lapse monitoring of, e.g., production-related changes in the reservoir.

6.3. DAS signal quality

VSP measurement data is typically represented in a *depth-time plot*[3] (Figure 6.3a). The first arrival represents the wave front, emitted by the surface source, travelling down into the subsurface and arriving at subsequent depths along the length of the cable. Upon encountering an acoustical impedance contrast, due to a change of properties between rock layers, energy is partially reflected back. For the ideal case of a vertical well and a horizontal layer interface, the depth of the layer interface can be read at the intersection between first arrival and reflection slope.

One of the most straightforward applications of such dataset is the generation of *checkshot* velocity profiles. By using the time-lag in first arrivals between subsequent channels, interval velocities can be deducted as plotted in Figure 6.3b. Now that we have obtained seismic velocities, we can compare them with velocities obtained from well-logging tools, such as the sonic tool measurement in Figure 6.3b. A logging tool is lowered in a well-bore and can include a range of sensors, including electrical, nuclear and acoustic measurements, providing detailed information in close proximity to the borehole. In Figure 6.3b, good agreement is observed between geophone data and the sonic log, as can be expected. The DAS curve also corresponds well with the available sonic logs.

[3] A depth-time plot typically plots depth on the horizontal axis, which might be counter-intuitive at first sight. Originating from surface seismic, where channels represent lateral distance, this convention is widely adapted in the geophysical community.

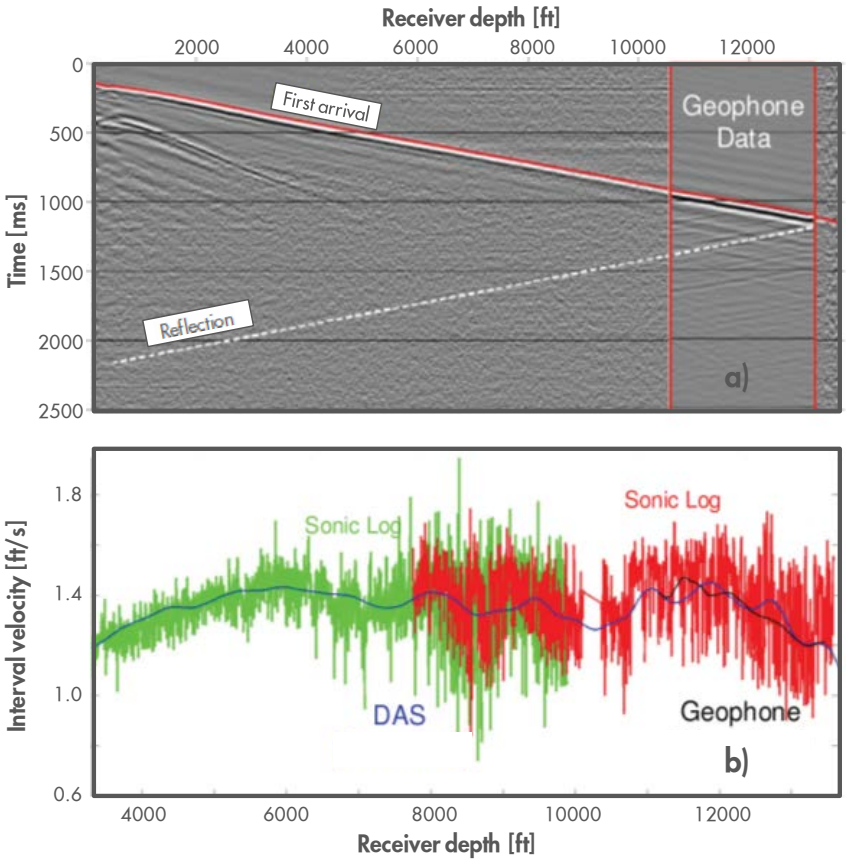

Figure 6.3: **(a) Zero-offset VSP recorded on DAS, with the first arrival highlighted in red. The rather small depth range recorded on the conventional geophone array is also shown. The strongest reflector observed is shown with a dashed white line. (b) Interval velocities calculated from DAS (blue, smoothed) and geophone (black, smoothed) data and their comparison with sonic logs. Please note that the depth scale is in feet and not in metres. [63]**

The checkshot velocity profile is used to convert travel times in surface seismic data to depth. Combined, this allows integration of the areal – but rather coarse – coverage provided by surface seismic between wells, with detailed property information obtained by logging tools in the vicinity of each well.

Figure 6.4 shows data simultaneously taken with DAS and geophones from the same well. The reflections are easier to see on the geophone record. The underlying reason can be derived from spectral plots of geophone and DAS data. As indicated by the boxes in Figure 6.4, signal spectra are obtained around the first arrivals, whereas noise spectra are taken after a long time when no signal is received anymore. It can be observed that the resulting *signal-to-noise ratio* (*SNR*) is substantially lower for DAS compared to geophones, especially at deeper locations where instrument noise is dominant. The full-depth coverage of the fibre-optic cable compared to the typically limited depth range of the geophone array, as indicated in Figure 6.3a, is a significant advantage of DAS compared to traditional geophone deployments.

The development of interrogation units, as described in Chapter 5, is illustrated by the data quality of VSP measurements in Figure 6.5. Data from 2009 (not shown) taken with an early

prototype showed characteristics similar to an amplitude-based C-OTDR system: significantly suffering from phase instabilities and amplitude variations, the measurements were not interpretable yet. The implementation of a dual-pulse setup in combination with spatial diversity sampling led to an improved version, the ODH3. With the introduction of ODH3 prototypes and production versions in 2010 and 2011, respectively, highly improved data is acquired as can be seen in Figure 6.5a and Figure 6.5b. Further improvements in repeatability and reduction of instrument noise floor lead to an increased visibility of reflections in 2011.

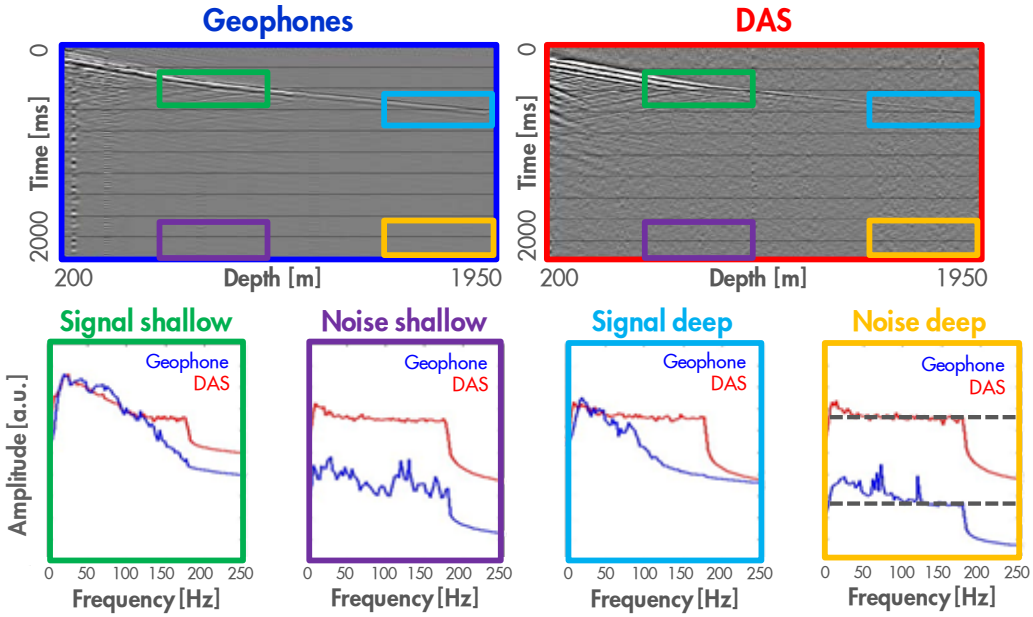

Figure 6.4: **Top: Geophone and DAS data and the windows used for signal- and noise-spectra. Bottom: Scaled frequency spectra for geophone (blue) and DAS (red) data for the indicated windows. [63]**

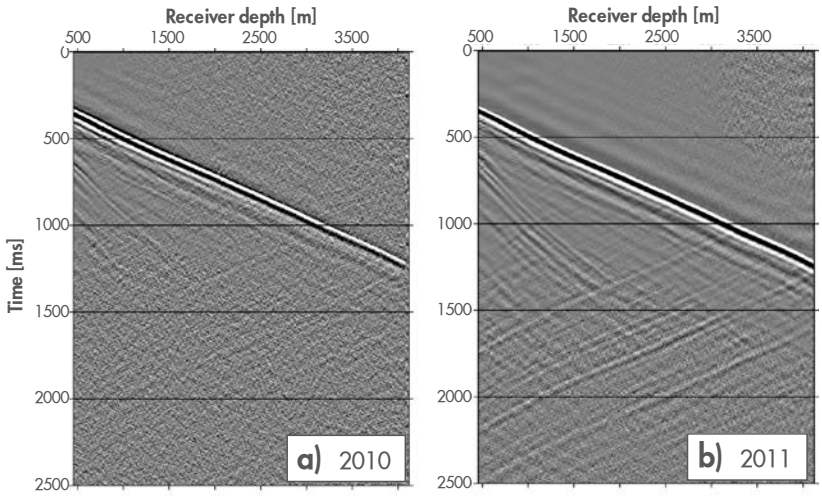

Figure 6.5: **Zero-offset VSP recorded by DAS: (a) 2010 data from Pinedale with an ODH3 prototype, (b) 2011 data from Pinedale with an ODH3 production version. Each set is a stack of 32 sweeps (Automatic Volume Control applied (1s gate)). [64]**

Although the DAS instrument noise-floor is still significantly higher than for a geophone, stacking of multiple measurements can reduce the noise to a level that already is often sufficient. The impact of this result is dramatic since it shows that DAS technology can yield a useful VSP result, despite the fact that there is still significant scope for further improvement in the DAS SNR.

The field trial results discussed so far have been obtained in North-American assets, and have been presented to show the applicability of the newly-developed interrogation units. The next Sections focus on further extension of the applicability of DAS technology, with major involvement of the author of the thesis in coordination, execution and interpretation of described activities.

6.4. Angle-dependent sensitivity

All data shown in the previous section are the result of zero-offset VSP measurements. For zero-offset VSPs, sensitivity is mainly limited by the inherent noise level of the interrogation unit. The dual pulse interrogation concept has some limitations due to the integration of induced strain over the gauge length l_G (Chapter 5), resulting in differential displacement Δl_G . The response to primary (compressional) waves essentially scales with the *apparent* wavelength $\lambda = v/(f \cos\theta)$, determined by a combination of wave velocity v, frequency f, and incidence angle θ of the acoustic wave with respect to the axis of the fibre-optic cable [65]:

$$|\Delta l_G| \approx \cos\theta \sqrt{1 - \cos\left(2\pi \frac{f l_G}{v} \cos\theta\right)}. \tag{2}$$

By assuming that a conventional down-hole fibre-optic cable is – for P-waves – only sensitive to signals propagating along its length, which will be explained further in Chapter 7, this relationship implies zero signal in two situations. First, if the wavelength of a P-wave travelling along the length of the cable is exactly equal to the gauge length, the strain over one channel will integrate to zero differential displacement. This results in a comb-like spectral response as indicated in Figure 6.6. The dependence on wavelength (or equivalently, frequency) is challenging to characterize experimentally, since transmission through the subsurface is heavily reduced for

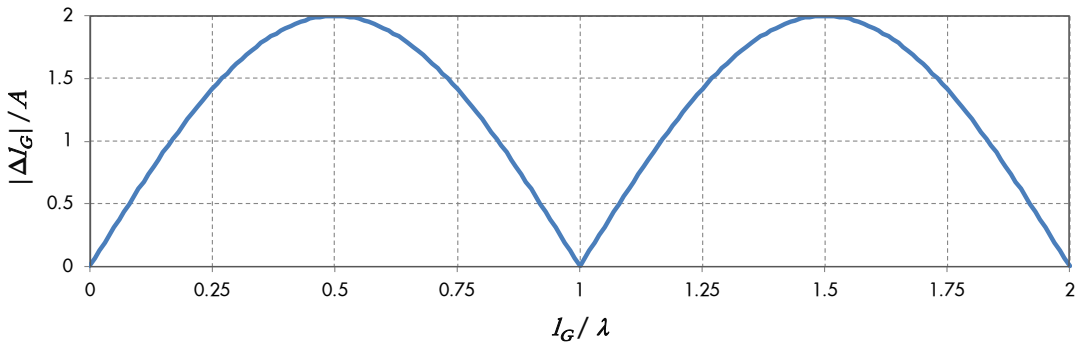

Figure 6.6: **Differential displacement Δl_G between the two pulses effectively separated by the gauge length l_G, as a function of the ratio between gauge length and apparent wavelength λ, normalized with the amplitude A of the incident wave on the fibre. Maximum sensitivity corresponds to displacement in counter-phase between the two pulse locations. The transfer function through the well- and cable-construction has been neglected here, but will be further treated in Chapter 7. [65]**

increasing frequencies. For example, at a formation velocity of 2500 m/s and a gauge length of 10 m [66], the sensitivity would drop to zero at 250 Hz. At this frequency, experimental data so far has been found to have insufficient incident energy at depth to allow a proper characterisation.

Second, if the apparent wavelength is very long compared to the gauge length, the pressure gradient and hence the differential displacement in a channel is negligible. This is represented in Figure 6.6 by the zero crossing at $l_G/\lambda = 0$. Practically, such long apparent wavelength can be the result of signals at a very low frequency or low velocity. Alternatively, the same situation arises if the apparent wavelength approaches infinity as a result of a *broadside* incidence angle. Broadside means that the wavefront arrives perpendicular to the length of the fibre, or in other words $\theta = 90°$. For such broadside wavefront, the pressure gradient along the length of the cable is negligible, thus resulting in zero signal. Characterisation of the incidence angle dependence is less problematic. Field data indeed confirms this behaviour (Figure 6.7), often simplified to $\cos^2\theta$ for wavelengths much larger than the gauge length.

Not only is this $\cos^2\theta$ behaviour worse than for conventional geophones, which exhibit an angle-dependence proportional to $\cos\theta$, it also implies that DAS in combination with traditional cables is only a single-component receiver. Geophones often have three-component sensitivity, allowing measurement of signals arriving at any incidence angle. The angle-limitation of DAS reduces the walk-away angle range that can be addressed, and reduces the sensitivity for well trajectories where the source is predominantly perpendicularly oriented towards the well (such as for a source placed above a horizontal well). The development of cables with improved directional sensitivity will be discussed in Chapter 8.

Summarizing, a number of applications exist in which useful VSP data can be acquired, despite the directional limitations of conventional fibre-optic cables. Good results have been obtained for cable cemented behind casing; the potential use of cable installed on-tubing will be investigated in the next Section.

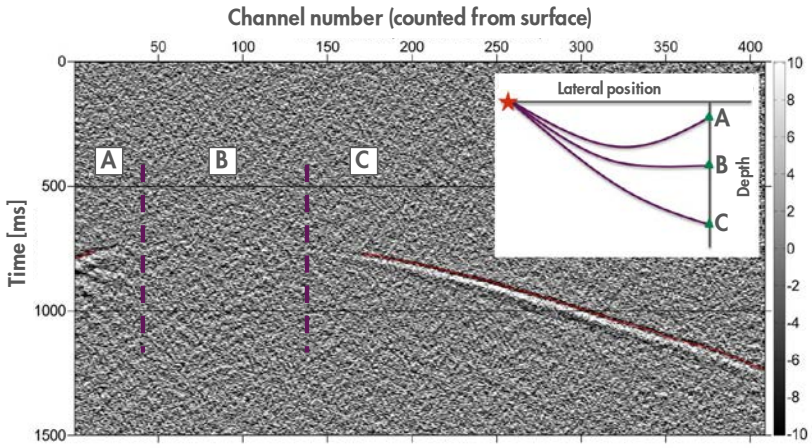

Figure 6.7: Far-offset shot gather from Pinedale 2011 illustrating broadside insensitivity of DAS acquired with standard fibre-optic cable – the amplitude of the first arrival dims as the incidence angle approaches 90° with respect to the well. [64]

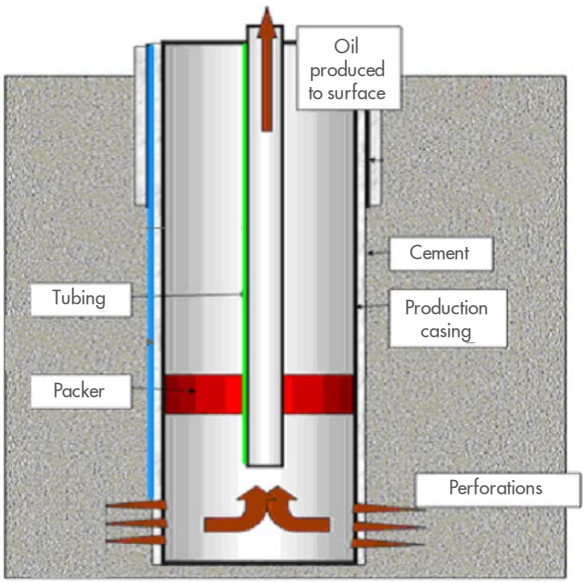

Figure 6.8: **Schematic of a well. The blue line and the green line represent two typical deployment locations of the fibre-optic cable: (blue) On the outside of the casing, cemented in place, in direct contact with the formation; (green) clamped to the tubing, surrounded by fluid, and acoustically coupled through – potentially multiple – casing strings.**

6.5. Cemented vs tubing-conveyed cable deployment

All field trial results discussed so far have been acquired with fibre-optic cable cemented behind casing. For this deployment model, the cable is installed on a casing string, and subsequently cemented in place together with the casing as illustrated in Figure 6.8. This was the initial deployment model as introduced for the hydraulic fracturing application (Chapter 5): at the time of fracturing operations, no other *completion* pipe string is installed in the well yet. However, deployment behind casing is not always the preferred approach. First, it is not allowed everywhere because of well integrity concerns. Depending on the well design, a leak path to the surface might form in a *micro-annulus* between the cement and the fibre-optic cable. Second, since a cemented cable cannot be retrieved anymore, exchanging the cable in case of failure is not possible[4]. Installation on a *tubing* string as part of the completion would allow retrieval and replacement during the lifetime of the well, and is more cost-effective as well. Third, if it would be possible to use such existing cable installations as well, opportunities for deployment of DAS would increase significantly. Most existing fibre-optic installations (especially for *Distributed Temperature Sensing*) have cable already installed on tubing.

Acoustic coupling is expected to be much better if the cable is in direct and solid contact with the formation, compared to being shielded by multiple casing layers, essentially hanging or laying loose inside the casing immersed in fluid. A first field trial to assess the sensitivity in on-tubing installations was conducted in Schoonebeek [67]. An existing cable – installed for DTS – was used to acquire VSP data [68].

[4] Please note that it is possible to install fibre by pumping it into a pre-installed capillary tube, a means of fibre deployment that will allow periodic exchange of the fibre. However, we have not verified acoustic coupling of such installation yet.

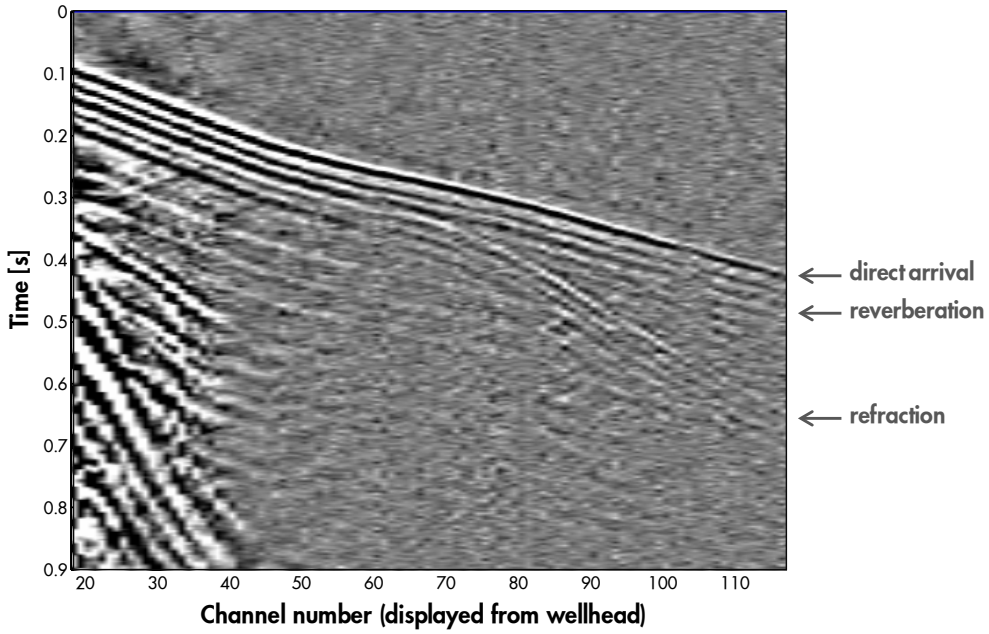

Figure 6.9: **Shot-record from a near-offset VSP at Schoonebeek (deviated well, ~900 m vertical depth; stack of 109 AWD shots). In the figure can be observed: the largest peak corresponding to the first arrival, a down-going wave transmitted directly from the surface source and arriving to the fibre-optic cable along the well trajectory; followed by some source-related reverberations; and, starting from approximately channel 75, the arrival of a refracted wave. [64]**

The results in Figure 6.9 clearly show that also in this case there is sufficient sensitivity [69]. The SNR is lower than in some other field trials, but this is partially caused by the use of a less powerful (AWD) source [70]. Still, the results show first arrivals of sufficient quality to extract a checkshot velocity profile [64]. Describing the exact coupling mechanism is challenging due to the fibre-optic cable being positioned inside a complex well configuration, but it should be appreciated that any acoustic signal coupled in the axial direction along the cable is integrated over multiple meters of cable and in that way the overall sensitivity is increased. More details on acoustic coupling into fibre-optic cables will be discussed in Chapter 7.

The same favourable coupling in on-tubing installations was identified in other subsequent field trials. This insight allows a major increase of the applicable range to wells where cable has already been installed on tubing, or to cases where installation on casing is not allowed or not cost-effective [71].

6.6. Micro-seismic monitoring

Micro-seismicity is another geophysical application that has been evaluated in field trials. Passive, continuous acquisition monitors seismic activity originating from the subsurface. Such activity can include naturally-occurring earthquakes, but in the context of the oil- and gas industry mainly focuses on production-related events. A field trial has been conducted in Oman (2011), in a field where micro-seismic activity is related to compaction due to subsidence and reactivation of faults, driven primarily by gas depletion [74]. A fibre-optic cable was installed, collocated with an array of eight geophones in a vertical observation well of 400 m depth. The combination of the geophone system and a fibre-optic cable was then cemented all the way to surface in order to realize a permanent installation with optimal coupling. The field trial took place seven months later. Meanwhile, the geophones had already been recording and detected on average 1 to 4 events per day.

The field trial consisted of two phases. First, high-quality VSP data was acquired using a vibroseis, confirming that fibre and instrument were working as expected [72]. In the second phase, DAS data were recorded passively and continuously for about one week [73].

During this period, eight micro-seismic events were detected by the geophones. The main location of the seismic activity occurred along a system of normal faults crossing the field approximately northeast-southwest (Figure 6.10). *Hypocentres* – the origins of the micro-seismic

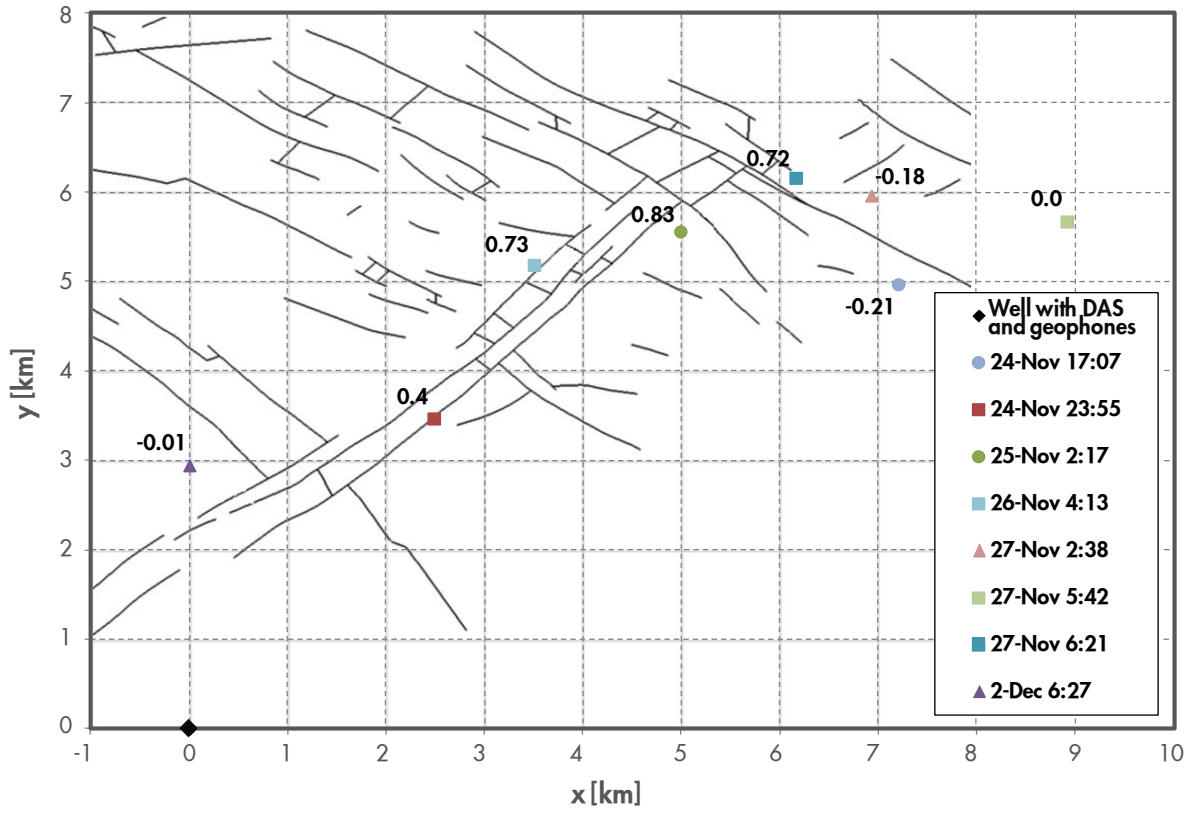

Figure 6.10: **Map of the trial location in Oman, the eight events detected by the geophone network during the DAS trial period, and main faults in the area. Date and time of the events are given in the legend; the moment magnitude is indicated at the site of the event. The well with DAS and geophones is located at position (x,y) = (0,0). [74]**

events – were located between 3 and 10 km away from the DAS well and about 1 km below the surface. Although some of the micro-seismic events were quite large, at this initial stage of data processing no significant signal in the DAS continuous record has been observed. It is likely that these events are simply undetectable given the current noise floor of DAS in combination with the limited angular sensitivity and wavelength dependence of a conventional down-hole cable. The higher noise floor of DAS compared to geophones has already been illustrated in Figure 6.4, while the directional sensitivity and wavelength dependence are described by Eq. (2).

A sensitivity analysis was carried out to quantify how strong the micro-seismic signals would look in DAS. The SNR of the P-wave arrival from the micro-seismic events as detected in the geophone array varies between 1.4 dB and 11.2 dB, as summarized in Table 6.1. The lower limit corresponds to the event on November 27th, originating 9 km away with a *moment magnitude* of 0.72, whereas the upper limit is the SNR of the strongest event. Moment magnitude is a scale used by seismologists to measure the size of earthquakes in terms of energy released. Signal and noise were estimated as the *root-mean-square* (*RMS*) amplitude during and before the P-wave arrival on the vertical component geophone data, respectively.

To calculate the equivalent signal measured in DAS, the geophone particle velocity measurements are translated into DAS differential displacements [65], and the dependence of DAS with respect to incidence angle and seismic wavelength (Eq. (2)) is taken into account. Calculation of the DAS noise floor resulted in a RMS value of 1.7 nm differential displacement over one gauge length. Table 6.1 displays SNR values obtained from comparing expected DAS signal to measured DAS noise, indicating the contributions of wavelength- and angle-dependencies. Note that signal reduction as a result of the wavelength-dependency is much lower than as a result of the angle-dependency: the events originate from a location such that their wavefronts arrive at the fibre-optic cable under an almost broadside incidence angle (Section 6.4). Taking all factors into account, the SNR is in the best case scenario -9 dB, which is about 20 dB below the best SNR of the geophone data and explains why micro-seismic events are not observable in these DAS records. Our basic processing increases this SNR only by 3 dB. Without the influence of angle and wavelength dependency, the SNR of the largest event would have been 4.6 dB (only 6.6 dB lower than geophones), indicating that not only the current DAS noise floor is a limitation, but also its directional sensitivity. Hence, development of cables with improved directional sensitivity has a significant impact.

Table 6.1: Measured geophone signal magnitudes vs calculated SNR levels for DAS, for representative micro-seismic events in Oman. Estimates assume a P-wave velocity of 2750 m/s, a peak energy centred at a frequency of 40 Hz, and a DAS noise floor of 1.7 nm differential displacement over a gauge length on the order of 10 m.

Event	24-Nov 23:55	25-Nov 2:17	27-Nov 6:21	2-Dec 6:27
Moment magnitude	0.4	0.83	0.72	-0.01
Measured SNR in geophones [dB]	9.66	11.22	1.41	8.82
Calculated SNR in DAS, instrument noise floor only [dB]	3.46	4.64	-4.79	2.62
+ sensitivity to incident angle [dB]	-13.90	-14.49	-22.02	-6.14
+ wavelength sensitivity [dB]	-16.65	-17.23	-24.76	-8.93

This sensitivity analysis is exclusively for P-waves. The SNR for shear waves in the geophone data is about 12 dB higher than that of P-waves, and that would increase the chance for DAS to detect them, provided that the noise floor is the main limitation for shear waves. However, ray tracing modelling suggests that with the characteristics of this field, shear-wave apparent wavelength and incidence angles are likely to be less favourable for DAS than those of P-waves.

The sensitivity analysis shows that situations exist in which DAS as of today is able to successfully detect micro-seismicity. In fact, DAS has detected micro-seismic events associated to hydraulic fracturing in another Shell field [75], where the distribution of events with respect to the location of DAS was more favourable than in this Oman field trial. Proximity, direction of propagation, frequency content, and magnitude, all play a role in successful detection.

Meanwhile, DAS can still represent a complementary solution to monitoring the field in Oman, provided the network is designed differently: DAS should be deployed preferably closer to the main area of seismic activity. DAS wells could cover more densely this area, while leaving the geophone installations for farther, sparser wells. Additionally, the sensitivity of geophones, either collocated with the fibre-optic cable or in separate wells, could be used to identify an event and trigger the DAS recording, reducing data volumes and processing times. Although the SNR of the raw DAS signal is likely not sufficient for instant event identification, DAS might provide additional information after more extensive (post-)processing taking into account its superior spatial resolution and spatial distribution [76].

6.7. Conclusions

Field trial results of both Vertical Seismic Profiling and micro-seismic monitoring have been discussed. Apart from the promising results obtained so far, the data also indicates limitations resulting from the current DAS noise floor and the directional sensitivity. Future hardware versions are planned to improve the noise floor (Section 5.6) and current cable developments (Chapter 7 and 8) are ongoing to increase directional sensitivity, thus broadening the probability of success for a wider range of applications.

7. DAS for Geophysics: transfer function

Existing down-hole fibre-optic cables provide good sensitivity for axially-incoming signals, but show poor broadside sensitivity. This conclusion is based on a mix of numerical modelling and experimental studies to characterize the acoustic coupling through cable- and fibre-layers.

7.1. Traditional down-hole fibre-optic cable

For down-hole use, optical fibres have historically been incorporated in *control-lines* of ¼" outer diameter as introduced in Section 1.3. The first use of such metal pipes in wells was as hydraulic lines to actuate down-hole valves. Another application involves housing of electrical wires, which allow connection of multiple down-hole sensors or actuators. Alternatively optical fibres can be included: typical down-hole cable designs can include ten or more optical fibres, and multiple sensors can be multiplexed on each fibre. The cylindrical metal control-line structure provides the required robustness: it has a good pressure rating, the metal can be chosen to withstand down-hole corrosive conditions, and an additional (plastic) encapsulation can further increase crush-resistance and provide grip for clamping the cable to tubing or casing strings.

Figure 7.1 shows a typical down-hole cable structure. Several variations exist: some of them are displayed in Figure 7.1a. Most designs contain the optical fibre(s) in an inner tube (Figure 7.1b). Both the inner and outer tubes are typically manufactured from flat metal strips which are folded around the optical fibres and then welded to form a pressure-tight tube. The inner tube, with a smaller diameter and wall thickness, is formed by a special burr-less welding process to reduce the risk of mechanical or thermal damage to the fibre. The inner tube is often filled with an immobilizing gel during the welding process. A plastic buffer is often applied around this inner tube to fill the void space between inner tube and outer tube. Because the optical fibre is already protected by the inner tube, the thick outer tube can be formed by standard processes used for the traditional control-lines as well.

These fibre-optic control-lines have already been deployed for tens of years, predominantly for Distributed Temperature Sensing or to connect discrete fibre-optic point sensors such as pressure-gauges [78]. As such, these fibre-optic control-lines are generally well accepted within the industry: their capability to maintain well integrity is accepted, and cable costs are already at a reasonable level due to the high quantities being produced. Additionally, rig crews know how to handle control-lines.

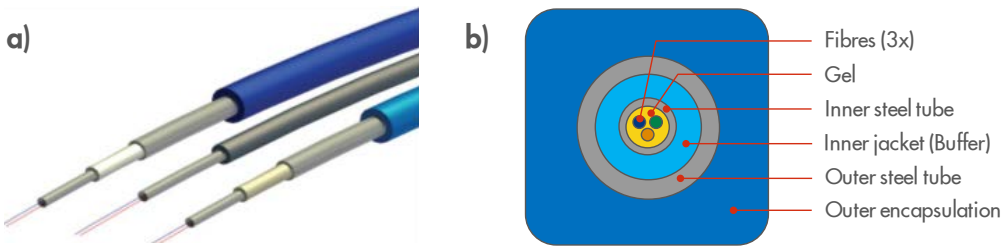

Figure 7.1: Down-hole cables [77]. (a) Typical products available on the market. (b) Cross-sectional view, with outer encapsulation (in dark blue), two metal tube layers (in grey), buffer (in light blue), and fibres embedded in gel (in yellow) in the inner tube.

Looking at the sensing capabilities of such cables, their thermal conductivity is sufficient for (DTS-based) temperature measurements. However, the use of these cables to measure acoustic signals with Distributed Acoustic Sensing (DAS) is a recent development. Field trials, as presented in Chapter 6, indicate that standard cables show enough acoustic sensitivity for signals impinging along the length of the cable to be detected. For signals impinging perpendicularly to the cable, *broadside*, the sensitivity observed in field trials is insufficient.

To provide a theoretical understanding of the acoustic sensitivity of standard down-hole cables, a study has been conducted to characterise the acoustic coupling through the different cable-layers. This study includes a combination of numerical modelling (Section 7.3) and experiments (Section 7.4).

This work has been conducted at an early stage of the project, partially in parallel to the field trials as discussed in Chapter 6. At that time, the main goal was to get an initial understanding of important factors determining the sensitivity of fibre-optic cables. As such, the work involved a number of embryonic, exploratory efforts. While such work might not always be clearly defined, it enables crucial insights in an early project phase. Retrospectively, the combination of modelling and experimental results provides useful conclusions in two respects. First, it gives an understanding of the reason for the good axial sensitivity as encountered in field trials (Chapter 6). Second, it indicates whether significant broadside sensitivity improvements can be likely achieved by mere modifications to the traditional cable designs.

7.2. Fibre-optic sensitivity to strain

Before considering the impact of various cable layers on acoustic sensitivity, the sensitivity of a bare optical fibre is defined. As introduced in Chapter 5, DAS is sensitive to changes δt in the travel-time t of back-scattered light pulses travelling through the fibre. Such a phase lag can essentially be introduced in two ways. First, physical elongation of the fibre, equivalent to an axially applied strain, leads to a shift of the scatter centres contributing to that particular pulse reflection. Second, strain causes a change in the density of the fibre material, which modifies the refractive index and hence the effective speed of light in the fibre. This relation between applied strain and refractive index is described by the *photo-elastic effect* and the related *Pockel* tensor P_{ij} [79]. The tensor component that is normally measured in Bragg scattering experiments by longitudinal waves is P_{12} while for scattering by a shear wave the effective component is P_{44} [79]. Assuming an axial strain ε_z and a radially-uniform broadside strain, the resulting change in travel time is described by:

$$\frac{\delta t}{t} = \varepsilon_z - \frac{\epsilon_0}{2}[(P_{11} - P_{44})\varepsilon_\perp + (P_{11} - 2P_{44})\varepsilon_z], \tag{3}$$

where ε_0 is the dielectric constant of vacuum and the broadside strain $\varepsilon_\perp = \varepsilon_x + \varepsilon_y$. The assumption of a radially-uniform broadside strain corresponds to a hydrostatic pressure: this is an acceptable approximation for most of our applications, in which the acoustic wavelengths are significantly larger than the cross-section of the cable. The coordinate system is defined in Figure 7.2. For a bare optical fibre with both core and cladding layers of glass, the Pockel tensor can be experimentally evaluated [80] and Eq. (3) becomes:

$$\frac{\delta t}{t} = 0.7\varepsilon_z - 0.2\varepsilon_\perp. \tag{4}$$

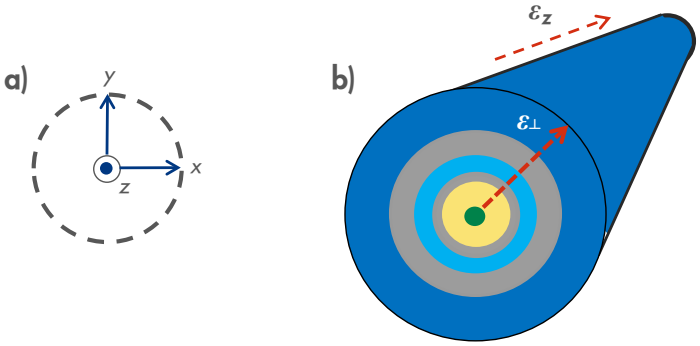

Figure 7.2: Coordinate system as used in this Chapter. (a) The axial coordinate z is perpendicular to the paper plane and is directed along the length of the cable; the coordinates x and y are perpendicular to the axis of the cable. (b) Axial strain ε_z and radially-uniform broadside strain are defined in this coordinate system.

Summarizing, the effect of axial strain on a bare optical fibre is approximately 3.5 times larger than the effect of broadside strain. Note that the broadside sensitivity is entirely due to the photo-elastic effect.

So far, only the effect of strain on pulse propagation in the bare optical fibre has been considered. The bare fibre is normally covered by a coating layer and integrated in a fibre-optic cable structure (Section 1.3). The transmission loss through the package of all these layers decreases the impact of the externally applied strain on the bare fibre. Hence, these layers determine to a large extent the effective acoustic sensitivity of a fibre-optic cable. Characterisation requires an acousto-mechanical analysis of the acoustic coupling through such fibre- and cable layers, which will be presented in the next Sections.

7.3. Modelling of axial and radial strain coupling

Based on first analytical studies [78], it was recognized that the interaction of acoustic waves with a multitude of cable layers is preferably approached numerically. Hence, the strain distribution throughout fibre- and cable-layers was studied by means of a finite-element model implemented in a commercial software package [82]. Realistic modelling of a down-hole cable in its down-hole environment involves an extreme range of length scales. A wave with a wavelength typically on the order of 10 to 100 m arrives along a well which is several kilometres deep. This wave is measured by means of DAS with a spatial resolution on the order of 10 m, using a fibre-optic cable that is less than 1 cm wide and contains an optical fibre of only 250 µm thickness. With reasonable computing resources, it is difficult to accurately model dynamic strain in such a geometry with a difference in length scales up to $1{:}10^7$. Two simplifications were introduced to provide a fit-for-purpose model in a reasonable timeframe.

First, instead of modelling acoustic – *dynamic* - strain, *static* strain was studied. This assumption is reasonable as long as the *bulk modulus* and *shear modulus* do not significantly change as a function of frequency, and furthermore *damping* is not significant. This assumption is valid for most fibre- and cable-layers since they consist of stiff, solid materials, such as metal, glass, polyethylene and acrylate. The gel typically used in cables (see Section 7.1) does not fulfil this criterion. Therefore, the mechanical characteristics of various gels have been experimentally evaluated by means of *rheometer* measurements [82]. Bulk and shear moduli values reasonable for the acoustic frequency

range of interest have subsequently been selected and used in the static models. This approach provides sufficient insight into the influence that the cable construction has on acoustic sensitivity of fibres in down-hole cables.

Second, in view of the large range of length scales, the model only considers the impact of an acoustic signal directly incident on the cable itself. The interaction with the environment is represented by defining the incident signal in two extreme cases: a *displacement-limited* and a *force-limited* regime. Along the length of the cable, the effective stiffness is fairly low and as a consequence the cable will comply with its surroundings: the displacement or strain at the cable boundary is the same, irrespective of the mechanical properties of the cable. In the radial direction, the cylindrical cable is – relatively-speaking – much stiffer. The presence of the cable influences the strain distribution around the cable as well, and imposes limits to the forces – stress – exerted by the surroundings onto the cable. Hence, a force-limited regime can be assumed. These two cases can also be explained in terms of *acoustic impedance*: in the axial direction the impedance of the cable matches with its surroundings, while a large contrast exists between the two in the radial direction.

Axial sensitivity

First, the axial sensitivity of a typical fibre-optic cable structure has been considered by using the displacement-limited approach. This has been realised by imposing a fixed axial strain as boundary condition on the outside of the cable. A two-dimensional axially-symmetric model allows evaluation of the strain distribution throughout the cable, into the optical fibre (Figure 7.3). The loss of axial strain while being transmitted through the cable structure is displayed in Figure 7.3. Most cable layers transmit strain with low loss: the thin layers of solid materials support transmission of shear strain very well. An incremental improvement of approximately 2 dB might be realised by removing the outer encapsulation.

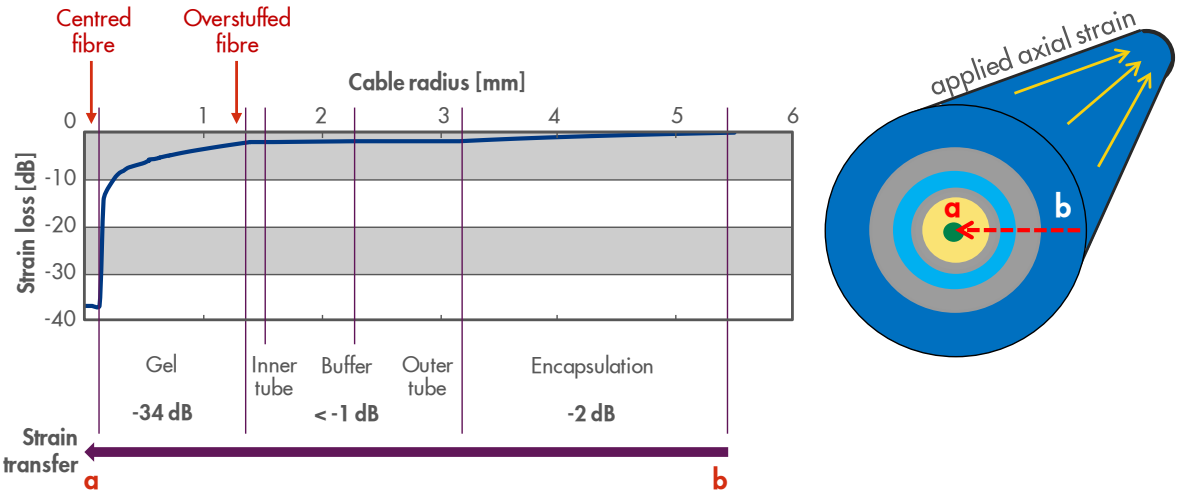

Figure 7.3: **Numerical model of strain distribution throughout cable layers, in response to axial strain on cable exterior. The cable includes an outer encapsulation and gel-embedded optical fibre. Depending on the location of the fibre, either stretched and located in the middle of the gel layer, or overstuffed and close to the inner wall of the inner tube, the reduction in strain at the fibre location, compared to the strain at the cable exterior, can vary between 37 dB and 3 dB, respectively.**

Strain transfer through the gel is much less efficient, because it does not support shear forces well. The axial sensitivity depends heavily on where the fibre is located in the inner tube. If the fibre is located in the centre, fully surrounded by gel, this leads to a huge signal loss: in this model estimated at 34 dB. On the other hand, the loss of strain is negligible if the fibre is located near the inner wall of the inner tube, especially if the fibre is in direct frictional contact with the metal tube. By positioning the optical fibre close to the tube wall, a fibre-optic cable with high axial sensitivity can be realised. The most likely location of the optical fibre inside the inner tube will therefore be studied further in Section 7.4.

Radial sensitivity

The modelling efforts also enable a characterisation of the radial sensitivity. For this purpose a force-limited approach has been chosen: a radially-uniform static stress has been applied to the exterior of the cable (Figure 7.4). The strain distribution into the optical fibre has again been evaluated. Figure 7.4 shows that the inner and outer tubes dominate the loss of radial stress in the cable. Determination of the absolute strain magnitude also requires taking into account the contrast in acoustic impedance between materials. Nevertheless, the poor radial transfer efficiency can largely be attributed to the inherent radial stiffness of cylindrically-shaped, metal tubes in combination with Eq. (4). Summarizing, traditional down-hole cable designs are in first approximation significantly less sensitive to broadside signals. This results from a combination of poor mechanical coupling through the cable in combination with the lower broadside sensitivity of the optical fibre itself.

The conclusions presented in the above Section are based on the work of Di Wu [82], who joined the IWT team as a trainee from the Design and Technology of Instrumentation (DTI) technological design programme at Eindhoven University of Technology. His project was supervised by the author of this thesis.

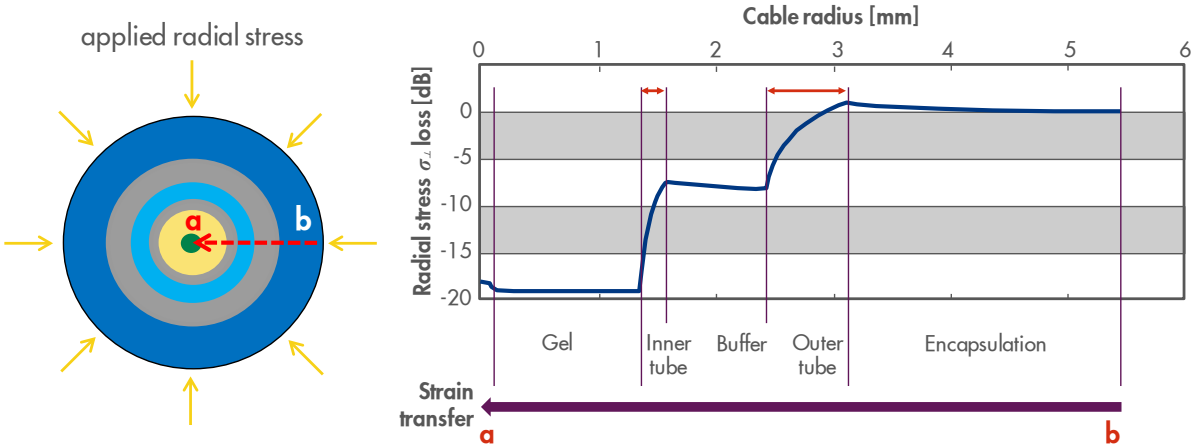

Figure 7.4: **Numerical model of the response to applied radial symmetric stress on the exterior of the cable. The stress drops mostly on the outer tube and the inner tube (indicated by red arrows); hence those layers are responsible for the majority of radial stress absorption. Due to stress concentration with a $1/r$ dependency, we can observe an effective gain in stress.**

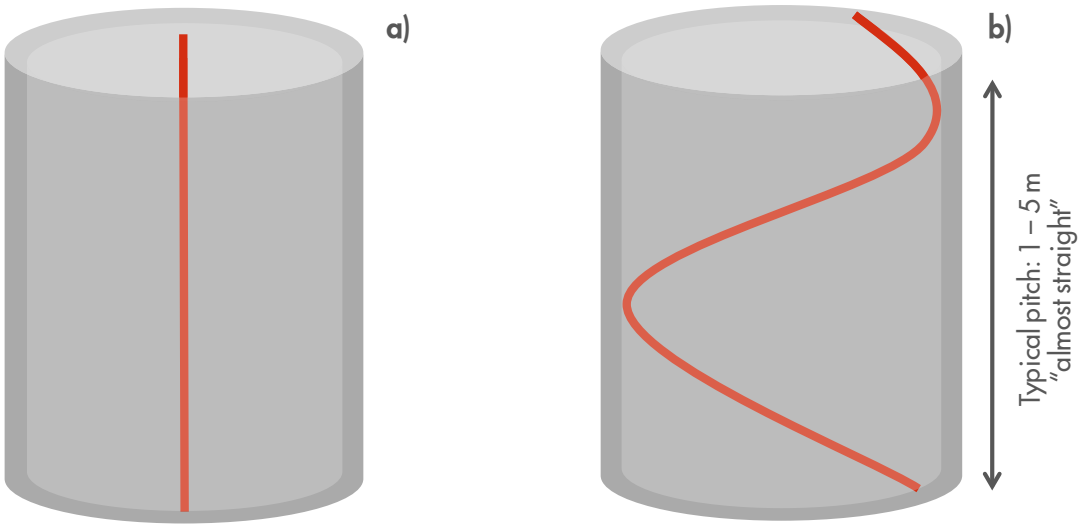

Figure 7.5: **Two possible locations of the fibre in the inner tube. (a) The fibre can be located straight in the centre of the tube. (b) However, practice showed that due to fibre overstuffing in the cable's inner tube, the fibre will naturally shape in its lowest energy state: a helical path along in the inner tube wall.**

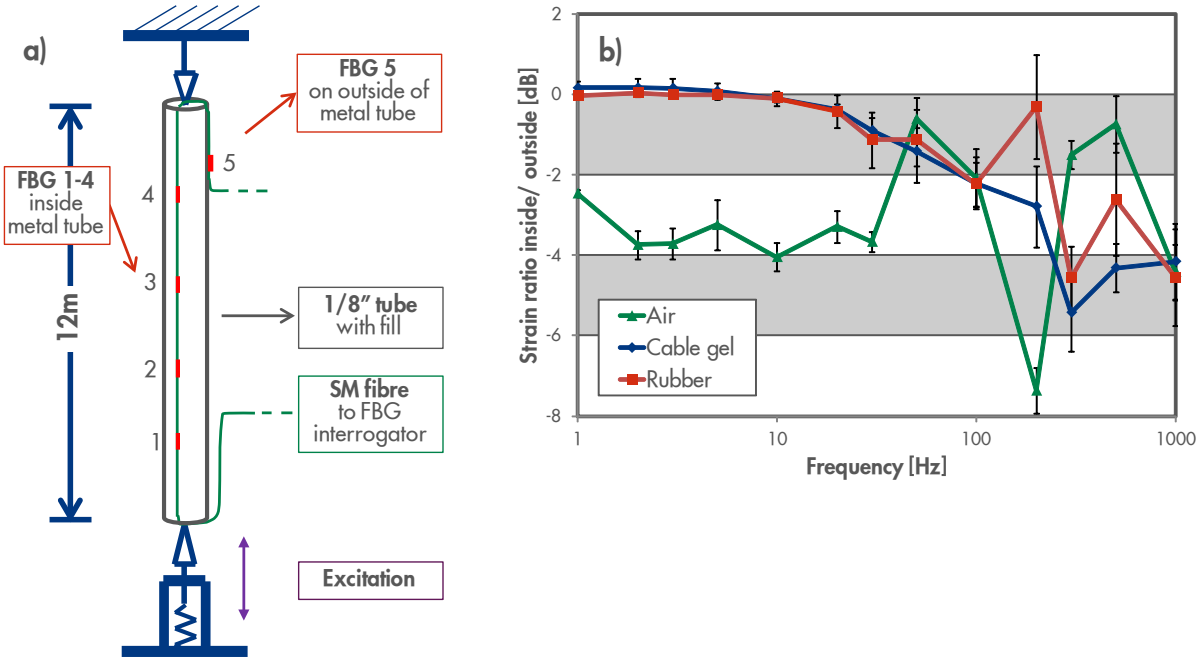

Figure 7.6: **Laboratory-scale setup to characterize the axial strain transfer into a fibre-optic cable. (a) The setup comprises a ⅛" metal tube spanned between a ceiling-suspended mounting point and a mechanical vibrator. The tube is subsequently filled with air, a typical cable gel, and a rubber. An overstuffed fibre with FBGs is incorporated in the tube fill. One additional FBG is attached to the outside of the tube. (b) The strain ratio between the FBG on the outside and the FBGs on the inside ($\langle FBG_i / FBG_5 \rangle_{i=1-4}$) is plotted, as a function of excitation frequency and tube fill.**

7.4. Axial strain coupling in practice

Modelling of the axial sensitivity, as described in Section 7.3, indicated that a large difference in sensitivity can be expected based on the actual position of the optical fibre within the inner tube. If the fibre is located at or near the inner tube, good sensitivity is expected. On the other hand, if the fibre is centred in the gel layer (Figure 7.5a), transmission losses up to 34 dB occur.

Field trials demonstrate the ability to measure seismic signals, despite the currently higher instrument noise floor of DAS compared to geophones (Chapter 6). If one would additionally assume high signal loss related to a centred fibre, observation of any signal would become very unlikely. Hence, the fibre is more likely positioned at or near the wall of the inner tube, in more direct contact with the surroundings.

This assumption is actually very likely, since the optical fibre is typically incorporated in a cable with an intentional *overstuffing* of 0.3 to 0.7%: the cable is shorter than the fibre inside [83]. Such fibre overstuffing is realised during the production process by bending the cable considerably, which results in additional fibre being pulled into the cable. Overstuffing improves the reliability of the cable: it compensates for differences in thermal expansion between the metal tubes and the glass of the fibre, and provides some slack to mitigate bending-induced strain. However, the additional length of fibre has to fit in the cable. Naturally, an overstuffed fibre will shape itself in a helical shape with the maximum possible diameter to minimize its energy state [84]. As a result, it will curl up against the inner tube walls, as illustrated in Figure 7.5b. Nevertheless, this can still be considered a "straight" fibre for DAS measurements, since the pitch resulting from typical overstuffing is between 1 and 5 m.

Direct contact between fibre and inner tube should result in negligible signal loss. This has been demonstrated in a laboratory experiment [85], as illustrated in Figure 7.6a. A cable-segment was prepared to resemble the ⅛" inner tube of a typical down-hole cable. This cable segment was vertically spanned between a fixed mounting-point in the ceiling and a shaker on the laboratory floor. The shaker was actuated to produce vertical vibration displacements, inducing an axial strain in the inner tube at frequencies between 1 and 1,000 Hz.

The cable segment was 12 m long, limited by the ceiling height of the laboratory building. The large aspect ratio between cable length and diameter ensures that this test represents a continuous cable segment. An issue is that the cable length is still on the same order as the DAS gauge length. As such, a DAS measurement might still be affected by non-homogeneous strains induced at the ends of the cable. For this reason, a fibre with multiple FBGs was used instead of a standard fibre with DAS. Both fibre-optic measurements are sensitive to axial elongation and changes in refractive index as a result of applied strain. FBGs were positioned away from the ends, providing point-measurements representative of a continuous cable segment. The optical fibre incorporated five FBGs. A part of the fibre was in-house loosely inserted in the metal tube such that four FBGs are distributed over the length of the tube. These measurements are assumed to be representative of the acoustic sensitivity of a fibre in a down-hole cable. The fifth FBG was attached to the outside of the tube, delivering reference measurements to quantify the amount of axial strain induced in the tube wall. The combination of FBGs allows measuring the transfer function for axial strain from the inner tube into the optical fibre. This experiment has been conducted for three different tube fills: air, a typical cable gel, and a rubber-like material.

The results, presented as the ratio between FBG readings inside versus outside the tube, are displayed in Figure 7.6b. At frequencies up to approximately 100 Hz, the axial strain transfer is almost without loss for gel and rubber, while even for air the transfer efficiency is still only

reduced approximately by a factor two. Numerical simulations (Figure 7.3) indicate a significant loss if the fibre would be centred in the inner tube. Hence, the combination of results indicates that the optical fibre is located loosely in contact with the inner tube wall. Strain transfer is to a large extent provided via simple frictional contact, directly between inner tube wall and optical fibre. While we cannot guarantee the position of the fibre in this experiment, tube fill likely provides stabilisation to the position of the fibre against the wall.

At frequencies above 100 Hz, the induced signal is limited by the maximum force delivered by the shaker and as such error-bars in the transfer-ratios are larger. Nevertheless, the observed transfer loss up to 1,000 Hz is still typically only 6 dB. Summarizing, especially for frequencies up to 100 Hz, the main frequency range of interest for many seismic applications, the combination of modelling and experimental evidence indicates that the loss of axial signal is negligible, almost independent of tube fill.

7.5. 2D directivity

The coupling of strain through cable layers has been discussed in the previous Sections. Further investigations in this Section focus on the coupling of strain from the outside of the fibre into its core. A numerical model of the core, cladding and coating layers has been developed [82]. The investigation parameter in this study is the coating material.

Table 7.1 illustrates the resulting strain transfer efficiency for fibres coated with *acrylate* versus *copper* [86]. Acrylate is a typical coating material for standard telecommunications-grade fibre, while copper was chosen to show the influence of a significantly stiffer coating. A force-limited regime has been assumed for all cases: the gel will not be able to support large radial strains, and also the axial strain that can be transmitted onto a stiff copper-coated fibre will be limited.

Firstly, we consider the acrylate-coated fibre. The axial strain transfer ratio is almost unity. This result supports the good sensitivity found in experiments (Section 7.4) and field trials (Chapter 6). The radial sensitivity is significantly less, analogous to the reduced sensitivity due to losses through cable layers as presented in Figure 7.4.

The copper-coated fibre is less sensitive to both axial and radial strain because of its larger stiffness. The model shows that the ratio between axial and radial sensitivity is different for acrylate-coated versus copper-coated fibres. This characteristic can be used to provide a sensor that can differentiate broadside from axial signals: locating both fibres in exactly the same environment and interrogating both fibres simultaneously provides two signals with different contributions from axial and radial strain [86]. The combination of these two measurements can be used to distinguish these two directional components. This concept can be realised by integrating the two fibres with different coatings inside the same cable and connecting both

Table 7.1: Difference in axial and radial strain transfer into the fibre core, for acrylate and copper fibre coatings. A force-limited coupling regime and identical coupling to the environment are assumed. [86]

	Transfer efficiency for		Axial/ radial transfer ratio
Fibre coating	**Axial strain**	**Radial strain**	
Acrylate	99.2%	0.18%	551:1
Copper	17.9%	0.13%	138:1

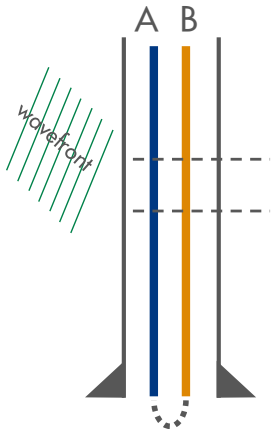

Figure 7.7: **Proposal for broadside signal analysis. By installing two fibres A and B in an identical way next to each other, only differing in the coating of the fibre, the axial and broadside response can be differentiated from each other. Significantly different coating materials, for example acrylate and copper, lead to different axial and radial strain transfer into the core. [86]**

fibres in series, as indicated in Figure 7.7. This setup provides a *directionally-sensitive sensor* in two directions, allowing independent determination of axial and broadside signal components. However, the two orthogonal broadside components cannot be distinguished yet. State-of-the-art geophones can provide directional sensitivity in all three orthogonal directions independently, as will be further discussed in Chapter 8. As such, a 2D directionally-sensitive sensor is an important step in that direction.

This concept unfortunately does not provide a solution for the low radial sensitivity of the combination of down-hole cable and optical fibre. Observing radial strain contributions due to weak seismic signals is currently unlikely, considering the current DAS instrument noise floor (Chapter 6). This concept has not been evaluated in a field situation yet. Nevertheless, the concept provides a way of realising independent determination of the broadside signal component, especially in view of future improvements in DAS instrument noise floor. This only requires inclusion of an additional optical fibre in a standard down-hole cable design.

7.6. Lessons learned

The combination of numerical modelling and experimental tests, as presented in this Chapter, indicates that the axial sensitivity of traditional down-hole fibre-optic cables is sufficient for DAS measurements. The broadside sensitivity, on the other hand, is significantly lower: without a major reduction of the instrument noise floor of current DAS interrogation units, broadside sensitivity is negligible. As such, typical down-hole cables are essentially one-dimensional sensors in the axial direction. This behaviour is also seen in field trials (Chapter 6) and has meanwhile been confirmed in additional, large-scale, experiments.

Based on a sensitivity-analysis of optical fibres with different coatings, a first concept for directional sensitivity is presented. Using two parallel fibres with coatings of different stiffness, axial and broadside signal can be independently determined. Unfortunately, this concept suffers from low radial sensitivities compared to the current instrument noise floor. Hence, more advanced ideas are required to improve broadside sensitivity and directional selectivity. This will be the topic of the next Chapter.

8. DAS for Geophysics: directionally-sensitive cable design

A range of geophysical DAS applications is in need of a directionally-sensitive cable. A broadside-sensitive cable has been developed and tested, incorporating a helically-shaped fibre. As a next step, component-selective cable designs are proposed, designed and tested.

8.1. Applications

The field trials and sensitivity analysis presented in Chapter 6 and 7 indicate that typical down-hole fibre-optic cables are predominantly sensitive in the axial direction and lack sensitivity perpendicular to this axis. Further efforts are required to provide cables which have better directional sensitivity, i.e., are not only sensitive along the length of the cable. These enhanced cables can serve a range of promising geophysical applications. Figure 8.1 gives an overview of such applications and their required directional sensitivity.

Vertical Seismic Profiling (*VSP*, Section 6.2) in *vertical* or moderately deviated wells is often sufficiently served by a cable that – to a large extent – is only sensitive along its length (Figure 8.1a). If the deviation of a well increases towards *horizontal* trajectories and hence the angle of incidence increases towards perpendicular – or *broadside* – to the cable length, cable sensitivity is significantly reduced (Figure 8.1b). As introduced in Chapter 6, if the angle between the seismic propagation vector and the direction of the cable is θ, then the sensitivity of a cable with a straight fibre is approximately proportional to $\cos^2\theta$. A cable with a straight fibre will therefore not detect P-waves propagating perpendicular to the cable length. This limited directional sensitivity is also a constraint for *micro-seismic* monitoring applications (Section 0), e.g., passive micro-seismicity induced by reservoir-compaction or hydraulic fracture characterisation, where seismic waves originate from events in the subsurface 'next to the well' (Figure 8.1c). Whereas for down-hole applications the suitability of traditional cables depends on the specific geometry as depicted in Figure 8.1a through c, *surface seismic* always suffers from the low sensitivity at broadside incidence angles (Figure 8.1d).

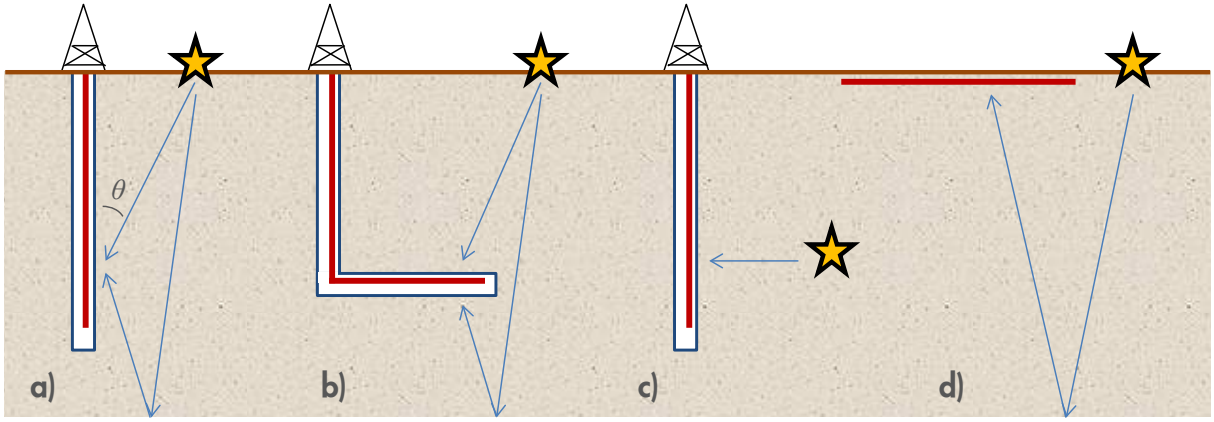

Figure 8.1: **Schematic representation of several geophysical monitoring applications and the orientation of the fibre-optic cable (red line). Vertical Seismic Profile acquisition with the cable installed (a) in a vertical well or (b) in a strongly deviated or horizontal well. (c) Micro-seismic monitoring of subsurface events. (d) Surface seismic. The sensitivity in applications b) through d) is currently limited by the predominantly axial sensitivity of traditional fibre-optic cables. [97]**

Table 8.1: **Overview of cable requirements for a range of down-hole (top) and surface (bottom) geophysical applications, compiled by analysing common knowledge in the oil and gas business. [87]**

REQUIREMENTS	DOWNHOLE APPLICATIONS					
#	A	B	C	D	E	F
Application	**VSP** *Vertical Seismic Profile in simple vertical well structure*	**VSP** *Vertical Seismic Profile in deviated well structure*	**VSP** *Reelable Vertical Seismic Profile in vertical well structure*	**VSP** *Reelable Vertical Seismic Profile in deviated well structure*	**Cross-well** *Detection of active source in neighbouring well*	**Microseismic** *Hydrofrac or reservoir surveillance monitoring*
Cable orientation	Vertical	Deviated	Vertical	Deviated		
Duration of use	Permanent	Permanent	Reelable	Reelable	Permanent	Permanent
1. Axial sensitive to signals along direction of cable	●	●	●	●	○	●
2. Broadside sensitive to signals impinging perpendicular to cable	○	●	○	●	●	●
3. Component selective sensitivity to one broadside comp.						
4. 3C sensitive to three orthogonal components	○	○	○	○	○	●
5. High sensitivity geophone-like sensitivity if high SNR required	○	○	○	○	○	●
6. Ruggized to survive (mainly in-well) deployment	●	●	●	●	●	●
7. Size limitation to fit in typical well dimensions	●	●			●	●
8. Extended length for >5km sensing lengths						

● Required	○ Desired

REQUIREMENTS	SURFACE APPLICATIONS					
#	G	H	I	J	K	
Application	**Monitoring** *4D reservoir monitoring in trench*	**Datahole** *4D reservoir monitoring in shallow dataholes*	**Subsea** *Deployment on ocean bottom*	**Exploration** *Temporary deployment on surface*	**Microseismic** *Hydrofrac or reservoir surveillance monitoring*	
Cable orientation	Horizontal	Horizontal	Horizontal	Horizontal	Horizontal	
Duration of use	Permanent	Permanent	Permanent	Temporary	Permanent	
1. Axial sensitive to signals along direction of cable					●	
2. Broadside sensitive to signals impinging perpendicular to cable	●	●	●	●	●	
3. Component selective sensitivity to one broadside comp.	●	○	○	●	●	
4. 3C sensitive to three orthogonal components	○	○	○	○	●	
5. High sensitivity geophone-like sensitivity if high SNR required	○	○	○	○	●	
6. Ruggized to survive (mainly in-well) deployment		○	●	○		
7. Size limitation to fit in typical well dimensions						
8. Extended length for >5km sensing lengths			○	●		

● Required	○ Desired

Table 8.1 provides a more detailed overview of applications for cables with enhanced directional sensitivity [87]. This overview is based on a market study of possible geophysical applications in the oil and gas industry in general.

Eight requirements have been defined in order to differentiate between applications. First, we have the regular *axial sensitivity* (#1). Next, *broadside sensitivity* (#2) is an essential first step towards enhanced cables as indicated in Figure 8.1. Some applications not only require sensitivity to broadside-incident signals, but also need the ability to distinguish between energy incident from different directions, i.e. *components*. Surface seismic applications benefit from this single-*component selectivity* (#3) by being only sensitive to the vertical direction: this is the direction in which subsurface reflections (and refractions) are incident. Moreover, being only sensitive to the vertical component reduces the noise-contribution from ground-roll energy which is also present in the horizontal directions. For micro-seismic monitoring, it is important to know the origin of a sub-surface event. Micro-seismic signals have often only low signal-strengths. The required *high sensitivity* (#5) makes micro-seismic monitoring a challenging application: even with dedicated geophones, the signal of an event is sometimes sufficiently weak to be only detected by sensors in one well. The ratio between incident energy in different directions is typically used to determine the event's origin, for each well individually. Whereas for surface seismic only the vertical direction is sufficient, in this case all three components need to be measured independently (a *three-component* sensor (#4)). Apart from ensuring a cable has sufficient sensitivity, it also has to withstand the deployment. In general, down-hole applications typically require more *ruggedized* cable designs (#6) in order to survive deployment and long-term down-hole conditions (Chapter 2) compared to surface deployment. Limited well-bore space also imposes more stringent *size limitations* (#7), whereas some surface applications require *extended sensing lengths* (#8) to achieve sufficient spatial spread.

DAS can provide a viable solution for above applications if the directional sensitivity of fibre-optic cables is improved. Such development for *Distributed Geophysical Sensing* (*DGS*) aims at extending the applicability of DAS and its potential advantages such as lower cost, user-controlled spatial sampling and small footprint.

In general, two ways to improve directional sensitivity with DAS are being considered: fibre shaping and cable shaping.

Fibre shaping aims at incorporating the fibre in the cable in such a way that it has a projection in the broadside direction. While different realisations to achieve this are possible, a *helically-shaped fibre* is introduced in Section 8.2. This concept fundamentally has *broadside* sensitivity to radial *strain* induced by changes in pressure, resulting from an impinging acoustic wavefront.

Cable shaping, on the other hand, involves construction of a cable so that an axial movement of the fibre is obtained when the cable experiences a transverse *motion*. Mass-spring-system-based realisations are introduced in Section 8.3, employing an *inertial member* to induce axial strain in the optical fibre. Proof-of-principle experiments have been conducted and confirm increased broadside sensitivity (Section 8.4), while introduction of asymmetries in the design results in a *component-selective* cable.

A field trial of both concepts will later be presented as well. The results of this field trial indicate the feasibility of the concepts to improve directional sensitivity, and provide an outlook (Section 8.6) for further development into deployable versions.

8.2. Helically-shaped fibre

Shaping fibre in a cable such that it has a projection in the transverse direction can be achieved by incorporating the fibre in a helical shape along the axial direction of the cable. The transverse projection of such helically-shaped fibre is significantly larger than for an overstuffed fibre in a traditional down-hole cable as discussed in Chapter 7.

The response as a function of the angle of incidence θ, with respect to the axis of the cable, is given in Figure 8.2. The response is calculated taking into account the orientation of the incident wave with respect to the axis of the helically-shaped optical fibre. A cable with a helically-shaped fibre is nearly equally sensitive in all directions (red solid curve). A specific linear combination can be made mathematically with the shaped fibre and the straight fibre response (green curve) that results in a response without inline sensitivity (purple curve). In other words: a broadside-sensitive cable [88].

A broadside-sensitive cable is then sensitive to radial *strain* coupled from the formation into the cable. As such, the response depends on the acoustic impedance contrast, resulting from the difference between cable material and soil properties. As an example, the dotted lines in Figure 8.2 show the reduced sensitivity in case the soil is harder than encountered in Schoonebeek [97]. This creates a challenge in manufacturing of the cable: optimal materials should be chosen to minimize the impedance contrast and hence maximize sensitivity. The properties of these materials should meanwhile also allow efficient use in the cable production process and result in a cable that can be successfully deployed.

An 800-metre long cable has been manufactured and deployed in a surface-seismic field trial in Schoonebeek, an oilfield in The Netherlands operated by NAM. The cable was installed in a trench (Figure 8.9a), alongside an array of accelerometers to provide a reference measurement.

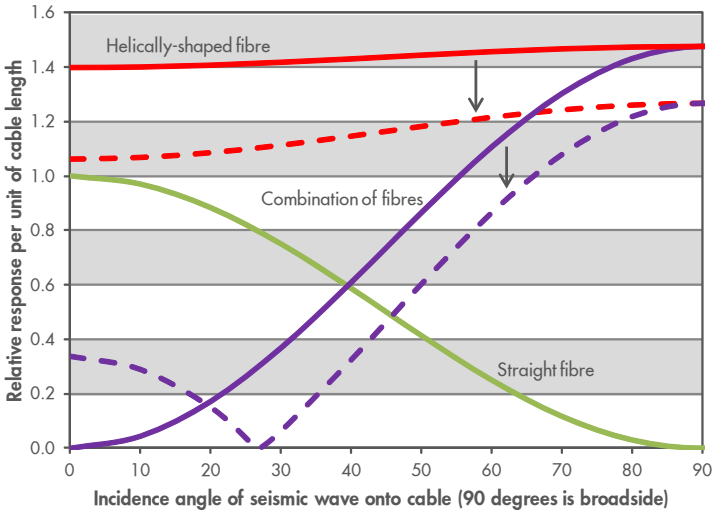

Figure 8.2: **Amplitude response as a function of the angle of incidence θ for a cable with a straight fibre (green), a (helically-) shaped fibre (red) and a mathematical linear combination (1*shaped – 1.37*straight) of these two for ground conditions as seen in Schoonebeek (purple). For a harder soil than encountered in Schoonebeek, the response would be as shown with the dotted lines, resulting from a change in sensitivity of the shaped fibre. All curves are normalized based on the response at $\theta = 0°$ of a cable with a straight fibre. [97]**

Trial results are shown in Figure 8.3. It clearly shows that the cable with the shaped fibre records reflection energy, which is absent from the cable with the straight fibre. The *ground-roll*, a surface wave which has inline and vertical components, is seen by all systems. It can also be observed that the cable with the shaped fibre is more sensitive to ground-roll from ambient noise sources than the vertical accelerometer: ground-roll is indicated by red arrows in Figure 8.3c, while it is largely absent in Figure 8.3a [89].

The experimental results of this helically-shaped fibre concept show that it is an interesting solution for applications that require broadside sensitivity. Further research activities were carried out, confirming the radially-symmetric broadside sensitivity [89]. Component-selectivity is the next step, and will be discussed in Section 8.3.

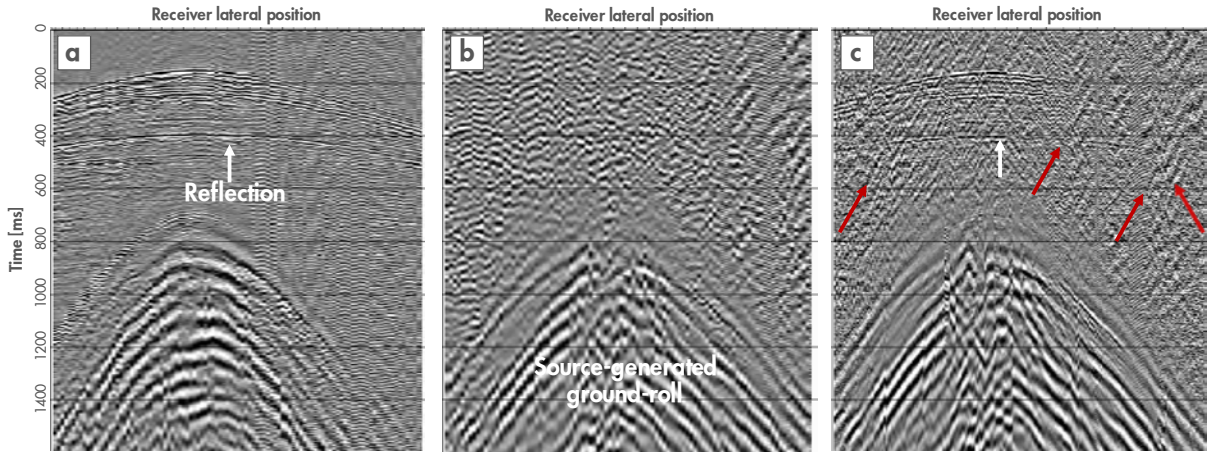

Figure 8.3: Shot records recorded in three collocated detector systems: (a) vertical accelerometers; (b) a straight fibre; (c) a shaped fibre. The white arrows point at reflection energy, absent on the straight fibre; the red arrows on the shaped fibre record (c) point at ground-roll from ambient noise sources. [97]

The author's involvement with development of the helically-shaped fibre mainly entailed support to the design, execution and analysis of field trials. Involvement with the development of inertial-member designs, as described in the next Sections, is significantly more extensive, ranging from initial idea generation, via proof-of-principle laboratory experiments and field trialling, to follow-up development efforts.

8.3. Inertial members

The broadside-sensitive cable has a disadvantage as illustrated in Section 8.2: it can distinguish between inline and broadside signal components, but not the azimuthal incidence angle, i.e., not between broadside waves that arrive – in this horizontal deployment – from up, down, left or right. Ideally, a cable sensitive to one broadside direction only would be preferred for certain applications. In surface seismic, such a component-selective cable oriented vertically would reduce the sensitivity to surface waves. A three-component cable could be used in a range of applications, e.g., in (down-hole) micro-seismic monitoring where one wants to distinguish between the different directions to determine where the event originates from.

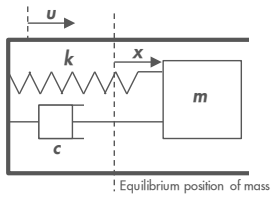

Figure 8.4: Diagram of an inertial sensor, showing the mass *m* free to move uni-directionally within the case under the influence of a spring (spring-constant *k*) and damper (damping coefficient *c*). [93]

A potential cable design is based on the same concept as traditional geophones: a mass-spring system as illustrated in Figure 8.4. By suspending a *mass* inside a *case* using a *spring*, motion of the case is transmitted to the mass. The finite *stiffness* of the spring causes an *inertial* effect with at least one *resonance frequency*: the mass will follow the motion of the case at frequencies significantly below the resonance, while the motion of the mass will be in counter-phase at frequencies above the resonance: a frequency-dependent difference in motion of the mass versus motion of the case is the result. The large amplitude-response at the resonance frequency is suppressed by including a fine-tuned *damping*. By limiting the motion of the mass mechanically to one direction only, a component-selective sensor is created. Such sensor can be placed in the soil using a spike to pick-up surface seismic, or lowered in a well to conduct, e.g., VSP surveys (Chapter 6). After almost a century of development efforts and further improvements, electrical geophones have evolved into extremely accurate and reliable sensors [91].

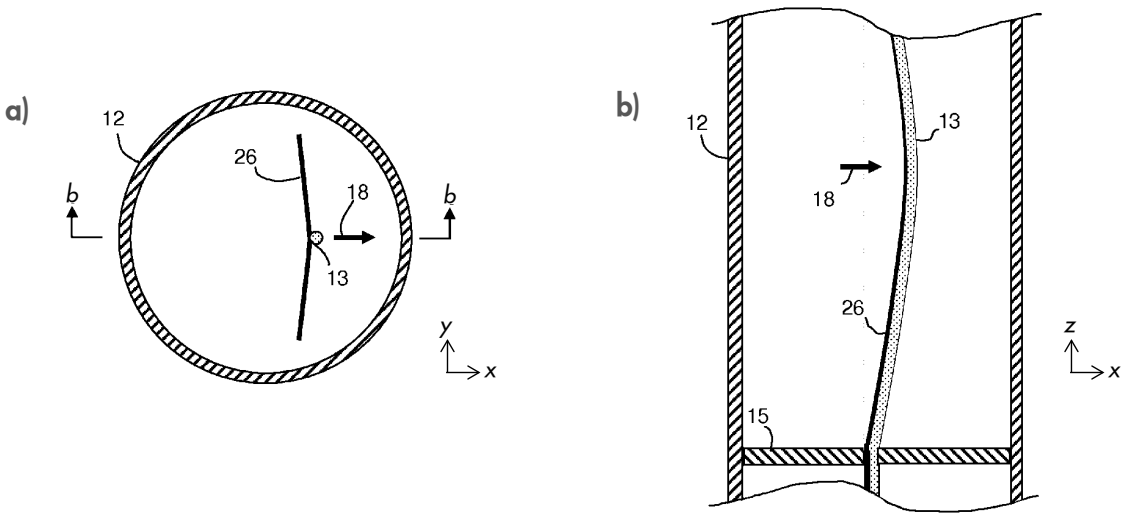

Figure 8.5: Fibre-optic cable concept exploiting inertial members (#26) to induce strain on an optical fibre (#13), by means of an inertial member flexing between supports (#15). (a) Perpendicular cable cross-section. (b) Longitudinal cable cross-section as indicated in a). Analogues to a basic mass-spring system, the inertial member fulfils the combined role of mass and spring. Broadside motion of the cable case (#12) will cause a differential displacement (#18) of the inertial member, resulting in an axial strain on the fibre. Figure from patent application [92].

An electrical geophone combines this mechanical system with an electrical pick-up of the motion of the mass within the case, resulting in a sensor-reading proportional to the velocity of the case. The same concept can be used to realise a fibre-optic sensor, by using an optical fibre to detect the relative movement of the mass compared to the case. Realisations of fibre-optic geophones exist already [90]. Still, there is a challenge in translating such concepts into a fully-distributed sensor. Creating a distributed mass-spring system, along the entire length of a sensing cable, allows the use of Distributed Acoustic Sensing to interrogate such distributed *inertial assembly*. While multiple realisations can be envisioned, two specific concepts will be presented here: a *strip*-based inertial member and a *bowspring*-based inertial member.

One realisation is depicted in Figure 8.5. This involves attaching a *strip* (#26) to the optical fibre (#13) and supporting the strip periodically along the length of the fibre (#15). In this way, a mass-spring system is created. The strip's density is providing the mass and the strip's stiffness is acting as a spring. Broadside signal now leads to flexing of the strip (#18). The fibre, attached to the side of the strip, will experience an axial strain as a result of the strip's flexing motion. Thus the axial strain is now related to the broadside dynamic displacement of the cable.

By shaping the strip such that the stiffness in the two broadside directions is different, the fibre can be made predominantly sensitive in one particular broadside direction. An example can be found in Figure 8.5a, where the strip has different dimensions in the *x*- and *y*-direction. The higher stiffness in the *y*-direction, due to a wider cross-section, limits the deflection, resulting in a lower signal compared to the more sensitive *x*-direction: hence a component-selective sensor has been created [92].

Another realisation involves the use of *bowspring*-like components. In analogy to the flexing of the strip in the previous concept, the bowspring assemblies convert the broadside motion of an inertial mass into an axial strain on the optical fibre. Figure 8.6 shows a bowspring assembly with two pairs of bowspring blades (#50A, 50B and #51A, 51B). One end of each bowspring blade is connected to a sleeve (#53A, 53B) which slides along the central member. The other end of each bowspring blade is fixed to an elongate central member (#52), which serves as inertial mass. The bowspring blades serve as springs to suspend the mass of the central member within the cable. An optical fibre is fixed between the two sliding sleeves. The central member will move out of phase with the cable's inner wall (#55) in large parts of the frequency spectrum. This will cause the sliding sleeves to move and vibrate in opposite longitudinal directions relative to each other

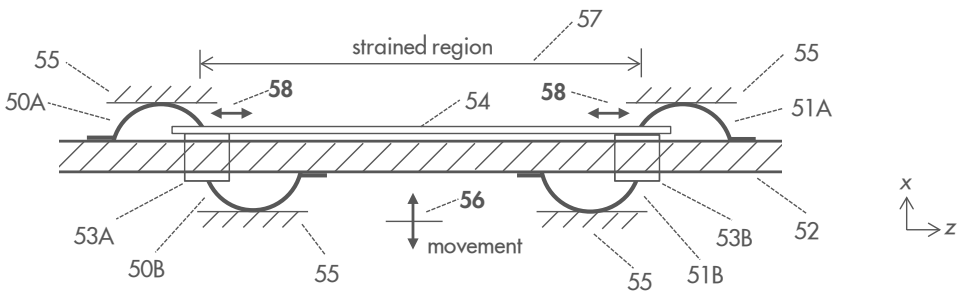

Figure 8.6: Fibre-optic cable concept exploiting inertial members to induce strain on an optical fibre (#54), by means of a central member (#52) suspended between two pairs of bowspring blades (#50A,B and #51A,B). Broadside motion results in axial strain (#58) on the part of the optical fibre attached between the two sliding sleeves, resulting from an inertial differential movement (#56) between central member and cable enclosure (#55). Figure from patent application [93].

as illustrated by the arrow (#58), inducing an axial strain on the optical fibre attached between the sliding sleeves. Because the bowspring blades only support inertial motion of the central member in one broadside direction, again a component-selective sensor is created [93].

These inertial sensors are sensitive to ground motion rather than to strain. Hence, the acoustic impedance contrast between sensor cable and soil has a lower impact on the sensitivity than for, e.g., the helically-shaped fibre (Section 8.2). A *three-component* sensor can be realised by combining multiple component-selective sensors: two orthogonally-oriented component-selective cables can be combined with a straight fibre to enable independent measurements of all three components of a seismic wave. The result is a sensor with directional sensitivity similar to a geophone. The maximum number of sensors in a sensing cable is now only determined by the channel length of the DAS interrogation unit. This setup has the potential to provide a more densely-distributed array of sensors than typically economically achieved with geophones.

8.4. Proof of principle

A laboratory experiment was set-up to generate the proof-of-principle test of such inertial member designs (Figure 8.7). The primary goal was to show increased broadside sensitivity. Ultimately, the inertial sensor design has to be of down-hole cable dimensions, with typical down-hole cables having a ¼" outer diameter. A vibration stage has been fitted with cylindrical grooves of such dimensions in order to simulate the inside of such a cable. Inside these grooves, inertial member prototypes have been inserted.

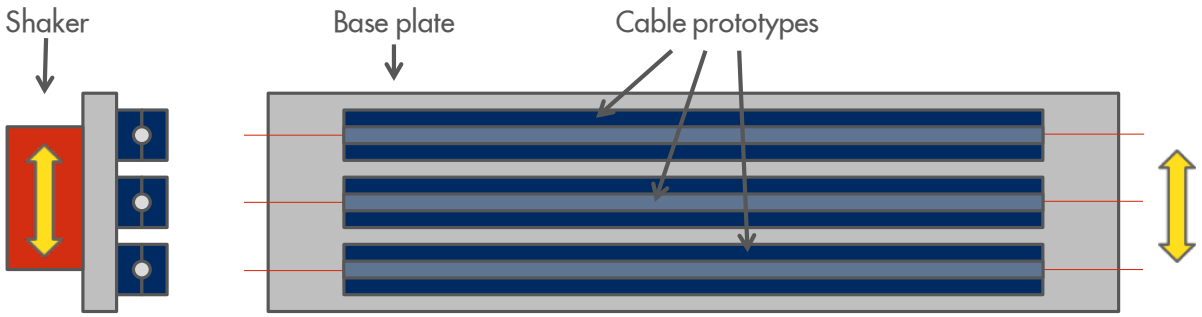

Figure 8.7: Schematic representation of the shaker table, showing the base plate with three grooved bars containing cable prototypes. The yellow arrows indicate the direction of shaking. [94]

Experimental results showed significantly increased broadside sensitivity of the inertial-member designs. The baseline for this measurement is a typical fibre in gel as used in conventional down-hole cables. To illustrate the improved sensitivity in a realistic frequency range, a seismic signal recorded in the field has been synthesized and fed into the driver of the vibration stage. The signal represents a dynamite shot and was originally recorded by geophones in an exploratory seismic survey. Figure 8.8 displays the raw time data for such an attempt for a DAS channel containing the (reference) fibre with gel, and for a DAS channel containing an inertial member assembly. While the signal observed in the fibre-in-gel is rather small (Figure 8.8a), the inertial-member assembly result clearly shows a response to the original input signal (Figure 8.8b). This clearly illustrates the increased broadside sensitivity [94].

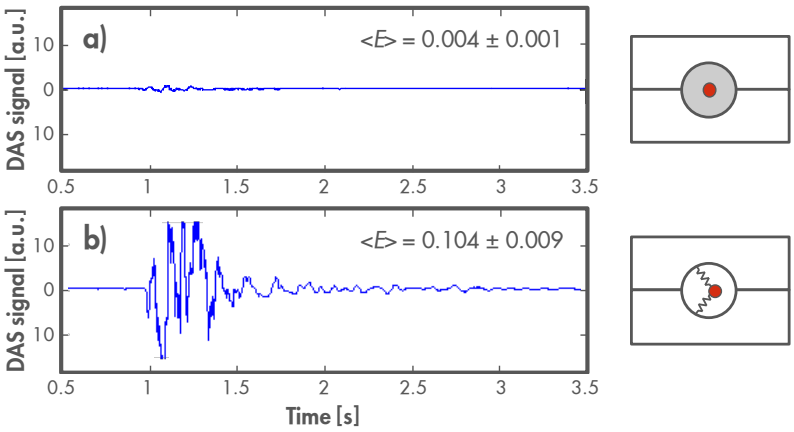

Figure 8.8: **Results for a dynamite-shot input signal to the shaker table [94], for two test assemblies (from top to bottom): fibre-in-gel (reference) and inertial member. Plotted is the measured DAS signal as a function of time. The RMS amplitude *<E>* in a frequency range 5-120 Hz, including noise, has been calculated. The indicated error represents the intra-experiment error of three repeated datasets.**

8.5. Field trial

Demonstration of the improved sensitivity in the lab, for both designs as introduced in Section 8.3, was followed by manufacturing and deployment of prototypes in a field trial. The cable prototypes have been deployed in the same surface seismic field trial in Schoonebeek as the helically-shaped fibre (Section 8.2). Deployment of this cable is illustrated in Figure 8.9a. As discussed in Section 8.2, the helically-shaped fibre prototype is a continuous cable allowing fully-distributed broadside measurements.

The inertial member prototypes have been installed alongside the helically-shaped fibre prototype, in the same trench [95]. So far, only point sensors have been built as illustrated in Figure 8.9b. To enable characterisation of their component-selectivity, three-component accelerometers have been collocated to provide a reference measurement. Based on our analysis of the experimental results [96], it can be concluded that all prototypes delivered promising results, despite the non-optimized frequency response of these first prototypes. We are sufficiently encouraged to continue our investigations.

8.6. Outlook

The cable prototypes with improvements to broadside and component-selective sensitivity – incorporating fibre shaping and cable shaping concepts – are valuable solutions for both surface and down-hole applications (Section 8.1). Improved directional sensitivity has been successfully demonstrated in a surface-seismic field trial.

Further development of both concepts is planned. The broadside-sensitive helically-shaped fibre will be trialled in other environments to investigate the fidelity of the signal, including other ground conditions and down-hole installations. The fully-developed cable shall be a readily deployable, continuous cable for both surface and down-hole broadside sensitivity.

To aid the development and characterisation of distributed sensors further, a novel test setup has been developed based on the initial setup as depicted in Figure 8.7. This setup enables input of arbitrary wave-fronts, irrespective whether these are combinations of axial, broadside, compressional, or displacement signals. In this way it is possible to test the response of a sufficiently long test piece under conditions as encountered in the field, at the benefit of improved development cycle-times inherent to controlled laboratory experiments [98].

Using this facility, the component-selective inertial-member concept will be further developed towards a distributed, integrated prototype cable with optimized frequency response in three components.

The combination of these cable solutions has the potential to provide the required degree of directional sensitivity to further enhance the application scope of DAS for geophysical applications such as found in Table 8.1.

Figure 8.9: **Deployment of prototype cables in Schoonebeek for a surface seismic field trial. (a) Broadside-sensitive cable is spooled from a transport reel and positioned in a trench. (b) Several component-selective prototype sensors installed in a ruggedized box, ready for deployment next to the broadside-sensitive cable prototype in the trench. [97]**

9. Depth calibration for DAS: design

The Magnetic Depth Locator (MDL) is a tool which provides a non-intrusive means of depth referencing for fibre-optic Distributed Acoustic Sensing (DAS) in-well measurements. The possibility of repeating the calibration at negligible incremental cost, makes it very suitable for safeguarding the depth reference accuracy of time-lapse well and reservoir monitoring.

9.1. Well-logging accuracy

Depth referencing is a crucial aspect for traditional *well-logging* operations. Well-logging includes geophysical measurements in a well-bore, as well as *petrophysical* measurements. Geophysical measurements – such as VSP acquisition as introduced in the previous Chapters – provide an areal coverage away from the wellbore. The field of petrophysics aims at characterising the rock properties and fluid distribution in greater detail and at a better depth resolution than typical geophysical methods can achieve, however, typically limited to the immediate vicinity of the well-bore (typically up to about 1 metre away). Petrophysical evaluation tools include nuclear logs (such as a *GR log*, detecting natural gamma rays), *electrical resistivity* logs, down-hole nuclear magnetic resonance (*NMR)* scanners, rock samplers (*coring*), flow sensors, pressure measurement and fluid-collection devices. Whereas individual tools can provide information down to the molecular level of the sub-surface, it is the *combination* of these individual measurements that provides the most valuable information. *Logging tools* are typically only temporarily lowered in a well using an electric *wire-line* providing real-time data-transfer to surface. The depth of each individual measurement in a well-bore has to be accurately known, in order to compare and integrate various datasets at the correct location. Eventually, the results have to be related to depth in the formation, rather than just to a depth relative to the well-bore. Therefore, *depth referencing* is of paramount interest in well-logging quality-control procedures.

Continuous measurements along the well-bore by means of fibre-optic cables are becoming an increasingly valuable surveillance solution, complementary to well-logging. They allow acquisition of (cased-hole) petrophysical and geophysical data in real-time without well-intervention unlike wire-line tools. These datasets show changes during the life of a well, also in well-configurations where deployment of traditional logging tools is not possible or too expensive. Distributed Acoustic Sensing can measure acoustic signals along a fibre-optic cable, which can be used for a variety of applications: seismic surveys, flow assurance, performance monitoring, hydraulic fracture monitoring and many others. Like in conventional well-logging, it is crucial to calibrate the fibre length to a common depth reference. This allows such fibre-optic datasets to be compared against each other and to integrate them with other well-logs and areal datasets.

This Chapter provides an overview of typical depth inaccuracies in fibre-optic installations (Section 9.2), followed by an example of the accuracy that is required for field application (Section 9.3). Starting from Section 0, a novel non-intrusive depth-referencing tool for DAS measurements will be introduced.

9.2. Depth accuracy

Fibre-to-formation depth conversion has many possible sources of error. These inaccuracies – and the calibration steps required to correct them – can be summarized in three contributions

(Figure 9.1). First, the calibration from the distance as inferred by the DAS interrogation unit to the physical *length in the fibre*. Second, the relation between physical length of the fibre and location with respect to the well-configuration, the so-called *drillers' depth*. And third, the correlation between the drillers' depth and *formation depth* as typically established using standard practices from a wire-line logging survey. The main goal of depth referencing is to relate (sensor) measurements accurately to important features in the formation, e.g., reservoirs or other zones-of-interest. Generally less important for data interpretation are, e.g., the absolute depth all the way from surface or the drillers' depth, although these can be valuable intermediate steps in a depth-referencing procedure.

Figure 9.1: Typical calibration steps to achieve calibration from measured fibre length to position in the formation.

Uncertainties in the conversion from drillers' depth to formation depth are: stretching of the pipes due to being hung-off in the well, thermal expansion of the pipes (e.g., due to reservoir temperatures typically ranging from 50°C up to approximately 300°C in case of steam injection) and differences in reference depths (e.g., referenced from the drill floor versus a reference to a part of the well-head assembly, such as the *top bottom flange*).

A number of techniques have been proposed to provide a direct calibration from fibre-to-formation by using wire-line logging tools. One of the most promising techniques measures the acoustic signature of a logging tool travelling upwards through the well-bore [99]. A depth reference can be obtained by combining the location in the fibre where the noise is generated with the wire-line depth at each moment in time. Such a *cased-hole* wire-line survey accurately measures the depth location of the DAS channels, which can be tied to formation depth if the cased-hole survey also contains a logging tool – such as a GR log – which can read formation properties through the casing.

Unfortunately, the use of logging tools is not always an option. The well might not be accessible to logging tools due to the inability to slide tools into the well, for example in long horizontal, snake or fishhook wells, subsea wells, or due to restrictions in the wellbore such as narrow tubing. In observation wells, it might not be economically feasible to log the well with conventional logging tools [100]. These economical and practical limitations play an even more important role in time-lapse monitoring for well and reservoir management. Although the calibration should be confirmed over time, periodic running of logging tools is likely too expensive, especially if production deferment is also taken into account. In such cases, it would be valuable to have *depth markers* as part of the well-configuration. If such permanent depth markers can be observed in a DAS measurement, they would provide a *non-intrusive* means of *depth calibration*.

Since usually depth markers are attached to the well-configuration, they do not provide a marker relative to the formation. Previously described uncertainties in the conversion from drillers' depth to formation can therefore not be corrected for in this way directly. In Chapter 10 a combination of calibration steps will be presented as solution for this. However, there is a significant number of error sources related to the calibration from fibre to well length, and these can be calibrated with such depth markers attached to the well configuration. For example:

- The fibre is installed in the cable with a certain *overstuffing* to withstand thermal expansion, and the cable is generally not installed along the pipe in a straight line but rather (partially) wrapped around it due to installation procedures. Both fibre-overstuffing and cable trajectory might change over time due to, e.g., temperature cycles and slow downward migration of fibre and cable. Fibre-overstuffing is typically 0.5% to 1% of the cable length [101], and it might potentially – for example under influence of gravity – fully stretch over time. Partial wrapping of cable around the pipes can be of similar magnitude or larger, and can also change over time – for example due to temperature cycles.
- Connection of different DAS interrogation units also introduces significant errors, especially for drive-by solutions, repeated often and with varying equipment. Each time, the interrogation unit can have a slightly different fibre distance offset and fibre length conversion. Most likely, different lengths of lead-in cables will be used, which also affects the calibration each time. Although channel offsets and lead-in cable length can be calibrated by a surface marker, even the smallest change in fibre length conversion creates significant errors.
- Considering the refractive index value only down to two decimals already introduces an error of about 0.5% in the length conversion. For example, both 1.47 and 1.465 are common refractive index values depending on which fibre is used, and often not known by the installer and cable vendor. A mismatch between the refractive index used for length conversion and the actual refractive index of the fibre, introduces a highly undesirable systematic error. This systematic error can easily occur, and change between surveys, due to differences in acquisition equipment, fibre specifications and installation documentation.
- Splice chambers along the optical path, e.g., to feed the cable through a packer, have some extra length of fibre. Also, the cable is often wrapped multiple times around the tubing just before exiting at the well head. This makes calibration methods using acoustic signals along the cable at surface significantly less useful, adding to the need for down-hole depth markers especially if wire-line tools cannot be deployed for an initial calibration to formation depth.

As summarized in Table 9.1, if depth markers would not be implemented, the above-mentioned errors in fibre length over time can easily add up to 2% of the cable length (which corresponds to the average total error in Table 9.1). For a 1 km long well, this results already in a depth inaccuracy of 20 m, or more than two DAS channels, assuming a channel length on the order of 10 m (Chapter 5), and can potentially vary over time.

Table 9.1: Typical sources of errors and their influence on depth accuracy for a 1 km deep well. Please note that the errors given are only crude estimates based on general cases. The majority of errors is always leading to additional fibre length and hence individual errors can be linearly summed.

Error source	Error	Remark	Length error for a 1 km well [m]
Fibre overstuffing in cable	0.5 – 1.0 %	of cable length	5 – 10
Refractive index variation	±0.005	refractive index difference	-3 – 3
Splice chamber	1 – 10 m	extra fibre length	1 – 10
Cable not installed straight along pipe	0.5 – 1.0 %	of well depth (estimate)	5 – 10
Total per 1 km deep well (estimate)			**8 – 33 m**

9.3. Application

To show the impact of a fibre length error on the order of 20 m, consider a crucial *reservoir monitoring* application: *time-lapse* Vertical Seismic Profiles.

In-well DAS has been trialled (Chapter 6) for time-lapse purposes to monitor sub-surface changes over time due to, e.g., steam injection, together with dedicated time-lapse surface seismic systems which serve as a reference. First, consider the surface-seismic system, solely to quantify how accurate seismic travel times have to be for time-lapse monitoring. To minimize repeatability errors, sources and receivers are typically permanently installed. During periods of steam injection, typically observed maximum time shifts due to changes in the reservoir ranged from 0.2 ms to 5 ms [103].

Now we can have a look how these time shifts translate to repeatability requirements for a VSP acquisition with a down-hole receiver array, or fibre-optic cable for that matter. This situation is illustrated in Figure 9.2. First consider a time shift of 5 ms. This is considered a rather large effect, but it would still be masked by a down-hole sensor displacement – assume an average wave velocity of 2500 m/s [102] – of only 12.5 m: a shift in the order of 1.5 DAS channels. We estimated that DAS possibly has an error of 20 m or more (Section 9.2); clearly this is a large error for which we should find a way to calibrate for.

On the low end, a time shift of 0.2 ms equals only 0.5 m of sensor position inaccuracy. Such extremely high accuracy is not always required because of the expected magnitude of the time shifts, and relative depth calibration might often be sufficient for time-lapse monitoring: The aim is that DAS channels' depth positions should remain constant from survey to survey, or in other words, the relative depth calibration should be sufficiently constant over time. This is achieved in the surface time-lapse applications by having permanent installations. However, in a well, for the reasons explained in Section 9.2, fibre-to-depth calibration could change over time and therefore the relative depth calibration condition may no longer be met.

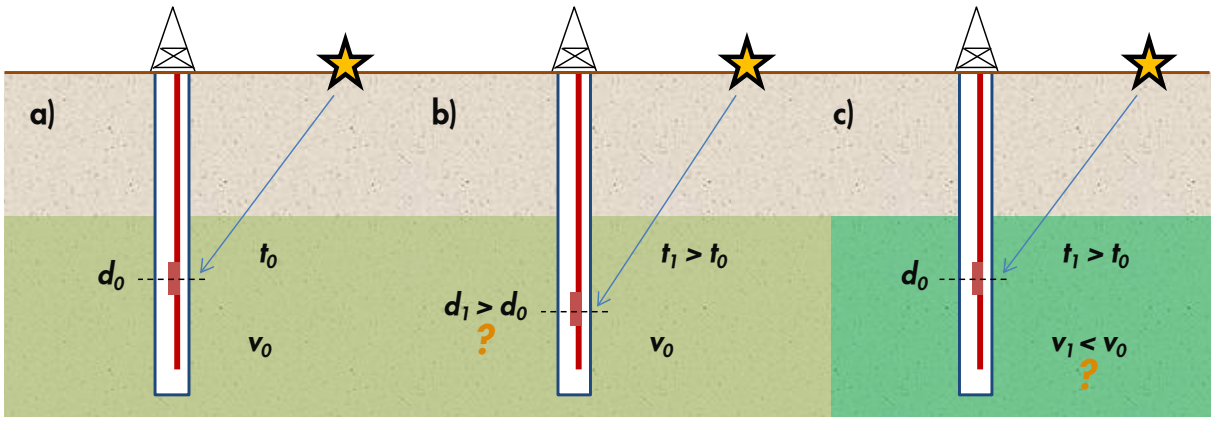

Figure 9.2: **Simple case of a check-shot in a VSP installation. (a) Initially consider a first arrival t_0 incident on a sensor in the well-bore at depth d_0. This part of the well is located in a formation with acoustic wave velocity v_0. An increase observed in arrival time t_1 in a repeat survey can be interpreted as either (b) a change in position of the sensor to depth d_1 or (c) by a change in properties of the formation resulting in a lower velocity v_1. Time-lapse depth calibration with the Magnetic Depth Locator cancels the impact of a change in sensor position over time as depicted in (b).**

Non-repeatability of the DAS channel to depth calibration reduces the possibility of success of in-well time-lapse monitoring programs, especially in fields where the reservoir time-lapse effects are small and increase slowly over time. Natural subsurface features – such as a time-invariant non-reservoir reflection – cannot always be used for depth calibration. Even if possible some inaccuracy might still be accumulated over the fibre length from that feature downward to the reservoir. Thus, suitably placed depth markers can facilitate calibration all the way down to the reservoir, and even further down to the end of the fibre when required.

Concluding, depth markers as part of the well-configuration can help significantly in correcting for a majority of depth-calibration inaccuracies. The *Magnetic Depth Locator* (*MDL*) concept, as will be presented in Section 0, provides such depth markers. In that way, it provides a non-intrusive on-demand depth calibration method enabling accurate time-lapse DAS measurements for well and reservoir monitoring.

9.4. Magnetic Depth Locator

Acoustic vibrations are generated locally in a fibre-optic cable at positions where a magnet is placed next to it, by applying an AC electric current through the cable's inner tube [104]. As depicted in Figure 9.3, the interaction between the applied current and the perpendicularly oriented magnetic field results in a Lorentz force on the inner tube containing the fibre. By applying an alternating current, the Lorentz force also alternates and thus induces an oscillation of the inner tube. This vibration is localized since the generation of Lorentz force only extends over the length of the field-generating magnets.

A standard down-hole fibre-optic cable can be used (Chapter 1), in which the inner tube is used to convey the electrical current and is insulated from the outer tube by a polymer buffer, e.g., polypropylene. This allows current flow along the length of the cable without shortcutting to the well environment. The cable's outer tube – *control-line* – or the well construction is used as a return path for the current.

The vibration induced in the fibre-optic cable can be picked up by DAS. In this way, the optical channel collocated with the magnet can be determined at the various magnet-positions along the

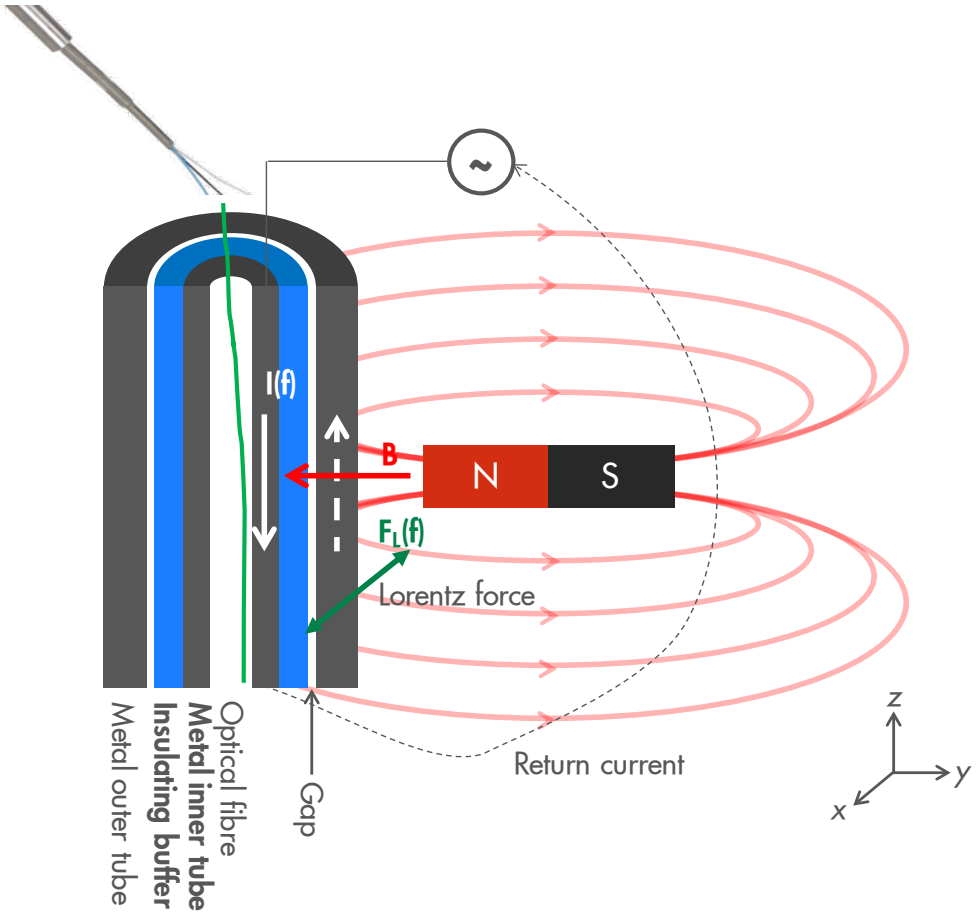

Figure 9.3: **Concept of the magnetic depth locator. The combination of an AC current *I(f)* through the fibre-optic cable and a local magnetic field *B* creates an AC Lorentz force $F_L(f)$ and hence a local vibration signal detected by DAS at the position of the magnet. The return path for the electric current is provided by either the outer tube or the adjacent formation. The gap between buffer material and outer tube is crucial to allow for vibration of the inner tube.**

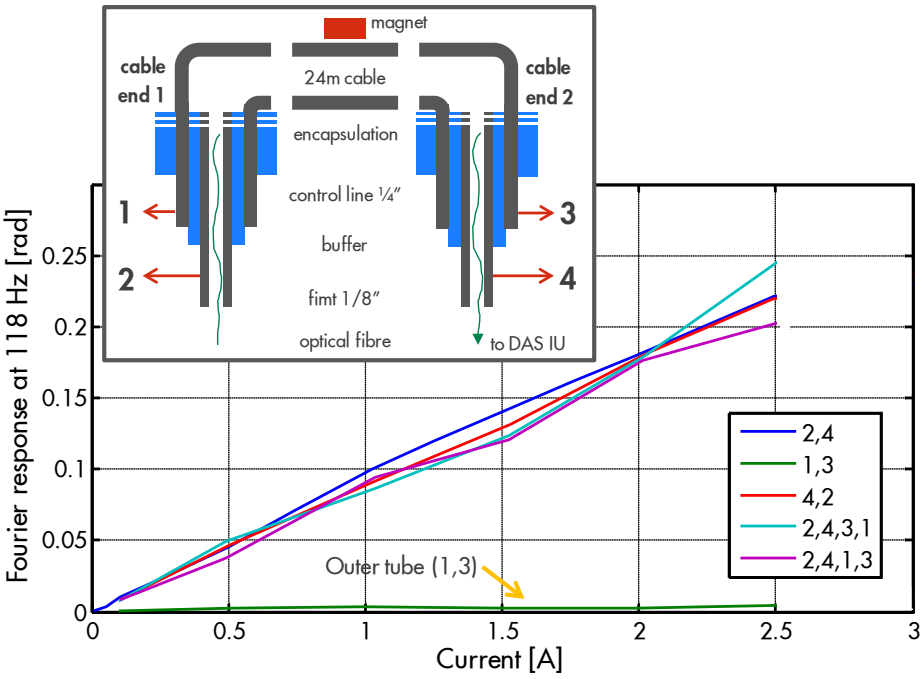

Figure 9.4: **MDL signal as a function of electrical current. The numbers *(i,j)* in the legend indicate the current path through the respective cable tubes. Within the limits of the power source, the signal is proportional to the current through the cable's inner tube. A current through the outer tube had a negligible influence on the acoustical signal generated, in line with the larger stiffness of the outer tube.**

cable length and thus a depth reference is provided. DAS measurements are entirely unaffected once the electrical current is switched off, while repeat calibrations only require applying the current again. The simple procedure of determining the optical channel which observes the MDL vibration provides only depth accuracy equal to the length of one channel, currently on the order of 10 m. A solution to obtain sub-channel accuracy will be presented in Section 9.6. The next Section will first describe optimisation of the signal reliability.

9.5. Reliability

To characterize the basic response function of an MDL depth marker, laboratory tests were conducted. A setup comprising of 24 m length of typical down-hole cable was used for this [103]. Magnets could be attached all along the length of this cable and an electrical current could be applied to the cable. The resulting response was then measured with DAS.

Initial tests indicated that the DAS signal-response to the induced vibration is proportional to the electrical current at a given frequency through the cable's inner tube, indicated in Figure 9.4. Current flow through the outer tube does not significantly influence the signal, since the larger stiffness of the outer tube reduces the induced motion. The acoustical signal is mainly due to vibration of the inner tube, due to alternating current through the inner tube interacting with the permanent magnetic field. This has the advantage that the motion is only limited by the free space between buffer and outer tube wall, and not by any restraints to the outside of the cable, for example clamps or cement.

Figure 9.5: **Magnet assemblies incorporating (a) one magnet and (b) five magnets as used in the laboratory reliability tests. The overall length of the five-magnet assembly is 0.4 m. Also note the fibre-optic cable underneath and the mounting clips used to immobilize the cable onto the substructure.**

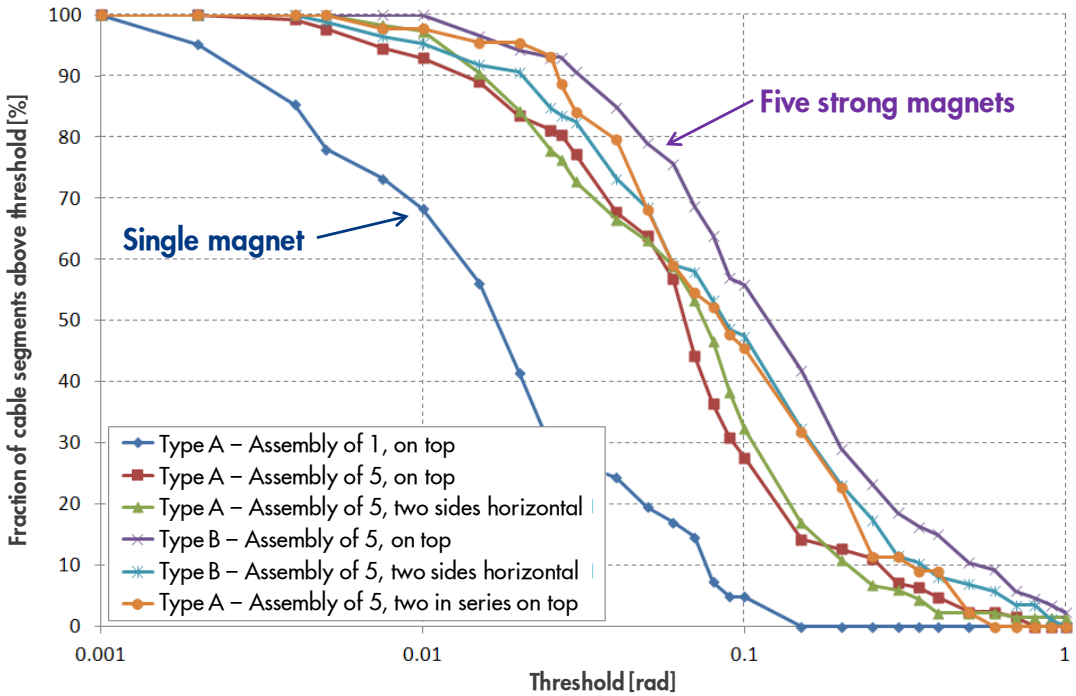

Figure 9.6: **Fraction of cable segments that show DAS signals above the threshold value, plotted for a six different magnet configurations and types. The 'Type B – Assembly of 5, on top' is currently considered for deployment, and displays a considerably increased performance compared to the single-magnet assembly.**

Tests have also shown that there is a variation in the signal along the length of the cable, caused by manufacturing variations in the thickness of the gap between buffer and outer tube [105]. Signal reliability tests have been performed and show signal variations of orders of magnitude. To improve the performance, these tests have been repeated for various magnet assemblies, ranging from one magnet (Figure 9.5a) to an assembly of five magnets (Figure 9.5b) of an approximately 20% stronger type.

Results of these reliability tests can be found in Figure 9.6. Here the fraction of cable segments having DAS signal amplitudes larger than the specified threshold value are shown. This fraction provides an indication of the reliability of generating sufficient signal with a magnet assembly. For this purpose the laboratory cable was divided into 48 segments and the DAS response was measured for the magnet assembly, subsequently being placed at each of these segments. If the signal strength would be the same in all cable segments, one would expect an instant signal drop from 100% to 0% as soon as the threshold increases above the signal strength. Due to variations in the gap between buffer and outer tube, the signal varies along the length of the cable.

For a single magnet the large variation in signal strength is shown by the gradual decrease in percentage. For assemblies of multiple magnets distributed over 0.4 m, the transition zone is much better defined. Moreover, the combination of multiple magnets and the choice for stronger magnets increases the average signal strength due to the increase of magnetic field. This additionally shifts the full curve to larger signal strength, resulting in a significantly larger percentage of cable segments showing good signal strength. Compared to the expected amplitude at 50% reliability of one magnet, the best performing magnet assembly shows a comparable or higher signal in 95% of all active cable segments – at the same electrical current. A 9x larger signal is observed in at least 50% reliability of all cable segments.

Summarizing, by using assemblies of multiple magnets close to each other, the cable response reliability has been substantially improved. For further enhancement of the reliability, the number of installed assemblies can be increased beyond the number needed for accurate calibration.

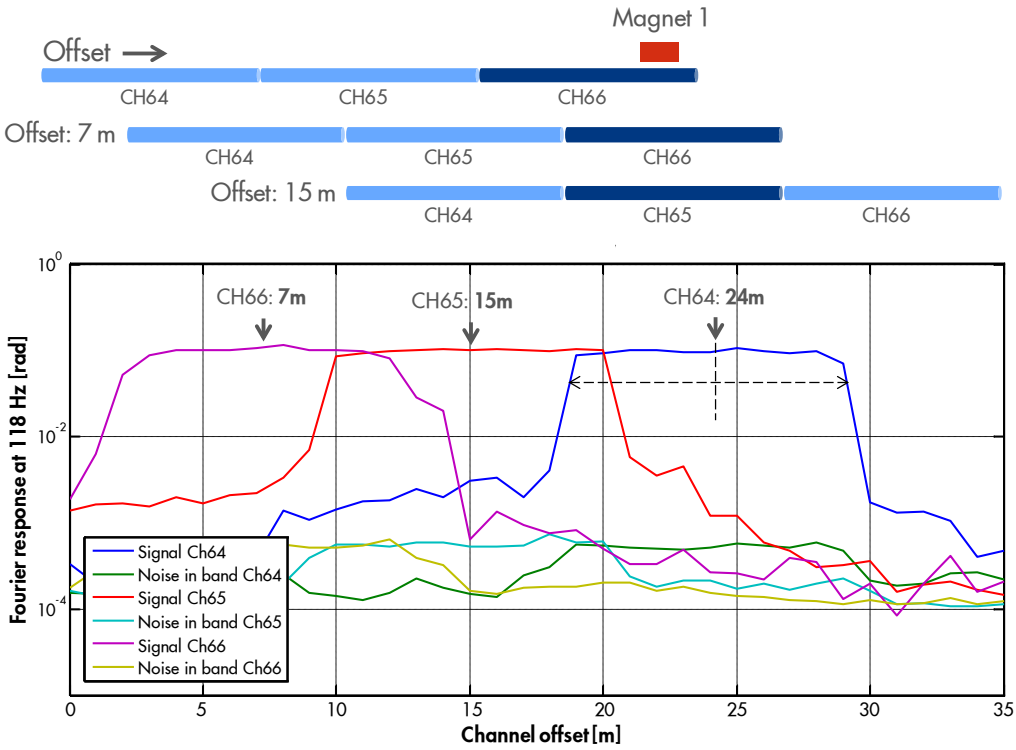

Figure 9.7: **MDL signal as a function of channel offset in the DAS box. As long as a particular magnet channel overlaps with the magnet position, a high signal is observed. The centres of the resulting plateaus are the centres of the full-width-half-maximum of each plateau. The offset corresponding to each channel centre is an independent measurement of the location of the magnet with respect to the fibre.**

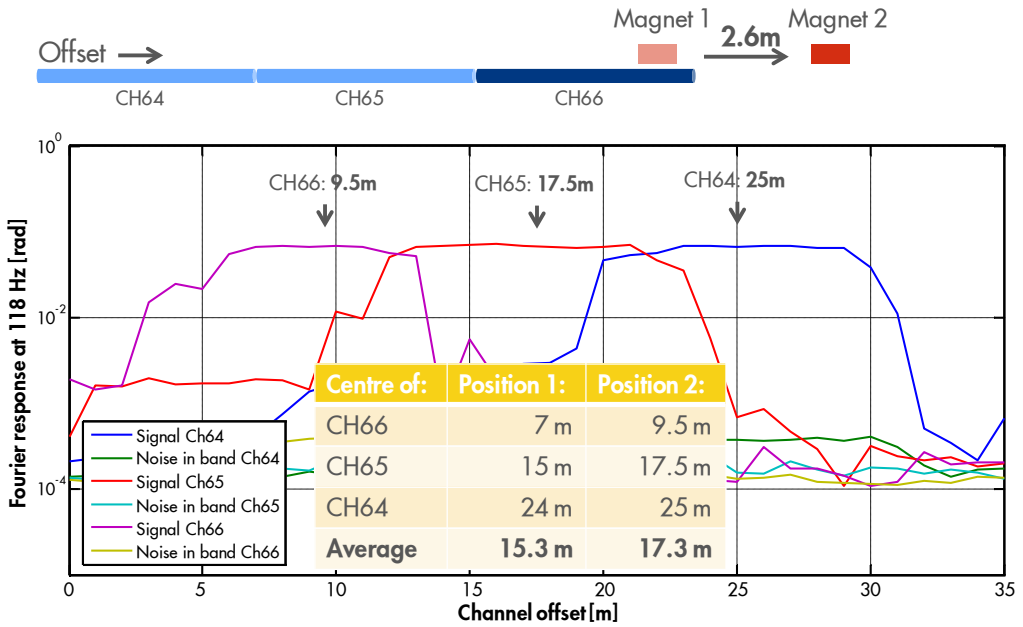

Centre of:	Position 1:	Position 2:
CH66	7 m	9.5 m
CH65	15 m	17.5 m
CH64	24 m	25 m
Average	**15.3 m**	**17.3 m**

Figure 9.8: **MDL signal as a function of channel offset in the DAS box. The measurement and analysis procedure is the same as in Figure 9.7, but now the magnet has been physically moved by 2.6 m. The measured average shift of the channel centres equals (2 ± 0.9) m, in good agreement with the physical offset.**

9.6. Sub-channel accuracy

DAS integrates signal impinging over the gauge length, typically on the order of 10 m. For a far-field wave, typical for geophysical applications, the observed – *averaged* – wave arrival will therefore correspond to the centre of each channel. Application examples discussed in Section 9.3 require the centre of each channel to be determined with an accuracy down to approximately 0.5 m. To achieve such positioning accuracy, the centre of each DAS channel has to be determined with sub-channel accuracy.

To achieve a position accuracy better than the DAS gauge length, the *channel offset* feature of the DAS ODH3 interrogation system can be used [103]. This feature allows bulk-shifting of all channels in sub-channel steps. The result of scanning through these channel offsets is illustrated in Figure 9.7. All optical channels are bulk-shifted by sub-channel steps and in that way essentially moved past the magnet assembly. By shifting the channel position over a sufficient distance, the boundaries of a particular channel can be observed. This enables determination of the channel offset for which the magnet assembly is centred in that particular channel.

By scanning the channel offset over more than one channel, the magnet assembly position can in this way be determined with accuracies better than 1 m. Figure 9.7 and Figure 9.8 demonstrate this accuracy by moving the magnet by a known physical distance (here 2.6 m) and calculating the change in position by repeating the channel offset scan.

9.7. Conclusions

The Magnetic Depth Locator (MDL) provides a non-intrusive method of depth referencing for fibre-optic DAS in-well measurements. The possibility of repeating the calibration at negligible incremental cost, makes it very suitable for safeguarding the depth reference accuracy of time-lapse well and reservoir monitoring.

This Chapter provided an overview of the feasibility and applicability of the MDL concept. The variety of laboratory experiments conducted – to optimize the method and find its limitations – has been translated into a magnet-assembly design, cable specifications and a calibration procedure. To move the concept into practice, ruggedized packaging and deployment procedures will be considered in Chapter 10.

10. Depth calibration for DAS: deployment

The Magnetic Depth Locator is a solution for depth calibration of a down-hole fibre-optic DAS cable. Field deployment requires functional and ruggedized system components. These are being developed and are part of an integrated calibration procedure from fibre to formation which has been trialled in a test well.

10.1. Towards a deployable system

The *Magnetic Depth Locator* (*MDL*) has been introduced in Chapter 9 as a tool for depth calibration of down-hole DAS measurements, especially suitable for repeated calibrations without well-intervention and at negligible incremental cost. Laboratory findings have enabled identification of a functional system configuration in terms of an effective current path and an optimised magnet assembly (Section 9.5). The Lorentz force, resulting from the combination of an AC current and a magnetic field, is most effective in inducing vibration in a typical down-hole cable's inner tube, also referred to as *fibre-in-metal-tube* (*fimt*). As such, it is only the vibration of the fimt, within the outer tube, which contributes to the depth reference signal induced by an electrical current through the fimt. As a result of cable manufacturing tolerances, variations in the void between fimt and outer tube can limit the vibration of the fimt in some sections of the cable. Hence, a spatially-distributed array of magnets can be used to ensure the generation of a sufficient signal.

An MDL installation in a well-bore consists of several components, as summarized in Figure 10.1. These components will now be briefly introduced [106]. A dedicated *power source* is required to provide sufficient AC current to generate a suitable acoustic signal. The current is coupled into the fimt of the down-hole cable at the point where this cable is terminated. Typically this is in a *pressure-barrier* which is usually attached to a well-head outlet, and hence such component requires modification to allow an insulated electric current path into the fimt. In case of a continuous *down-hole cable* throughout the well, the current is conducted by the fimt. Insulation to the outer tube is provided by a plastic buffer material between the fimt and the outer tube. At the down-hole end of the cable, a closed electrical circuit is realised by short-cutting the fimt to the outer tube and the tubing or casing. Such termination can be a *turn-around assembly*, typically installed to splice a down- and up-going fibre together allowing measurement of these two fibre-sections in series. Conducting well-components – such as casing – or, alternatively, the formation itself provide a return path to surface.

In case of a discontinuous down-hole cable, for example because of a packer or an unexpected cable break, a *splice-chamber* has to be used to connect two lengths of cable together. Packers are used as part of a completion to improve well-integrity and force production fluids through the tubing string while isolating the annular space between tubing and casing (Section 2.1). Only a short length of cable can be fed through a packer, requiring connection to a second length of cable above the packer. Since splice-chambers are typically made out of conducting metal, a modification is required here to connect the inner tubes together, i.e. ensure insulation from the environment. Last but not least, magnet assemblies are clamped to the cable at each position in the well where a depth marker is required (discussed later in Section 10.2).

The components listed are in various stages of design and manufacturing. The power source and magnet assemblies are dedicated core components of a MDL system. Other components,

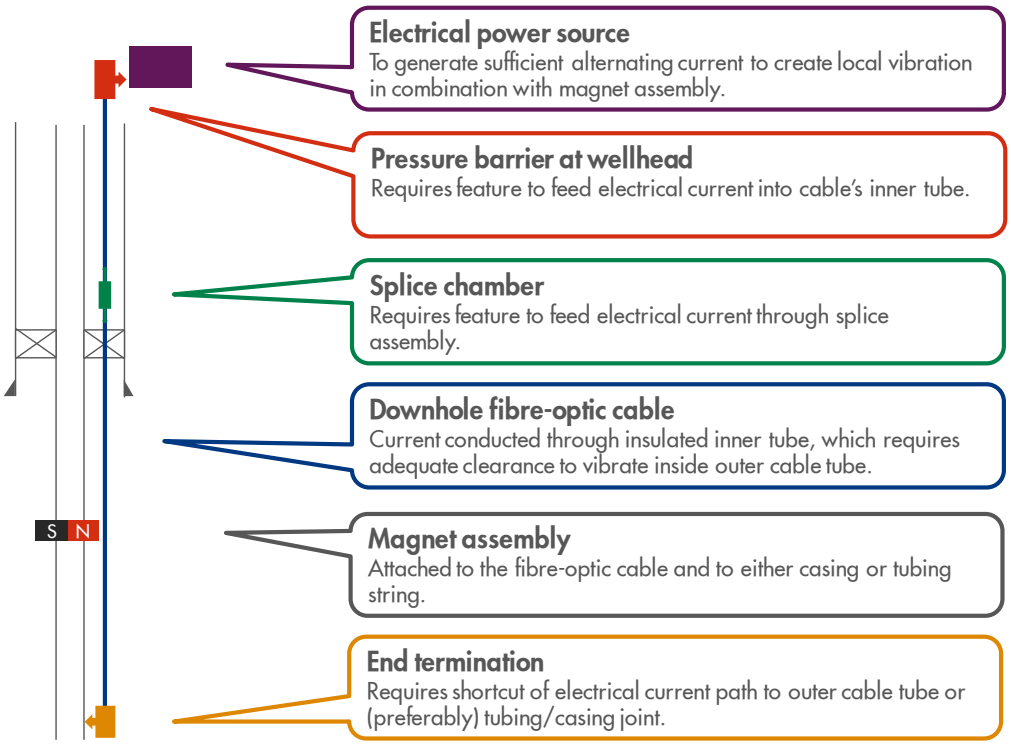

Figure 10.1: Overview of components required for deployment of the Magnetic Depth Locator in a well-bore. [106]

especially the pressure barrier, splice-chamber and turn-around assembly, are used in typical fibre-optic installations for well-integrity purposes and therefore need to be modified to allow a suitable electrical current path. These components are often integral parts of the fibre-optic installation as offered by vendors, and modifications are therefore preferably realised together with fibre-optic installers. The design and realisation of a magnet-assembly prototype – the core component of any MDL system – will be discussed in the next Section.

10.2. Assembly development

A housing has been developed to hold the assembly of magnets [106]. The design of this housing is aimed at a reliable deployment and optimum signal characteristics by focusing on three requirements:

- *Ruggedization*: The magnets are contained in an *insert*, fitting inside a metal sensor *clamp*. The insert can be manufactured using a quick and cost-effective rapid-prototyping process and consists of glass-reinforced nylon;
- *Alignment of magnets*: For optimum signal generation, it is important that the magnets in each assembly are properly aligned with and distributed along the cable. For this purpose, the insert consists of two parts: the magnets are held in a base-part, and the cable is placed so that it is flush and aligned with the magnets when sandwiched with the counter-part acting as a lid;
- *Ease of handling*: It is important to assure that the make-up of the insert and clamping on the rig-floor does not take too much time and minimises the risk of loose parts falling into the well. For that reason, the insert only consists of two parts, the holder and the lid, while the associated magnets are fixed to the holder. Moreover, the two parts *click* together and in that

way hold the assembly together and aligned. A clamp rigidly squeezes all parts against the pipe wall and provides further mechanical protection.

A prototype insert has been designed and manufactured to incorporate the above requirements. The 3D rendering in Figure 10.2a shows the *bottom-part* with an array of magnets. Figure 10.2b shows the *top-part* attached to the bottom part, ensuring alignment of all magnets and the fibre-optic cable. Before running-in-hole this insert is covered by a metal clamp, which protects it from being crushed while running in-hole and firmly holds the magnet assembly in place against the pipe.

The prototype is tailored to a 3½" tubing deployment. This is a size often found in operating units, however, the design can easily be scaled to fit other dimensions as well. The first installation of this magnet assembly has been performed in a dedicated *test well*. The completion in this test well also consists of 3½" tubing. More details regarding installation in the test well and use for depth calibration can be found in Section 10.4.

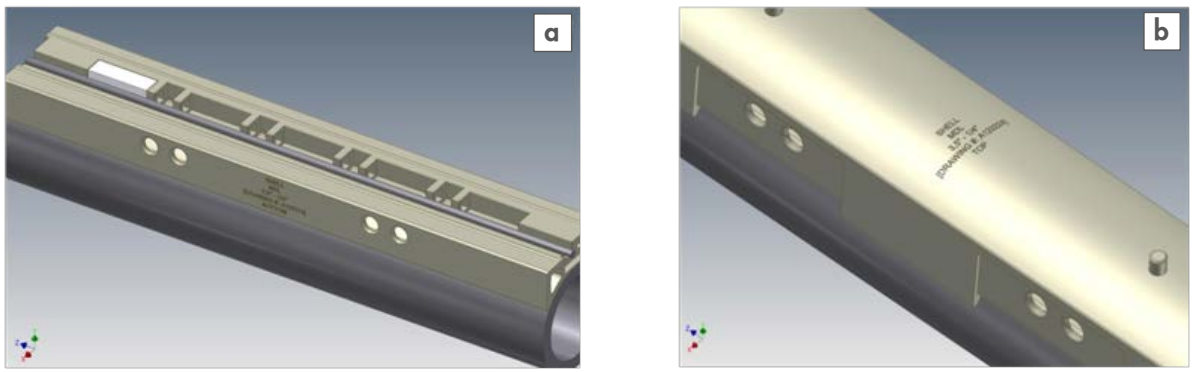

Figure 10.2: 3D renderings of the magnet assembly insert: (a) bottom part fitting onto a 3.5" pipe, showing the fibre-optic cable and space for five magnets; (b) top part 'clicked' onto the bottom part and in that way fixing the cable and magnets together in an aligned way. [106]

10.3. Integrated approach

The detection of magnetic-field-induced vibration in the DAS measurements results in a calibration of the fibre length to the exact location of each magnet assembly. The simplest way to determine the magnet assembly's position in the well, also referred to as driller's depth, is during installation. The position of the magnet assembly relative to the pipe joint on which it is mounted can be measured before running-in-hole when laying out the tally. The *tally* includes a list of measured lengths of all pipe-joints in order of installation. The lengths of all pipe joints installed above a magnet assembly in combination with the position of that magnet assembly on a particular pipe joint can be used to obtain an initial estimate of the magnet assembly's position in the well. The length of pipe-joints measured at surface is however not accurate in absolute terms: pipes stretch in the well because of the weight of the pipes hanging off from them and also due to thermal expansion. Generally speaking, human errors in manual length measurement happen and can lead to a significant cumulative error over a large number of joints. Hence, depth accuracy is not necessarily guaranteed. Depending on the application and the required depth

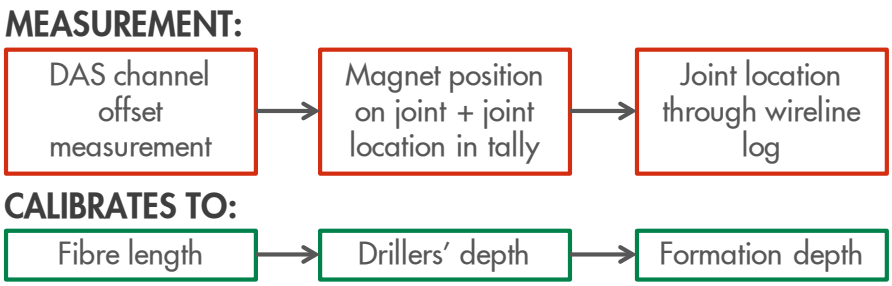

Figure 10.3: Steps for depth calibration with the Magnetic Depth Locator. To calibrate fibre length to position in the formation, a combination of several measurements is advised. [106]

accuracy, additional calibration steps can be included to provide a more accurate calibration to drillers' depth and eventually to formation depth (Figure 10.3).

A verification of the position of the magnet assembly in the well can be obtained by lowering a logging tool in the well which detects pipe collars. The position of a magnet assembly can be marked by mounting it on a pipe joint with a significantly different length, e.g. a *pup joint*, causing a clear deviation from the otherwise regular pattern of pipe-collar signals along the depth of the well. Such *relative* depth measurement is often used to relate logging measurements to well features. In combination with the fairly accurate measurement of the distance between nearest pipe collar and magnet assembly, the actual position in the well can established [106].

Alternatively, the position of a magnet assembly can also be detected *directly* [107]. A magnetically-sensitive logging tool, such as a *casing collar locator* (*CCL*), is sensitive to an induced magnetic field. Acoustic logging tools, such as a sonic *cement-bond log* (*CBL*), are sensitive to the amount of metal around the tool. Depending on the deployment cost and sensitivity of the various logging tools in a particular well configuration, either direct or relative methods may be used to verify the position of a magnet assembly in the well.

This position in the well can also be related to a position with respect to the formation. The same (wire-line) tool-string can also include a tool – such as a *Gamma Ray log* – which can read formation properties through (tubing and) casing. This combination allows relating the position of the magnet assembly in the well to a position with respect to the formation [106].

Together, these measurements ensure an accurate calibration of fibre length to location in the formation and enable comparison of fibre-optic datasets with other well logs and areal, e.g., surface seismic, datasets. After an initial calibration to the formation, repeat calibrations to mitigate changes in the length conversion in the fibre-optic installation only involve additional MDL calibrations. Such repeat calibration can be executed at negligible additional cost without well-intervention, as only a power source and DAS interrogator are required. The next Section describes a trial in a test well in which this integrated calibration approach has been tested.

10.4. Test-well trial

Depth calibration with the Magnetic Depth Locator was investigated in a dedicated test well [108]. This trial involved the installation of five magnet assemblies distributed over a 300 m long production tubing. This installation was used to perform test-calibrations with the MDL system in combination with wire-line tools as described in Section 10.3.

Figure 10.4 shows the installation of a magnet assembly before running-in-hole. The two parts of the magnet assembly are clamped together to provide alignment between the cable and the magnet assembly (Figure 10.4b). A metal clamp is placed over the insert to provide mechanical protection (Figure 10.4c). The installation procedure took only five minutes for each of the assemblies, and was successfully completed for all five magnet assemblies. At the end of the test period of about four weeks, the assemblies were retrieved. Visual inspection did not show any damage: the magnet-assembly is sufficiently ruggedized for down-hole deployment.

The drillers' depth of each magnet assembly was carefully monitored during well-completion, providing information on which assemblies were installed at which depths. This involved length-measurements of all pipe-joints as well as measuring the distance from each magnet assembly to the nearest pipe collar. After completion of the well, the position of each magnet assembly was verified using a wire-line logging run [109]. Such a logging run also provides the opportunity to relate the position of the magnet assembly to a position in the formation when using specific formation-reading logging tools.

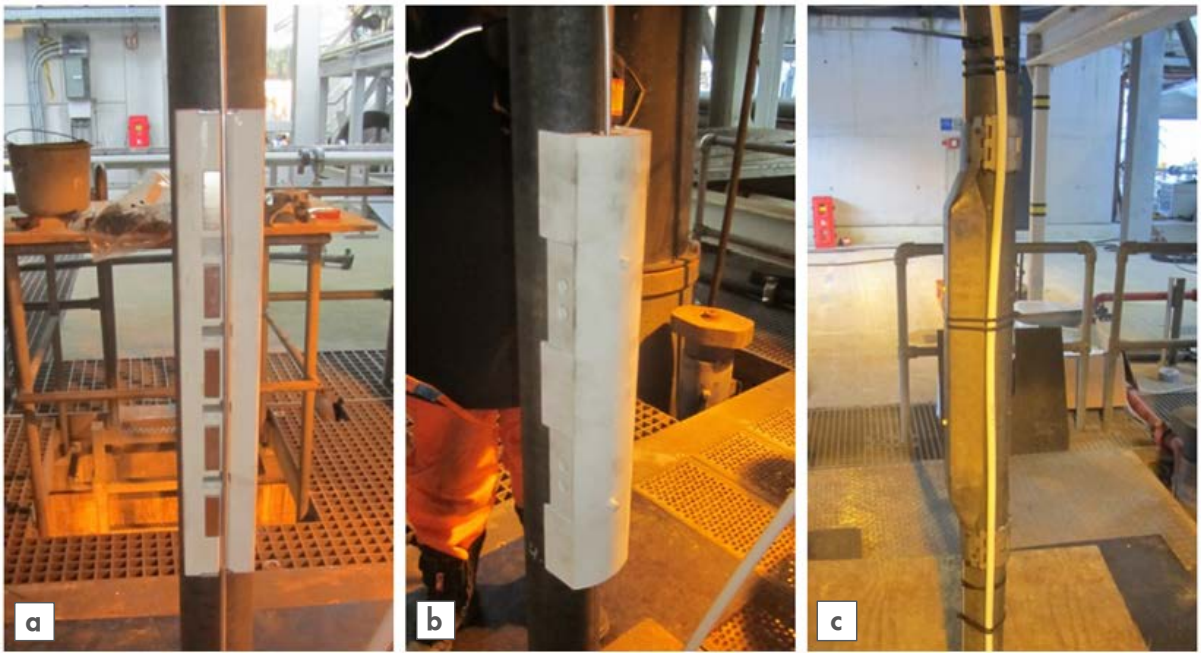

Figure 10.4: **Installation of a magnet assembly: (a) bottom part of the insert with five magnets aligned flush with the fibre-optic cable; (b) top part of the insert 'clicked' onto the bottom part; (c) a down-hole instrumentation clamp positioned over the insert and clamped to the tubing joint. This provides a ruggedized assembly for reliable down-hole deployment. [108]**

After having established the physical position of each magnet assembly, the MDL system can be used to calibrate the fibre length in a DAS measurement. Several calibrations were executed to verify the signal reliability and calibration accuracy in a real well environment. These tests were completed successfully and provided insight in the operating range of the MDL system. While the detailed results are under consideration at the moment of writing and are not presented here, the results indicate errors in depth assignment as expected based on the a priori analysis given in Section 9.2 [110].

10.5. Way forward

The deployment of the MDL system should preferably be done by the service company that installs the entire fibre-optic system in a particular well. The concept is well suited for this approach because it uses standard fibre-optic cable and magnet assemblies that can be easily clamped to the cable. Furthermore, implementation of electrical current paths in fibre-optic components – such as pressure barrier and splice chamber – is handled best by the service company itself, because of company-specific component designs, regional differences in legislative requirements and to assure the overall reliability of the fibre-optic system. The results from the test-well trial show enough evidence to consider discussing further development of selected components with service companies.

Field trials are a logical next step for further development of the MDL system and should include jointly developed components. Such trials should aim at demonstrating the MDL system as a non-intrusive depth reference for DAS fibre-optic well and reservoir monitoring.

11. Concluding remarks

A number of novel fibre-optic sensing technologies have been described in the preceding Chapters, with significant contributions to the ability to obtain detailed sensor readings in a well-bore. This Chapter reviews the progress to date as well as identifies additional steps towards a step-change in well and reservoir surveillance.

11.1. Strategic approach to develop in-well fibre-optic sensing tools

Cooperation with *industry partners* is an essential part of Shell's approach to *innovation*. This applies to further development of components in a Magnetic Depth Locator installation, but has also been an essential aspect in all other projects described in this thesis. Shell does not intend to produce their own fibre-optic sensing systems, but aims to stimulate the fibre-optic sensing industry to develop an appropriate solution for the upstream applications in question. The development of key technologies is, however, an enabler to optimise production and to obtain a license-to-operate, thus gaining a competitive advantage. To generate sufficient novel technology concepts and guide development into suitable solutions, adequate in-house expertise is required. This vision has resulted in an R&D capability which operates at the frontline of fibre-optic sensing research in the upstream industry. The multi-lateral working relationship with academia, commercial research institutes and commercial companies provides a good illustration of Shell's efforts in maturation of new technologies: synergies between the different entities are multi-fold in the frontline research to provide novel sensing concepts. Cooperation with universities also has the advantage of nurturing the academic qualifications of young Shell staff, as is the case in this PhD-on-design thesis.

This thesis reports on fibre-optic sensor developments for application in oil and gas wells. Such developments have to advance through subsequent stages of *maturation* before achieving the goal of commercial *deployment* in upstream operating units. This section provides a short recap of the *progress* described in this thesis and the *next steps* towards further technology maturation. The advances in fibre-optic sensing system development described in this thesis involved a major contribution from the author. Next steps provide a general outlook for further development, but not necessarily reflect actual activities planned to be carried out by the author or the IWT team as can be expected in such multi-faceted research organisation.

The development of an interrogation unit for point sensors based on fibre Bragg gratings (FBG) is a nice example of the initial stage of such an approach. *Proof-of-principle* was obtained for a low-cost high-temperature interrogator. This result confirmed, in an early project stage, the *feasibility* of field-wide deployment of low-cost Quasi Distributed Pressure Sensing (QDPS) systems, as well as, e.g., temperature or chemical sensing systems. Now, about four years later, when Shell-(co-)developed FBG-based sensors are becoming available for deployment, a dedicated test programme allows *evaluation* of *commercially-introduced* interrogation units before implementation in *field trials*.

Distributed Acoustic Sensing (DAS) has *matured* most rapidly in its development towards a successful tool for operating units. After lab and field evaluation of prototype interrogation units, further development has led to improved interrogators which have been trialled in a range of different scenarios. As a result, DAS is currently already being *deployed* on a commercial basis for

selected geophysical and flow applications. This success provides a basis for enabling an additional number of novel applications, triggering further developments of which two are introduced in this thesis: *directionally sensitive cables* and *depth calibration*.

The first is directed to improved directional sensitivity as an important enabler for additional geophysical applications which require sensitivity to broadside-incident waves. Novel cable prototypes have been *developed* and *demonstrated* in field trials. Further developments are planned to result in readily deployable, continuous cables for both surface and down-hole directional sensitivity.

The second promising development is the Magnetic Depth Locator (MDL). This device, with its integrated calibration workflow, has been developed to provide a non-intrusive method of depth referencing for repeated fibre-optic DAS in-well measurements. A first *test-well trial* of the core components was completed successfully.

11.2. Commercial success

Ongoing development has the potential to provide a capable suite of fibre-optic sensors for the upstream business. While this is a promising prerequisite, the effective use of fibre-optic sensing in the oil and gas industry requires consideration of two crucial aspects: *value-of-information* and the *integration* of multiple data sources. Only this approach leads to the commercial success required by IOCs to operate.

The value of fibre-optic sensing technologies is in the information that can be extracted from the measurement data. For day-to-day production monitoring, data analysis should be *automated* and the resulting information should be *actionable*. Operators do not have the time nor the expertise to analyse raw measurement data manually. Therefore, intelligent processing systems should be implemented to automate data analysis. The outcome of such analysis should contain information that can be used to optimise production operations, either directly by adjusting production parameters or as input to models such as a reservoir simulator. For longer-term field-development purposes, streamlined processing workflows can assist local teams in interpreting data and assuring that the resulting information is adequate input for further field development decisions.

Whereas individual sensing technologies might provide usable insight, it is the *combination* of several sensing technologies that will lead to the most *conclusive information*. As an example, temperature profiles (from DTS) and noise logs (from DAS) can both provide valuable information about flow behaviour into and along the well-bore. However, in most scenarios, it is the combination of these two that leads to the most clear conclusions. The challenge here is in the processing and analysis capabilities to combine multiple datasets, and solve for the larger set of related parameters in an advanced, automated manner.

The combination of multiple fibre-optic sensing technologies with advanced processing algorithms and workflows will provide a significant advantage in optimising efficiency, safety and ultimate recovery. In that way, the densely-distributed measurements in time and along the entire length of the fibre have the potential to revolutionise *well and reservoir surveillance* in the *oil and gas* industry. This thesis provides tools to travel along this road to advanced diagnostics in oil and gas wells.

References

[1] "2012 Key World Energy Statistics", International Energy Agency (IEA), Paris, 2012

[2] C. Rühl, P. Appleby, J. Fennema, A. Naumov, and M. Schaffer, "Economic development and the demand for energy: A historical perspective on the next 20 years", Energy Policy, Volume 50, Pages 109-116, 2012

[3] "Discover the processes at Pearl GTL", Shell, 2013, retrieved from http://www.shell.com/global/future-energy/natural-gas/gtl/acc-gtl-processes.html.

[4] New Lens Scenarios", Shell, The Hague, 2013

[5] "Shell moves forward on new Gulf of Mexico development at Stones", Shell, 2013, retrieved from http://www.shell.com/global/aboutshell/investor/news-and-library/2013/new-gulf-mexico-stones-08052013.html.

[6] E. Tzimas, A. Georgakaki, C. Garcia Cortes, and S.D. Peteves, "Enhanced Oil Recovery using Carbon Dioxide in the European Energy System", European Commission Joint Research Center, Petten, 2005

[7] "OPEC Annual Statistical Bulletin 2010/2011 Edition", OPEC, Vienna, 2011

[8] F. Berghmans, "Reliability of optical fibers and components", Proc. SPIE 5855, 17th International Conference on Optical Fibre Sensors, 2005;

[9] A. Othonos, and K. Kalli, "Fiber Bragg Gratings: fundamentals and applications in telecommunications and sensing", ISBN 0890063443, Artech House, Norwood, 1999

[10] K.O. Hill, Y. Fujii, D.C. Johnson, and B.S. Kawasaki, "Photosensitivity in optical fiber waveguides: application to reflection fiber fabrication", Appl. Phys. Lett. 32 (10): 647, 1978

[11] J. Hecht, "Understanding fiber optics", 4th edition, Prentice Hall, London, 2002

[12] C.V. Raman, "A new radiation", Indian J. Phys. 2: 387–398, 1928

[13] Raymond M. Measures, "Structural Monitoring with Fiber Optic Technology", Academic Press, San Diego, USA, 2001

[14] "The 2012 EU Industrial R&D Investment Scoreboard", European Commission Joint Research Centre, Institute for Prospective Technological Studies, Seville, 2013

[15] "DTI PhD on Design", TU Eindhoven, retrieved from http://www.3tu.nl/en/education/sai/programmes_and_tracks/dti/career_perspective/phd_on_design/ .

[16] Ley, Brian, "Diameter of a Human Hair", 1999, retrieved from http://hypertextbook.com/facts/1999/BrianLey.shtml .

[17] A.T. Bourgoyne, M.E. Chenevert, K.K. Millheim, and F.S. Young, "Applied Drilling Engineering", SPE Textbook Series, Vol. 2., Society of Petroleum Engineers, Richardson, 1991.

[18] "International Petroleum Industry Multimedia System", IHRDC, Boston

[19] R.C. Selley, "Principles of Petroleum Geology", W.H. Freeman & Co., 1983

[20] T.O. Allen, and A.P. Roberts, "Production operations 2: Well completions, workovers and stimulations", Oil and Gas Consultants, Inc., Tulsa, 1978

[21] K.W. Waterfall, C.A.T. Willink, and D.J. Milne, "Incident Investigation and Analysis for E&P Operations", Journal of Petroleum Technology, Society of Petroleum Engineers, Richardson, 1995

[22] "ALARP Suite of Guidance", UK Health and Safety Executive, retrieved from http://www.hse.gov.uk/risk/theory/alarp.htm .

[23] J. Kemp, "Bakken revolution is only half-complete", Reuters, 2012

[24] R. Garifi, "Oil Industry Innovations Prove Valuable to Space Exploration", Space safety magazine, 2013, retrieved from http://www.spacesafetymagazine.com/2013/06/12/oil-industry-innovations-prove-valuable-future-exploration/ .

[25] "OPEC Annual Statistical Bulletin 2010/2011 Edition", OPEC, Vienna, 2011

[26] R. Newton, "Project Management – Step by step", Pearson Education, Harlow, 2006

[27] A. Othonos, and K. Kalli, "Fiber Bragg Gratings: fundamentals and applications in telecommunications and sensing", ISBN 0890063443, Artech House, Norwood, 1999.

[28] H. den Boer, A. Franzen, B. Birch, and E. Moes, Shell Journal of Technology, SR.13.10266_20, SGSI, Rijswijk, 2013 [Doc #3.4]

[29] P. Lumens, Shell report EP-2009-5413, SGSI, Rijswijk, 2009 [Doc #3.2]

[30] P. Lumens, Shell report EP-2009-5412, SGSI, Rijswijk, 2009 [Doc#3.1]

[31] J.J. den Boer, A. Franzen, and P.G.E. Lumens, "Fibre Bragg Grating Measurement Method and System", Patent Application Publication WO2012/089816/A2, Shell, The Hague, 2012 [Doc#3.3]

[32] B.N. Taylor, and C.E. Kuyatt, "Guidelines for evaluating and expressing the uncertainty in NIST measurement results", Technical note 1297, National Institute of Standards and Technology, 1994

[33] S.L. Gilbert, and W.C. Swann, "Standard Reference Materials: Hydrogen Cyanide H13CN Absorption Reference for 1530-1560nm Wavelength Calibration- SRM2519", NIST special publication 260-137, National Institute of Standards and Technology

[34] F.G. Smith and J.H. Thomson, "Optics", John Wiley &. Sons, 1988, chapter 13

[35] "Oil&Gas Case Study - Multi-point downhole pressure & temperature monitoring system", Product brochure, SmartFibres, Bracknell, 2012 [Doc#4.1]

[36] H. den Boer, A. Franzen, B. Birch, and E. Moes, Shell Journal of Technology, SR.13.10266_20, SGSI, Rijswijk, 2013 [Doc #4.2]

[37] P. Lumens, and A. van Rooyen, Note-for-file, SGSI, Rijswijk, 2013 [Doc #4.3]

[38] Micron Optics sm125-500 FBG Interrogation unit, specifications can be found at: http://www.micronoptics.com/sensing_instruments.php .

[39] H.F. Taylor, and C.E. Lee, "Apparatus and method for fiber optic intrusion sensing", Patent Application Publication US 5194847, 1993

[40] M. Molenaar, D. Hill, P. Webster, E. Fidan, and B. Birch, "First Downhole Application of Distributed Acoustic Sensing (DAS) for Hydraulic Fracture Monitoring and Diagnostics", SPE Hydraulic Fracturing Technology Conference Paper 140561-MS, The Woodlands, 2011

[41] K. Tsujikawa, K. Tajima, and J. Zhou, "Intrinsic loss of optical fibers", Optical Fiber Technology 11, page 319-331, 2005

[42] Wikipedia, "Speckle pattern", http://en.wikipedia.org/wiki/Speckle_pattern.

[43] N. Lagakos, E.U. Schnaus, J.H. Cole, J. Jarzynski, J.A. Bucaro, "Optimizing fiber coatings for interferometric acoustic sensors", IEEE Journal of Quantum Electronics vol.18 no.4, page 683-689, 1982

[44] P. Healey, "Review of long wavelength single-mode optical fibre reflectometry techniques". J Lightwave Technol LT-3 (4), page 876-886, 1985

[45] P. Healey, "Instrumentation principles for optical time domain reflectometry", J Phys E: Sci Instrum. 19, page 334-341, 1986

[46] S. Wright, R. E. Epworth, D. F. Smith, and J. P. King, "Practical coherent OTDR at 1.3 pm", Proc. Optical Fibre Sensors (OFS) Conf., page 347-350, Stuttgart, 1984

[47] D. Considine, "Digital Complex Sampling", Electronics Letters, 1983

[48] A.H. Hartog, and K. Kader, "Distributed fiber optic sensor system with improved linearity", Patent Application Publication US 2012/0067118A1, 2012

[49] Wikipedia, "Coherence length", http://en.wikipedia.org/wiki/Coherence_length.

[50] J.P. Dakin, and C. Lamb, "Distributed fibre optic sensor system", Patent Application Publication GB 2 222 247A, 1990

[51] R.I. Crickmore, D.J. Hill, and M. McEwen-King, "Phase Based Sensing", Patent Application Publication WO2011067554A1, 2011

[52] S.J. Russell, J.P.W. Hayward, and A.B. Lewis, "Method and apparatus for acoustic sensing using multiple optical pulses", Patent Application Publication GB 2442745B, 2008

[53] A. Bauer, P.G.E. Lumens, P. in 't Panhuis, and D. Wu, Presentation slides, Shell, Rijswijk, 2010

[54] P. Healey, "Statistics of Rayleigh backscatter from a single-mode fiber", IEEE Transactions on Communications 35 (2), page 210-214, 1987

[55] B.P.M. Duijndam, Shell report EP-2010-5203, SIEP, Rijswijk, 2010 [Doc #5.2]

[56] P.G.E. Lumens, Presentation slides, Shell, Rijswijk, 2011 [Doc #5.6]

[57] A. Lewis, and S. Russell, "Seismic Geophysical surveying", Patent Application Publication WO2013/011283 A2, 2013

[58] P.G.E. Lumens, and R. Kusters, Presentation slides, Shell, Rijswijk, 2011 [Doc #5.7]

[59] P. Christie, K. Dodds, D. Ireson, L. Johnston, J. Rutherford, A. Hess, J. Schaffner, and N. Smith, "Borehole Seismic Data Sharpen the Reservoir Image", Schlumberger Oilfield Review, Volume 7, Issue 4, 1995

[60] J. Meunier, "Seismic Acquisition from Yesterday to Tomorrow", SEG/EAGE Distinguished Instructor Series, No. 14, 2011

[61] Z. Wei, "How good is the weighted-sum estimate of the vibrator ground force", SEG The Leading Edge, page 295, August 2009

[62] F.F. Reynolds, "Some notes on geophones", Mandrel Industries, Inc., 1970

[63] J. Mestayer, B. Cox, P. Wills, D. Kiyashchenko, J. Lopez, M. Costello, S. Bourne, G. Ugueto, R. Lupton, G. Solano, D. Hill, and A. Lewis, "Field Trials of Distributed Acoustic Sensing for Geophysical Monitoring", SEG Annual Meeting, San Antonio, 2011 [Doc#6.1]

[64] A. Mateeva, J. Mestayer, B. Cox, D. Kiyashchenko, P. Wills, J. Lopez, S. Grandi, K. Hornman, P. Lumens, A. Franzen, D. Hill, and J. Roy, "Advances in Distributed Acoustic Sensing (DAS) for VSP, SEG Annual Meeting, Las Vegas, 2012 [Doc#6.2]

[65] P.G.E. Lumens, Note-for-file, Shell, Rijswijk, 2011 [Doc#6.3]

[66] G. Mavko, T. Mukerji, and J. Dvorkin, "Rock Physics Handbook - Tools for Seismic Analysis in Porous Media", Cambridge University Press, 2003, Section 10.1 - Typical Rock Properties: A velocity of 2500 m/s is a typical value for poorly consolidated sandstone. In general for sandstones, this velocity is a lower bound.

[67] P.G.E. Lumens, and A. Franzen, Note-for-file, Shell, Rijswijk, 2010 [Doc#6.4]

[68] P.G.E. Lumens, Note-for-file, Shell, Rijswijk, 2011 [Doc#6.5]

[69] S. Grandi, P.G.E. Lumens, and B. Wyker, Note-for-file, Shell, Rijswijk, 2011 [Doc#6.6]

[70] S. Grandi, K. Hornman, and P.G.E. Lumens, Presentation slides, Shell, Rijswijk, 2012 [Doc#6.7]

[71] A. Mateeva, J. Mestayer, B. Cox, D. Kiyashchenko, P. Wills, S. Grandi, K. Hornman, and J. Lopez, "Distributed Acoustic Sensing (DAS) for Reservoir Monitoring with VSP", EAGE Borehole Geophysics Workshop, Malta, 2013

[72] P.G.E. Lumens, Spreadsheet, Shell, Muscat, 2010 [Doc#6.8]

[73] P.G.E. Lumens, A. Franzen, and S. Grandi, Presentation slides, Shell, Muscat, 2011[Doc#6.9]

[74] S. Grandi Karam, P. Webster, K. Hornman, P.G.E. Lumens, A. Franzen, F. Kindy, M. Chiali, and S. Busaidi, "Microseismic Applications using DAS", EAGE Fourth Passive Seismic Workshop, Amsterdam, 2013 [Doc#6.10]

[75] P. Webster, J. Wall, C. Perkins, and M. Molenaar, "Micro-Seismic Detection using Distributed Acoustic Sensing", SEG Annual Meeting, Houston, 2013

[76] P.G.E. Lumens, and S. Grandi, "Seismic monitoring", Patent Application Publication WO 2013/093460/A2, OptaSense, Farnborough, 2013 [Doc#6.11]

[77] AFL Telecommunications, retrieved from http://www.aflglobal.com/ .

[78] W.F. Geisler, "Fiber optics improves BHP monitoring reliability, World Oil, October 1993

[79] B. Budiansky, D.C. Drucker, G.S. Kino, and J.R. Rice, "Pressure sensitivity of a clad optical fiber", Applied Optics, Vol. 18, No. 24, 1979

[80] N. Lagakos, E.U. Schnaus, J.H. Cole, J. Jarzynski, and J.A. Bucaro, "Optimizing Fiber Coatings for Interferometric Acoustic Sensors", IEEE Journal of Quantum Electronics, Vol. QE-18, No. 4, 1982

[81] B.N. Kuvshinov, Shell report EP 2010-5301, SIEP, Rijswijk, 2010 [Doc# 7.1]

[82] D. Wu, Shell report SR.11.13242, SGSI, Rijswijk, 2011 [Doc#7.2]

[83] B.D. Johnson, W.C. Reed, C.G. Wilson, "Optical fiber communications cable", Patent Application Publication US4723831A, AT&T, 1985

[84] E.W. Weisstein, "Helix", MathWorld, retrieved from http://mathworld.wolfram.com/Helix.html .

[85] P.G.E. Lumens, Presentation slides, SGSI, Rijswijk, 2011 [Doc#7.3]

[86] P.G.E. Lumens, "Detecting the direction of acoustic signals with a fiber optical distributed acoustic sensing (DAS) assembly", Patent Application Publication WO 2012/084997/A2, Shell, Rijswijk, 2012 [Doc#7.5]

[87] P.G.E. Lumens, G. Hemink, J. La Follett, and B. Wyker, Shell report (draft), Shell, Rijswijk, 2013 [Doc#8.8]

[88] J.J. den Boer, A.A. Mateeva, J.G. Pearce, J.J. Mestayer, W. Birch, J.L. Lopez, K. Hornman, and B.N. Kuvshinov, "Detecting broadside acoustic signals with a fiber optical distributed acoustic sensing (DAS) assembly", Patent Application Publication WO2013/090544/A1, Shell, The Hague, 2013 [Doc#8.1]

[89] K. Hornman, B. Kuvshinov, P. Zwartjes, and A. Franzen, "Field Trial of a Broadside-sensitive Distributed Acoustic Sensing Cable for Surface Seismic", 74th EAGE Conference & Exhibition, London, 2013 [Doc#8.6]

[90] "Fiber Optic Seismic Technology", TechLink Vol. 6 No. 8, Petroleum Geo-Services, 2006, retrieved from: http://techlib.pgs.com/MediaFiles/46_TechLink34_Optical%20Seismic_A4_print.pdf .

[91] F.F. Reynolds, "Some notes on geophones", Mandrel Industries Inc., 1970

[92] J.J. den Boer, J.M.V.A. Koelman, J.G. Pearce, A. Franzen, P.G.E. Lumens, and D. Joinson, "Fiber optic cable with increased directional sensitivity", Patent Application Publication WO2012/177547/A1, Shell, The Hague, 2012 [Doc#8.3]

[93] J.J. den Boer, A. Franzen, L. Groen, D. Joinson, and P.G.E. Lumens, "Smart hydrocarbon fluid production method and system", Patent Application Publication WO2013/098321/A2, Shell, The Hague, 2013 [Doc#8.4]

[94] P.G.E. Lumens, L. Groen, and D. Joinson, Shell report SR.11.14211, Shell, Rijswijk, 2011 [Doc#8.2]

[95] G. Hemink, Shell report SR.12.14235, Shell, Rijswijk, 2013 [Doc#8.5]

[96] G. Hemink, Shell report SR.12.14234, Shell, Rijswijk, 2013 [Doc#8.7]

[97] P.G.E. Lumens, A. Franzen, K. Hornman, S. Grandi Karam, G. Hemink, B. Kuvshinov, J. La Follett, B. Wyker, and P. Zwartjes, "Cable development for Distributed Geophysical Sensing, with a field trial in surface seismic", 5th European Workshop on Optical Fibre Sensors, Krakow, 2013 [Doc#8.10]

[98] B. Wyker, P.G.E. Lumens, and J. La Follett, Shell report SR.12.13905, Shell, Rijswijk, 2013 [Doc#8.11]

[99] P. Webster, and Y. Wu, Shell, Calgary, 2012 [Doc#9.6]

[100] R. B. Snow, W. H. Throop, and J. A. Williams, "Logging offshore wells in the United States", Annual Logging Symposium, Society of Petrophysicists and Well-Log Analysts, 1968

[101] P. Lumens, L. Groen, and A. Franzen, RST Newsletter 2013 Issue II, Shell, Houston, 2013 [Doc#9.1]

[102] G. Mavko, T. Mukerji, and J. Dvorkin, "Rock Physics Handbook - Tools for Seismic Analysis in Porous Media", Cambridge University Press, 2003, Section 10.1 - Typical Rock Properties: A velocity of 2500 m/s is a typical value for poorly consolidated sandstone. In general for sandstones, this velocity is a lower bound.

[103] P. Lumens, and A. van Rooyen, Shell report SR.12.13904, Shell, Rijswijk, 2013 [Doc#9.4]

[104] D. Joinson, "Method and system for determining the location of a fiber optic channel along the length of a fiber optic cable", Patent Application Publication WO/2012/089818/A1, Shell, Rijswijk, 2012 [Doc#9.2]

[105] Email conversation, 2012 [Doc#9.5]

[106] P. Lumens, and A. van Rooyen, Shell report SR.12.13904, SGSI, Rijswijk, 2013 [Doc#10.2]

[107] D. Joinson, "Method and system for determining the location of a fiber optic channel along the length of a fiber optic cable", Patent Application Publication WO/2012/089818/A1, Shell, Rijswijk, 2012

[108] P.G.E. Lumens, Presentation slides, SGSI, Rijswijk, 2013 [Doc#10.3]

[109] P.G.E. Lumens, Presentation slides, SGSI, Rijswijk, 2013 [Doc#10.4]

[110] P.G.E. Lumens, Note-for-file, SGSI, Rijswijk, 2013 [Doc#10.5]

List of patents

September 2013

1. J.J. den Boer, A. Franzen, and P.G.E. Lumens, "Fibre Bragg Grating Measurement Method and System", Patent Application Publication WO2012/089816/A2, Shell, The Hague, 2012

2. P.G.E. Lumens, "Detecting the direction of acoustic signals with a fiber optical distributed acoustic sensing (DAS) assembly", Patent Application Publication WO 2012/084997/A2, Shell, Rijswijk, 2012

3. J.J. den Boer, J.M.V.A. Koelman, J.G. Pearce, A. Franzen, P.G.E. Lumens, and D. Joinson, "Fiber optic cable with increased directional sensitivity", Patent Application Publication WO2012/177547/A1, Shell, The Hague, 2012

4. P.G.E. Lumens, and S. Grandi, "Seismic monitoring", Patent Application Publication WO 2013/093460/A2, OptaSense, Farnborough, 2013

5. J.J. den Boer, A. Franzen, L. Groen, D. Joinson, and P.G.E. Lumens, "Smart hydrocarbon fluid production method and system", Patent Application Publication WO2013/098321/A2, Shell, The Hague, 2013

List of publications

September 2013

Conference Papers

1. A. Mateeva, J. Mestayer, B. Cox, D. Kiyashchenko, P. Wills, J. Lopez, S. Grandi, K. Hornman, P. Lumens, A. Franzen, D. Hill, and J. Roy, "Advances in Distributed Acoustic Sensing (DAS) for VSP, SEG Annual Meeting, Las Vegas, 2012

2. S. Grandi Karam, P. Webster, K. Hornman, P.G.E. Lumens, A. Franzen, F. Kindy, M. Chiali, and S. Busaidi, "Microseismic Applications using DAS", EAGE Fourth Passive Seismic Workshop, Amsterdam, 2013

3. P.G.E. Lumens, A. Franzen, K. Hornman, S. Grandi Karam, G. Hemink, B. Kuvshinov, J. La Follett, B. Wyker, and P. Zwartjes, "Cable development for Distributed Geophysical Sensing, with a field trial in surface seismic", 5th European Workshop on Optical Fibre Sensors, Krakow, 2013

Curriculum Vitae

Paul Gerard Edmond Lumens

Employment

03/2010 – present: Research Petrophysicist
Fibre-optic sensing for application in oil and gas wells.
Shell Projects & Technology, In-Well Technology team

Professional training

02/2008 – 03/2010: Professional Doctorate in Engineering
Two-year post-MSc programme "Design and Technology of Instrumentation"
3TU.School for Technological Design, Stan Ackermans Institute

04/2005 – 07/2007: Technical Management Certificate
Eindhoven University of Technology, Dept. of Technology Management

Education

09/2005 – 01/2008: M.Sc. Applied Physics
Eindhoven University of Technology, Department of Applied Physics

09/2002 – 07/2005: B.Sc. Applied Physics (cum laude)
Eindhoven University of Technology, Department of Applied Physics

09/1996 – 05/2002: VWO (cum laude), pre-university education
profiles "Natuur & Techniek" and "Natuur & Gezondheid"
Bisschoppelijk College Echt

Bibliographic information

Shell Global Information Centre

Classification	Unrestricted
Report Number	SR.14.10061
Title	Fibre-optic sensing for application in oil and gas wells
Author(s)	P.G.E. Lumens (PTI/RS)
Keywords	energy, oil and gas, upstream, well and reservoir surveillance, fibre, fiber, optic, distributed, sensing, pressure, QDPS, Bragg grating, FBG, interrogator, acoustic, DAS, geophysical, DGS, VSP, surface seismic, micro-seismic, cable, broadside sensitivity, directivity, inertial sensor, depth, reference, calibration, magnet, depth locator
Date of Issue	April 2014
Period of Work	November 2008 - August 2013
US Export Control	Non US - Non Controlled
WBSE Code	ZZPT/015243/010204
Reviewed by	A. Franzen (PTI/RS)
Approved by	J. van der Horst (PTI/RS)
Issuing Company	Shell Global Solutions International B.V. P.O. Box 60 2280 AB Rijswijk The Netherlands

The copyright of this document is vested in Shell Global Solutions International, B.V. The Hague, The Netherlands. All rights reserved.
Neither the whole nor any part of this document may be reproduced, stored in any retrieval system or transmitted in any form or by any means (electronic, mechanical, reprographic, recording or otherwise) without the prior written consent of the copyright owner. Shell Global Solutions is a trading style used by a network of technology companies of the Shell Group.